

DISSERTATION

INFLUENCE OF ADIPOSE-DERIVED MESENCHYMAL STROMAL CELLS
ON OSTEOSARCOMA MINIMAL RESIDUAL DISEASE

Submitted by

Megan Aanstoos-Ewen

School of Biomedical Engineering

In partial fulfillment of the requirements

For the Degree of Doctor of Philosophy

Colorado State University

Fort Collins, Colorado

Summer 2015

Doctoral Committee:

Advisor: Nicole Ehrhart

Matthew Kipper

Steven Dow

James Custis

Copyright by Megan Elizabeth Aanstoos 2015

All Rights Reserved

ABSTRACT

INFLUENCE OF ADIPOSE-DERIVED MESENCHYMAL STROMAL CELLS ON OSTEOSARCOMA MINIMAL RESIDUAL DISEASE

Introduction: Mesenchymal stromal cells (MSCs) have been shown to improve bone integration and healing in several preclinical studies and have therapeutic potential in limb salvage following massive bone loss due to tumor resection. However, MSCs have also been shown to promote primary and pulmonary metastatic tumor growth when injected in the presence of gross tumor or when co-injected with tumor cells in rodent models. While these results raise concerns about the safety of using MSCs in sarcoma patients, MSCs are unlikely to be utilized in a clinical setting when gross tumor is present.

The objective of this dissertation project was to develop murine models of minimal residual osteosarcoma following primary tumor removal then to utilize these models to determine whether the administration of adipose-derived MSCs with or without chemotherapy treatment in a minimal residual disease setting would promote either pulmonary metastatic osteosarcoma progression or local disease recurrence. We hypothesized that surgical site or intravenous administration of MSCs will influence either osteosarcoma pulmonary metastatic burden or local disease recurrence in a minimal residual disease setting.

Materials & Methods: Two syngeneic, orthotopic models of luciferase-expressing osteosarcoma were developed. In the first model, tumor-bearing mice underwent a coxofemoral amputation and were followed to assess development of pulmonary metastases. In the second model, a femorotibial amputation was performed in order to develop a model of consistent local

tumor recurrence. In this model, all gross tumor was removed, however, microscopic tumor remained at the surgical margin.

In this dissertation project, three principle projects were completed to test our hypothesis. The first project explored the use of MSCs delivered either to the surgical site or intravenously to ascertain their influence on pulmonary disease burden. A follow-on pilot explored concurrent MSC and chemotherapy treatment on development of pulmonary disease. The second project evaluated the use of MSCs delivered either to the surgical site or intravenously on local recurrence of osteosarcoma at the surgical site. Gross recurrent tumor size was measured for comparison between treatment groups. The third project examined the use of cisplatin and MSCs on survival of mice following removal of primary osteosarcoma.

Data were expressed in mean \pm SD or median with 95% CI. ANOVA test, Kruskal-Wallis test, Fisher's Exact test, Welch's test, t-test, and Mann Whitney test were used for statistical analysis. Significance was set at $p < 0.05$.

Results: Mice treated with intravenous MSCs had a faster time to first pulmonary metastatic disease detection than mice treated with MSCs injected into the surgical site or control mice (no MSCs) ($p = 0.022$). No treatment effect was seen between groups with respect to time to tumor recurrence or size of recurrent tumor in the second study. Survival curves were significantly different when comparing cisplatin, cisplatin and MSC treatment, MSC alone treatment and untreated mice ($p < 0.001$) as well as in pairwise comparisons. Mice treated with MSCs had a 73% chance of earlier death than untreated controls.

Discussion/Conclusion: Intravenous administration of MSCs in a minimal residual osteosarcoma environment resulted in a faster time to first detection of pulmonary disease and in a higher chance of earlier death compared to untreated mice. However, administration of MSCs locally in a surgical site following sarcoma excision appears to be safe, even in the

setting of known residual microscopic disease. Further, the use of cisplatin treatment appeared to ameliorate the effects of intravenous MSCs on survival. Based on these results, further study is warranted to evaluate the influence of intravenously administered MSCs on minimal residual pulmonary metastatic disease.

ACKNOWLEDGEMENTS

The support for this research came from the Laboratory of Comparative Musculoskeletal Oncology and Traumatology and the Limb Preservation Foundation.

A huge thank you to my adviser for giving me an opportunity to learn more about the world of veterinary medicine and oncology. From Dr. Nicole Ehrhart's first guidance into developing animal models to her assistance presenting my work in public forums to her invaluable editing, commenting, and encouragement for finishing, I really cannot state how much I appreciate having her as my adviser and mentor.

My committee has been exemplary as well – meeting often with me and giving insightful feedback to improve my work at every turn has helped make this dissertation project more than just one person. A special thank you to each of them as well for taking the time to guide me through the narrow walls of biomedical engineering and clinical science. Dr. Matt Kipper, Dr. Steven Dow, and Dr. James Custis – you are wonderful.

Finally, research is not completed in a vacuum and without the outstanding assistance, support, and encouragement of my lab, this project would have fallen by the wayside many times. Laura Chubb, my perfect lab manager, helped me with everything and anything and never minded giving her time and energy to making sure I succeeded. Our lab's post-doc, Dr. Ruth Rose, was always available for guidance, support, and made a wonderful surgeon for the many amputations this project demanded. The many students in our lab made for a supportive family offering advice, assistance, and encouragement along the way. Thank you to all these professionals and more for getting me through my doctoral degree!

DEDICATION

First I want to say thank you to my husband, Hunter Ewen, for his everything. Though he might not understand everything I do, he gives me support for it anyway.

Second, thank you to my family and friends and mentors for your help in everything from mental health to writing to goodies to keep me going. A strong network makes all the difference and I'm proud to know I have a great one.

Third, thank you to my kitties for letting me close the door on you so I could work and letting me come home smelling of mice without eating me.

Finally, I'd like to dedicate this work to my dog Jake, who was my first adult experience with the devastating disease that is osteosarcoma. For him and all those who suffer from cancer – stay strong, we are working on cures for you!

TABLE OF CONTENTS

| | |
|---|------|
| Abstract | ii |
| Acknowledgements | v |
| Dedication | vi |
| Table of Contents | vii |
| List of Figures | viii |
| Chapter 1 – Overview | 1 |
| 1.1 Research Objectives | 1 |
| 1.2 Scientific Rationale | 2 |
| 1.3 Hypothesis and Specific Aims | 4 |
| Chapter 2 – Review of the Literature | 9 |
| Chapter 3 – Development of a Luciferase expressing OSA Cell Line, In Vivo Model Development and Validation of MSC-Tumor Interaction | 29 |
| Chapter 4 – Do Mesenchymal Stromal Cells Delivered Intravenously or into the Surgical Site Promote Murine Osteosarcoma Pulmonary Metastases? | 69 |
| Chapter 5 – Influence of Concurrent Treatment of Mesenchymal Stromal Cells and Methotrexate on Long-Term Pulmonary Metastases Following Removal of Primary Osteosarcoma | 81 |
| Chapter 6 – Do Mesenchymal Stromal Cells Delivered Intravenously or into the Surgical Site Promote Murine Osteosarcoma Local Recurrence? | 88 |
| Chapter 7 – Influence of Concurrent Treatment of Mesenchymal Stromal Cells and Cisplatin on Survival Following Removal of Primary Osteosarcoma | 100 |
| Chapter 8 – Conclusions and Future Research | 114 |
| Appendices | 121 |
| Appendix A: Laboratory Operating Procedures | 121 |
| Appendix B: Scoring Assessments | 149 |
| List of Abbreviations | 153 |

List of Figures

| | |
|---------------------|---------|
| Chapter 3 | 29 |
| 3.2 – 1 | 36 |
| 3.2 – 2 | 37 |
| 3.4 – 1 | 45 |
| 3.4 – 2 | 45 |
| 3.5 – 1 | 50 |
| 3.6 – 1 | 53 |
| 3.7 – 1 | 58 |
| 3.7 – 2 | 59 |
| 3.8 – 1 | 65 |
| Chapter 4 | 69 |
| 4.3 – 1 | 76 |
| 4.3 – 2 | 77 |
| 4.3 – 3 | 78 |
| Chapter 5 | 81 |
| 5.3 – 1 | 86 |
| Chapter 6 | 88 |
| 6.3 – 1 | 95 |
| 6.3 – 2 | 96 |
| 6.3 – 3 | 97 |
| 6.3 – 4 | 98 |
| Chapter 7 | 100 |
| 7.3 – 1 | 107 |
| 7.3 – 2 | 108 |
| 7.3 – 3 | 109 |
| 7.3 – 4 | 110 |
| 7.3 – 5 | 111 |
| 7.3 – 6 | 112 |

Chapter 1: Research Overview

1.1 Research Objectives

The overarching purpose of the work reported herein was to address the question of whether mesenchymal stromal cells, given either in the surgical site or intravenously, will promote disease progression in the setting of minimal residual osteosarcoma following primary tumor removal. Our research objectives were to (1) create clinically-relevant murine models of minimal residual osteosarcoma (in both pulmonary and surgical sites) using luciferase-expressing, syngeneic, osteosarcoma cell lines, (2) validate metastatic progression within the pulmonary system after histologically complete primary tumor removal, (3) examine the effect of concurrent treatment of mesenchymal stromal cells and chemotherapy on survival and pulmonary metastatic disease after primary tumor removal, (4) confirm local recurrence following histologically incomplete primary tumor removal and, (5) ascertain the influence of mesenchymal stromal cells on tumor re-growth and progression of pulmonary metastasis in these microscopic minimal residual disease models following primary osteosarcoma removal.

We achieved these research objectives by completing the following experiments:

(1) Generation of an M1 DLM8 osteosarcoma cell line with stable luciferase expression

(2) Optimization of an orthotopic tibial osteosarcoma tumor model using the transfected DLM8-Luc-M1 cell line.

(3) Validation of the timing of amputation prior to the onset of grossly-detectable pulmonary metastasis and subsequently tracking progression of metastatic development, thus certifying the micrometastatic pulmonary disease model using the DLM8-Luc-M1 cell line.

- (4) Development and validation of a novel murine local osteosarcoma recurrence model using a narrow-margin amputation technique
- (5) MSC-Tumor interaction experiments and validation
- (6) DLM8-Luc-M1 and DLM8-Luc cell line chemotherapy sensitivity assays and comparisons
- (7) Assessment of the influence of adipose-derived mesenchymal stromal cells on progression of pulmonary metastasis following primary tumor removal when delivered either into the surgical site or intravenously.
- (8) Evaluation of the influence of chemotherapy with and without mesenchymal stromal cells on pulmonary metastasis following amputation for DLM8-Luc-M1 tibial osteosarcoma.
- (9) Confirmation of the influence of MSCs on local tumor recurrence in the presence of microscopic residual disease when delivered either into the surgical site or intravenously
- (10) Determination of the influence of chemotherapy with and without mesenchymal stromal cells on survival in mice following amputation for DLM8-Luc-M1 tibial osteosarcoma.

1.2 Scientific Rationale

Osteosarcoma (OS) is a malignant primary bone tumor that arises spontaneously in both canine and human species, typically in the appendicular skeleton. OS has a high metastatic rate, with the most common sites being lungs and other skeletal sites. Microscopic pulmonary metastasis is often present at initial diagnosis, although confirmation is difficult until the metastatic lesions become visible using current imaging modalities. Primary bone tumors account for 4-7% of childhood cancers and one type, osteosarcoma, is the second highest cause of cancer-related deaths in children and adolescents [13, 14]. It is also the most common bone cancer in dogs [6], making it an impactful disease in both human and pet populations. In humans, survival rates are

55-75% without metastatic nodules present at diagnosis [9, 14]; the survival rate drops to 30% when tumors are also present in a second site [13]. In patients older than 60 years, the survival rates are 18-55% [14]. Survival is lower in canines; 50% survive to 1 year and 20-25% to 2 years [16].

Treatment in humans usually involves preoperative chemotherapy – either given intravenously (IV) or intra-arterially (IA) – for several courses until the tumor is greater than 90% necrotic as observed using imaging modalities [16, 17]. The tumor is then surgically excised and the resulting bone defect is filled with an allograft or endoprosthetic implant. Limb salvage in canine OS patients is performed in some cases. In most canine patients, as well as in some humans, an amputation of the limb is performed instead [10]. Surgery is then followed with several more rounds of chemotherapy [17]. In cases where grossly-evident metastatic disease is present, the nodules are treated with preoperative chemotherapy, followed by surgical resection if the metastatic lesion is large enough and more chemotherapy [13].

Limb reconstruction (limb salvage) is the preferred treatment for human patients, yet several drawbacks to limb salvage treatment, including integration of implants with the host bone, a higher risk of local recurrence, and multiple, costly revisions, means it remains a clinical challenge and an area of active research. [1, 11, 13]. Recent investigations have focused on improving bone-implant integration through the use of mesenchymal stromal cells (MSCs). These cells, usually harvested from bone marrow (BM-MSCs) or adipose (AD-MSCs), can be used to coat the implants, or can be administered into the surgical site at or near the bone defect to aid in bony integration and reduce the number of revisions [3-5, 8]. In spite of their potential usefulness for bone healing in patients with reconstruction of large bone defects, there have been numerous rodent studies showing that MSCs promote both primary OS tumor growth and metastasis [7, 15, 18].

While these MSC – tumor interactions are disquieting, the aforementioned studies have been conducted when the primary tumor is still present *in vivo* or when tumor and mesenchymal stromal cell types are mixed *in vitro*. In typical clinical treatment, however, the primary tumor would be removed before MSCs were employed in the patient. While the behavior of MSCs in a post-operative microscopic disease setting may differ vastly from a setting in which the primary tumor is present, no previous work has been done looking at the influence of MSCs on minimal residual disease following removal of the primary tumor. Therefore, a study examining the interaction of MSCs and residual tumor or micrometastatic disease will provide relevant data for clinical treatment protocols.

1.3 Hypotheses and Specific Aims

This work addressed the behavior of AD-MSCs when used as part of a treatment protocol for mice undergoing surgery for osteosarcoma primary tumor removal. Prior research has shown that MSCs can promote primary tumor growth and decrease the time to metastatic occurrence when the primary tumor is present [2, 12, 18]. By determining the activities of AD-MSCs in a microscopic disease setting, after the primary tumor has been removed, treatment protocols and implant design can be adjusted to optimize healing – with or without the use of AD-MSCs. This information will be beneficial for physicians and veterinarians designing treatment protocols and engineers designing products for use in limb salvage situations where there is a need to improve bony integration and healing.

Our investigations were directed by the following **Fundamental Hypothesis**:

Adipose-derived mesenchymal stromal cells, delivered either into the surgical site or intravenously after removal of primary osteosarcoma tumor, will, in the presence of microscopic residual disease, influence metastatic pulmonary disease or local tumor regrowth.

To address this fundamental hypothesis we completed the following Specific Aims:

Preliminary Projects Specific Aim

Develop and validate murine models of minimal residual osteosarcoma (in both pulmonary and surgical sites) using luciferase-transfected, murine, syngeneic, orthotopic osteosarcoma cell lines.

Validation experiments:

- (1) Generate a murine luciferase-expressing syngeneic osteosarcoma cell line
- (2) Create clinically-relevant murine models of orthotopic osteosarcoma
- (3) Measure DLM8-Luc-M1 sensitivity to chemotherapy *in vitro*
- (4) Verify C3H AD-MSCs affect DLM8-Luc-M1 osteosarcoma *in vivo*
- (5) Demonstrate tracking of AD-MSCs to DLM8-Luc-M1 primary tumor
- (6) Validate metastatic progression within the pulmonary system after histologically complete primary tumor removal
- (7) Confirm local recurrence following histologically incomplete primary tumor removal

Specific Aim 1

Ascertain the influence of adipose-derived mesenchymal stromal cells on pulmonary metastatic disease burden following removal of the primary tumor.

Hypothesis1

Administration of AD-MSCs influences progression of metastatic pulmonary osteosarcoma following removal of the primary tumor.

Specific Aim 2

Assess the influence of concurrent treatment of adipose-derived mesenchymal stromal cells and methotrexate on long-term pulmonary metastatic disease burden following removal of primary osteosarcoma tumor.

Hypothesis 2

There will be no difference in long-term pulmonary metastatic disease burden between untreated mice or mice treated with methotrexate (MTX), AD-MSCs, or MTX and AD-MSCs.

Specific Aim 3

Investigate the influence of adipose-derived mesenchymal stromal cells on osteosarcoma local recurrence following narrow margin removal of the primary tumor.

Hypothesis 3

Administration of AD-MSCs influences time to local recurrence or size of local recurrence of osteosarcoma following removal of the primary tumor.

Specific Aim 4

Examine the influence of AD-MSCs with and without cisplatin on survival following removal of primary tibial DLM8-Luc-M1 osteosarcoma.

Hypothesis 4

There will be no difference in the survival curves or median survival time of mice untreated or mice treated with cisplatin (CIS), AD-MSCs, or CIS and AD-MSCs.

REFERENCES

1. Agarwal M, Anchan C, Shah M, Puri A, Pai S. Limb salvage surgery for osteosarcoma: effective low-cost treatment. *Clin Orthop Relat Res*. 2007;459:82-91.
2. Bian Z-Y, Fan Q-M, Li G, Xu W-T, Tang T-T. Human mesenchymal stem cells promote growth of osteosarcoma: Involvement of interleukin-6 in the interaction between human mesenchymal stem cells and Saos-2. *Cancer Science*. 2010;101:2554-2560.
3. Coathup MJ, Kalia P, Konan S, Mirza K, Blunn GW. A comparison of allogeneic and autologous mesenchymal stromal cells and osteoprogenitor cells in augmenting bone formation around massive bone tumor prostheses. *Journal of Biomedical Materials Research Part A*. 2013;101A:2210-2218.
4. Di Bella C, Aldini NN, Lucarelli E, Dozza B, Frisoni T, Martini L, Fini M, Donati D. Osteogenic Protein-1 Associated with Mesenchymal Stem Cells Promote Bone Allograft Integration. *Tissue Engineering Part A*. 2010;16:2967-2976.
5. Dupont KM, Sharma K, Stevens HY, Boerckel JD, García AJ, Guldberg RE. Human stem cell delivery for treatment of large segmental bone defects. *Proceedings of the National Academy of Sciences of the United States of America*. 2010;107:3305-3310.
6. Fenger JM, London CA, Kisseberth WC. Canine Osteosarcoma: A Naturally Occurring Disease to Inform Pediatric Oncology. *ILAR Journal*. 2014;55:69-85.
7. Grassi Rici RE, Alcântara D, Fratini P, Wenceslau CV, Ambrósio CE, Miglino MA, Maria DA. Mesenchymal stem cells with rhBMP-2 inhibits the growth of canine osteosarcoma cells. *BMC Veterinary Research*. 2012;8:17-17.
8. Kalia P, Bhalla A, Coathup MJ, Miller J, Goodship AE, Blunn GW. Augmentation of massive implant fixation using mesenchymal stem cells. *Journal of Bone & Joint Surgery, British Volume*. 2006;88-B:392.
9. Mirabello L, Troisi RJ, Savage SA. International osteosarcoma incidence patterns in children and adolescents, middle ages, and elderly persons. *International journal of cancer. Journal international du cancer*. 2009;125:229-234.
10. Mueller F, Fuchs B, Kaser-Hotz B. Comparative Biology of Human and Canine Osteosarcoma. *Anticancer Research*. 2007;27:155-164.
11. Ottaviani G, Robert RS, Huh WW, Jaffe N. Functional, Psychosocial and Professional Outcomes in Long-Term Survivors of Lower-Extremity Osteosarcomas: Amputation Versus Limb Salvage Pediatric and Adolescent Osteosarcoma. In: Jaffe N, Bruland OS, Bielack S, ed.: Springer US; 2010:421-436.
12. Perrot P, Rousseau J, Bouffaut A-L, Rédini F, Cassagnau E, Deschaseaux F, Heymann M-F, Heymann D, Duteille F, Trichet V, Gouin F. Safety Concern between Autologous Fat Graft, Mesenchymal Stem Cell and Osteosarcoma Recurrence. *PLoS ONE*. 2010;5:e10999-e10999.
13. Picci P. Osteosarcoma (Osteogenic sarcoma). *Orphanet Journal of Rare Diseases*. 2007;2:6.
14. Savage SA, Mirabello L. Using epidemiology and genomics to understand osteosarcoma etiology. *Sarcoma*. 2011;2011:548151.
15. Tsukamoto S, Honoki K, Fujii H, Tohma Y, Kido A, Mori T, Tsujiuchi T, Tanaka Y. Mesenchymal stem cells promote tumor engraftment and metastatic colonization in rat osteosarcoma model. *International journal of oncology*. 2012;40:163-169.
16. Withrow SJ, Vail D. *Withrow and MacEwen's Small Animal Clinical Oncology*: Elsevier Health Sciences; 2007.

17. Withrow SJ, Wilkins RM. Cross talk from pets to people: translational osteosarcoma treatments. *ILAR journal / National Research Council, Institute of Laboratory Animal Resources*. 2010;51:208-213.
18. Xu W-t, Bian Z-y, Fan Q-m, Li G, Tang T-t. Human mesenchymal stem cells (hMSCs) target osteosarcoma and promote its growth and pulmonary metastasis. *Cancer Letters*. 2009;281:32-41.

Chapter 2: Review of the Literature

2.1 Introduction

One goal of biomedical engineering is to utilize scientific innovation to improve medical technology for humans and animals. Under recent consideration is the use of “stem cells” to facilitate these advancements. There are two broad classifications of stem cells – embryonic and adult. The first category has received significant notoriety due to the need to harvest cells from fetal tissue, many times at the expense of the fetus. Due to these ethical concerns and issues with harvesting the cells, most translational research has turned to the alternative – adult stem cells.

Adult stem cells are divided into hematopoietic and non-hematopoietic classifications, based on tissue of origin and differentiation abilities. The focus of this review is on non-hematopoietic mesenchymal stem cells, also known as “multipotent mesenchymal stromal cells” (MSC) [29]. Characteristics of adult stem cells include multipotency, an ability to self-renew, adherence to plastic in culture, and expression of specific cytokine markers [39]. Mesenchymal stromal cells should be positive for CD105, CD73, and CD90, but negative for CD45 and CD34 [29]. The ability to cluster into colony forming units *in vitro* has also been accepted [19][55] as a way to differentiate the cells from other plastic adherent cells, such as fibroblasts. MSCs are multipotent cells that can differentiate into several lineages, including adipogenic, osteogenic, and chondrogenic. These cells are self-renewing and located in several organs in the body, including bone marrow [87], adipose [4], and muscle [19]. They have been shown to “home” to sites of injury and inflammation *in vivo*, including to tumors [31, 55, 72]. Additionally, these cells have been demonstrated to be clinically useful for various orthopedic applications, including fracture repair and bone-implant integration [36, 47, 51]. Consequently, the use of MSCs to aid

in bone regeneration for patients with orthopedic-related sarcomas is of great interest to researchers and clinicians.

2.2 Mesenchymal Stromal Cells

Although progenitor cells were postulated as existing as far back as the 1800s [41], it was the work of Friedenstein *et al.* in the 1960s and 1970s that provided a breakthrough into their characteristics and origins [32]. This work was further developed by Caplin *et al.* in 1991, when the cells were examined for their effectiveness in healing soft tissue and bone [16]. In the clinical setting, the most frequently utilized stem cells are derived from bone marrow (BM) [5]. These cells are harvested and expanded through culturing processes that select for MSCs from a mixture of other cells using cell sorting, plastic adhesion, or flow cytometry [50]. Due to their capacity for self-renewal and resistance to senescence, MSCs can be passaged many more times than somatic cells, although early passage cells are generally considered ideal for therapeutic purposes and for *in vivo* studies [12, 47, 93, 95]. Several labs have characterized BM-MSCs through the use of *in vitro* studies [10, 12, 13, 29, 66] and many studies in animals have been conducted to characterize BM-MSCs effect on critical sized defect healing [3, 33], integration of scaffolds into host bone [13, 50], and a myriad of other potential clinical uses [4, 8].

Current orthopedic research has focused on culturing MSCs in scaffolds [49, 50] that can be used for bone defect filler material, drug delivery, or implant design [44]. Results from *in vitro* studies have shown that MSCs in scaffolds can improve cellular growth [33, 44] and adhesion [49] and decrease the time needed for the bone to undergo osteogenesis and new mineral deposition [50]. Several animal models have been developed, including murine [25], sheep [9, 36], canine [3, 95], and goat [97], to evaluate utilization of MSCs in regeneration of bone, repair of bone defects, and enhancement of bone formation. These studies also demonstrated improved bone remodeling [3], union of the host-allograft interface, and enhanced mechanical

properties similar to host bone [27, 95]. In critical sized defects, when the defects were filled using scaffolds seeded with AD-MSCs, the defect healed quickly and was filled with bone-like tissue [24]. In some studies, scaffolds and MSCs have been combined with other biologics, such as bone morphogenetic protein-2 (BMP-2) [98] and fibrin [47], to further improve healing. In addition to scaffolds, the use of MSCs as a method for augmenting bone-endoprosthesis contact has been explored. Results of the study demonstrated an improvement in surface area contact and a higher quantity of bone formation [45].

2.3 Mesenchymal Stromal Cell Use for Bone Healing

Mesenchymal stromal cells (MSCs) have been shown to improve bone integration between native tissue and large segment cortical allografts or allo- endoprosthesis composites used in limb reconstruction [21, 28, 45]. As well, they have been shown to aid in healing of critical sized defects in several preclinical studies. MSCs therefore have potential for therapeutic use in limb salvage following large-segment bone loss resulting from trauma or tumor resection [30, 42, 54].

2.4 Osteosarcoma

Sarcomas are malignant tumors of mesenchymal origin [64]. They have the potential to metastasize to distant sites such as the lung or liver and tumor cells can remain dormant for several years [62]. Types of sarcomas most commonly known to affect the bone and surrounding soft tissue include osteosarcoma (OS), Ewing's sarcoma (EWS), rhabdomyosarcoma, and leiomyosarcoma. OS is the second highest cause of death in children and adolescents [56, 76] and the most common primary bone tumor in dogs making this disease an important health concern for both physician and veterinary orthopedic oncologists [62, 90, 92].

Osteosarcoma generally presents in the appendicular skeleton, most specifically in the tibia and femur in humans [62, 76] and the distal radius in canines [92]. Etiology of the disease is not

well established [80], although certain genetic disorders, such as hereditary retinoblastoma [76] or a mutation in the p53 gene [81] may increase the risk. Ionizing radiation has been implicated in 2% of osteosarcomas [64]. Prognosis is poor for long term survival, with children reaching 55-75% at 5 years without metastatic disease initially and 30% with metastases at initial presentation [76]. In patients older than 60 years, these rates drop to 18-55% [76] and in canines, survival is 50% at one year and 20-25% at two years [91]. There are eight subtypes of the disease with distinct behaviors: conventional, telangiectatic, small cell, low-grade central, secondary, parosteal, periosteal, and high-grade surface [94]. Radiographically, OS appears as a lobulated mass with central dense ossification and cortical thickening [94]. In order to obtain a confirmed diagnosis, a biopsy is required [62, 80] to supplement radiographic images. The next step is to determine whether metastatic disease is present at initial identification and this is done using MR, CT, and PET imaging [64]. Finally, a treatment regimen is planned for the patient.

Treatment options can vary among species. In canines, owners have a choice between palliative care for pain control or curative treatment. In cases where palliative care is chosen, pain management includes the use of analgesia, often in combination with radiation therapy for tumor control [22, 62, 67]. If the owner opts for curative care, the standard treatment protocol includes amputation of the affected limb or surgical resection of the tumor and the use of limb salvage to reconstruct the limb, followed by several rounds of chemotherapy [62, 91]. If the lesion cannot be resected, or in cases of metastatic nodules, the tumor is often treated with stereotactic radiation therapy to cause necrosis of the tumor cells, followed by chemotherapy. [22, 67, 91].

In humans, amputation is the less preferred option and many times, if possible, patients undergo pre-operative chemotherapy, surgical resection of the tumor, followed by limb salvage and further chemotherapy treatment [92]. Limb salvage consists of tumor removal, followed by reconstruction of the defect with either an allograft or an endoprosthetic implant. In both these

cases, residual tumor cells may be left in the surgical site. This could lead to local recurrence of the tumor. Other concerns include poor limb function, and cytotoxic treatments that prevent bone healing at the surgical site [1, 64]. Multiple revisions may be needed at great financial and psychosocial costs to the patients. Therefore, methods to reduce revisions and improve healing are critical components in improving patient quality of life. The use of stem cells may be one method to improve healing for such patients [45], based on the properties mentioned earlier, but there are several concerns that still need to be addressed.

2.5 Cancer Stem Cells versus Mesenchymal Stromal Cells as Sarcoma Origin Cell

The cancer stem cell (CSC) theory postulates that there is a small population of “stem cells” within tumors that have the ability to self-renew and differentiate into all the cells within a tumor [26]. CSCs have been isolated from osteosarcoma [37, 78, 89], Ewing’s sarcoma [79], and chondrosarcoma [83] as well as other tumors. It is believed that this sub-set of cells is responsible for initiating and maintaining tumor growth [38, 78]. Furthermore, if CSCs are not completely eliminated by chemotherapy or radiation treatments, they are believed to be partially responsible for tumor relapse, metastatic disease, and drug resistance [7]. Although CSCs are thought to share a common origin with MSCs and exhibit some similarities in surface markers, such as being CD90+ and CD105+, as well as traits such as self-renewal and multipotency, they are two distinct cell populations.

An alternative theory postulates that instability and mutations in MSCs lead to sarcomas [59]. In particular, there is concern about chromosomal instability [2] and malignant transformations at high passages in cell cultures [15, 57, 84]. Non-malignant MSCs have been isolated from the stroma of tumors [13, 60] and transformation, both regulated and spontaneous, of MSCs into sarcomas has been completed using several methods, explored in greater detail below [52, 69, 70].

The debate between adherents of these competing postulates -- whether tumors have their own stem cells that drive growth or whether they recruit MSCs to expand and proliferate -- has been covered by several authors [38, 59]. This review, however, moves the focus beyond that debate to explore some of the other ways MSCs have been shown to create and interact with sarcomas, the clinical importance of these results, and what questions remain to be answered.

2.6 Transformation of Mesenchymal Stromal Cells Using Oncogenes and Transcription Factors to Obtain Tumor Cells or Sarcoma Growth *In vivo*

The use of genetic manipulation to establish sarcomas from normal MSCs may provide insight into the development and mechanisms of these tumors [52, 77]. Oncogenes, isolated from fully formed sarcomas, have been implicated as vital for tumor formation. In some cases, such as EWS, the addition of a specific oncogene, in this case EWS-FLI-1 fusion gene, into MSCs is enough to obtain tumor formation [17, 58, 70]. However, in other situations, specific genes need to be knocked out. Isolation of BM-MSCs from mice with p16 and p19 deletions, both important in the p53 pathway, was completed. These cells were transduced with c-MYC transcription factor and GFP (Green Fluorescent Protein) and injected into syngeneic mice. Mice injected with these modified MSCs developed tumors histologically reminiscent of OS [77]. Rodriguez *et al.* demonstrates the relevance of the p53 pathway with regards to liposarcoma; AD-MSCs isolated from murine tissue were infected with viral particles expressing FUS-CHOP (Fused in Sarcoma, Translocated in LipoSarcoma-C/EBP Homologous Protein) and GFP. The p53 gene was deleted through the use of a lentiviral transduction in the FUS-CHOP AD-mMSCs. Mice inoculated subcutaneously with the p53^{-/-} FUS-CHOP AD-mMSCs induced liposarcoma formation but AD-hMSC, isolated from human donors, did not form tumors when subjected to the above treatments [71]. These results were corroborated in a model of myxoid liposarcoma in nude mice after injection of mesenchymal primary cells derived from murine bone marrow infected with FUS-CHOP [70]. The loss of the p53 gene was also necessary in an

alveolar rhabdomyosarcoma model before MSCs transfected with PAX-FKHR could form tumors [69]. Again, the loss of p53 was crucial to obtaining leiomyosarcoma *in vivo* [75]. The concern, however, is whether MSCs can create tumors when they have not been modified by genes known to be key in sarcoma formation.

2.7 Spontaneous Transformation of Mesenchymal Stromal Cells *in vivo* and *in vitro* into Malignant Tumors

One of the most noteworthy concerns in the literature is the safety of MSC use in human medicine [18, 20, 63, 68, 87]. Specifically, there has been some question about whether these cells will transform on their own into malignancies *in vivo*. Several authors have reported malignant transformation *in vitro*, both at low and high passages [15, 57, 84, 88]. *In vitro*, the cells transformed into poorly differentiated sarcomas [88] and fibrosarcoma [57]. When injected into mice, the cells formed tumors [2, 84] with characteristics similar to osteosarcoma, Ewing's sarcoma [15], or non-specific sarcomas. One lab reported obtaining sarcomas after seeding MSCs onto hydroxyapatite-collagen sponges that were used as bioscaffolds and implanted subcutaneously [82] although similar tests in another lab did not result in tumor formation from MSCs [20]. Some evidence suggests murine MSCs may be more likely to form tumors *in vivo* than human-derived MSCs [2, 71] but this remains undecided.

In contrast to the results reported above, several researchers have shown no transformation of MSCs and demonstrate no malignancies [40], both *in vivo* [68] and *in vitro* [10]. These results were confirmed by authors who at first reported malignant transformation of MSC cell lines [73, 74], but later redacted the results after finding the lines had been contaminated by tumor cells [35, 85]. Thus, there is still a question as to whether adult-derived MSCs can directly become malignant tumors, or whether they may merely assist in recruitment of cytokines that the tumor or cancer stem cells can then use to enlarge growth. Therefore, the debate as to whether they are safe to use in patients with malignances or a history of malignancy continues.

2.8 Interactions between Mesenchymal Stromal Cells and Sarcomas

Several investigators have examined interactions between MSCs injected into rodents with established primary sarcoma [46, 53, 61] or the interactions between MSCs and tumor cells *in vitro* [23]. It has been well-established that MSCs will “home” to areas of inflammation *in vivo* [31, 55]. In sarcoma models where gross tumor is present, MSCs have been shown to preferentially migrate to the primary tumor as well as to metastatic foci [43]. In a rat osteosarcoma model, co-implantation of MSCs and OS cells resulted in faster tumor development initially as compared to OS alone, but long term, there was no statistical difference in tumor volume [86]. When MSCs were injected after tumor development, the number of lung metastatic nodules was significantly increased compared to the control group which received no MSCs [86].

Perrot et al. [63] conducted a rodent study, using Saos-2 (human) osteosarcoma cells, to determine the effects of fat in the presence of osteosarcoma. A control group of osteosarcoma was compared to three other groups: OS and fat, OS and injury to the area used to mimic effects of surgery, and fat only. By three weeks, the tumor growth was significantly increased in the OS and fat group compared to the other mice. A second experiment by the same authors using POS-1 (murine) osteosarcoma cells was also conducted to determine the influence of murine MSCs on tumor growth. In this study, three groups were used: control with OS only, control with MSC only and a co-injection of MSCs and OS cells. Animals receiving a co-injection of OS cells and MSC developed tumors 1.5 times faster than OS animals alone. MSCs alone resulted in no tumor formation [63].

Interleukin-6 (IL-6) cytokines are also important for maintenance of stem cell proliferation. When MSCs or OS cells were exposed to IL-6, proliferation of both cell types was enhanced in a dose-dependent manner [11]. Additionally, IL-6 secretion from MSCs was elevated *in vitro* when exposed to OS cell culture media at different gradients. Recent research suggests the

possibility of a “positive feedback loop” of IL-6 existing between human MSCs and human osteosarcoma that allows OS tumor cells to enhance the proliferation of MSCs and MSCs to enhance the proliferation of osteosarcoma [11]. Further work on the IL-6 activation pathway revealed that dysregulation of signal transducer and activator of transcription 3 (STAT3) leads to promotion of tumor growth. Specifically, *in vitro*, the inhibition of STAT3 suppressed OS cell proliferation, even in the presence of MSC conditioned media or additional expression of IL-6. Therefore, it was concluded that MSCs secrete IL-6, which then activates STAT3 signaling in OS cells to promote the migration and invasion of OS cells [7]. This may explain why a co-injection of MSCs and OS cells increased tumor development compared to OS alone [86].

A model of primary osteosarcoma in the proximal tibia of nude mice was developed; when GFP labeled MSCs were injected through the caudal tail vein four weeks after tumor inoculation, OS growth was enhanced and the rate of pulmonary metastasis was much higher than groups without MSC exposure. Stromal derived factor-1 (SDF-1), which is a critical recruitment factor of MSCs, was measured and expression levels were higher near the tumor site. The authors proposed that OS cells *in vivo* secrete SDF-1 to recruit MSCs to the tumor and assert that based on the results of their study, it would be “irresponsible and risky” to use MSCs as a tool for the treatment of tumors [93].

Although the majority of the published research suggests MSCs increase sarcoma growth and time to metastatic disease, one study has shown that, in opposition to the results above, in Kaposi sarcomas, injection of MSCs will inhibit the tumor growth [48]. Unlike osteosarcoma, Kaposi sarcoma has a viral origin. It is also more likely to start in multiple sites simultaneously. Osteosarcoma, in contrast, usually has one focal primary site and is of mesenchymal origin, although etiology remains incompletely understood. MSCs intravenously injected into models of established hepatoma, carcinoma, and pancreatic cancer have led to an inhibition of tumor growth and have been shown to interfere with cancer cell proliferation by blocking G0/G1 tumor

cell cycle phases [14]. These examples of duality in MSC behavior highlight the complexity of the relationship between MSCs and sarcomas.

2.9 Mesenchymal Stromal Cells as Delivery Vehicles for Sarcoma Treatments

Results published to date indicate MSCs may not be safe for use in sarcoma-bearing patients. Due to their homing capabilities and subsequent interactions, they have nonetheless been explored as a modality for delivery of drugs for treatment of sarcomas. In particular, delivery of rhBMP2 using MSCs in a canine osteosarcoma model resulted in a decrease in p53 and Ki67 expression, an inhibition of osteosarcoma cell proliferation, and an increase in tumor cell death [43]. The use of MSCs as a vehicle for tumor necrosis factor-related apoptosis-inducing ligand (TRAIL) delivery to target rhabdomyosarcoma cells was effective in suppressing tumor cell growth [6]. Interleukin-12 (IL-12), a growth factor, was used for treatment in a murine Ewing's sarcoma model [96]. MSCs were infected through adenoviral vectors of IL-12 and Ewing's sarcoma was established in nude mice. Two injections of the genetically enhanced MSCs into the lateral tail vein, four days apart, resulted in inhibition of tumor growth and suppression of metastasis. Finally, MSCs have been explored as targeted-delivery vehicles for anticancer drug-loaded nanoparticles but at the present time complications have inhibited success (refer Gao *et al.* for a more extensive review of this research field) [34].

2.10 Clinical Results and Treatment Concerns

Perrot *et al.* [63] published a case study of recurrence of osteosarcoma that occurred 18 months after fat was used to augment shoulder tissue. As mentioned, one source of MSCs is from adipose tissue, and the authors postulated that the MSCs in the adipose could have resulted in the recurrence of osteosarcoma in the patient.

In a retrospective study, Picci *et al.* reported on 12 patients with a history of benign bone lesions that were treated with curettage and bone grafting. Of these, 8 developed osteosarcoma and 4

developed malignant fibrous histiocytoma (MFH). The authors suggest these results could have been due to the MSCs present and recommend caution in the use of bone grafts in cases where there may be a secondary late malignancy [65].

In both the clinical cases described above, the authors postulate that the use of MSCs was the result of the malignancy. However, in the first situation, the osteosarcoma could have remained behind after initial removal and was slow to reoccur. In the second study, a misdiagnosis of the primary disease could have also resulted in malignancy occurrence if residual disease had remained behind after the initial treatment.

Roodhart *et al.* [72] explored the interaction between MSC and chemotherapy using murine tumor models. BM-MSCs were harvested from syngeneic mice and injected intravenously into mice with established subcutaneous tumors. Four days after cell delivery, the MSCs were found in the tumors but not in any other organs. MSCs were then administered just prior to using cisplatin, a type of chemotherapy drug. Results demonstrated that the antitumor effects of the cisplatin were negated. This result occurred with as few as 50,000 MSCs being used. In animals given MSCs before cisplatin treatment, tumor volumes were similar to those of untreated control tumors receiving no cisplatin. MSCs were also injected subcutaneously at a site distant from the primary tumor. These proved to be even more potent, with as few as 1,000 MSCs resulting in a partial resistance of the tumor to cisplatin chemotherapy. Further work *in vitro* showed that even conditioned media from MSC cultures resulted in a resistance of OS cells to cisplatin if the MSCs had been cultured with a small amount of cisplatin for a short period of time before injection. The effects of the conditioned media could be negated with additional cisplatin treatments. However, MSCs harvested from healthy donors and injected once into nude mice with subcutaneous breast cancer tumors induced a continued resistance to cisplatin for 5 weeks, even with multiple cisplatin treatments.

Additional experiments from the same study revealed that platinum-based chemotherapy activates MSCs to secrete resistance-inducing factors and that these factors, once activated, will be present in endogenous MSCs in tumor-bearing mice [72]. Interference with the cyclooxygenase pathway also leads to a block in the resistance factor. The authors conclude that the injection of two doses of indomethacin or ozagrel before chemotherapy prevents the MSC-induced resistance. The inhibitory effect of MSCs on cisplatin treatment for OS was also observed by Tu *et al.* [7] who suggest that MSCs protect OS cells from cisplatin by producing IL-6. When IL-6 was neutralized, the effect disappeared.

2.11 Discussion

Based on investigations completed thus far, it has become apparent that mesenchymal stromal cells, while useful in a bone healing, may pose certain safety issues when used in sarcoma patients. They have been shown to transform into sarcomas when specific genes and cytokine pathways are manipulated and spontaneously transform into malignant tumors *in vitro* at high passages. The cells also release signals to increase proliferation of tumor cells, contributing to faster growth *in vivo*. However, mesenchymal stromal cells have proved useful for delivery of antitumor drugs, which resulted in a decrease in tumor growth and apoptosis of the malignant cells. In addition, because of their potent ability to form bone, aid in graft integration and allograft healing, MSCs have the potential to greatly benefit patients with large bone defects, such as those who have large segmental bone loss after sarcoma resection.

2.12 Rationale for Further Research

The conflicting results regarding the influence of mesenchymal stromal cells in the presence of sarcomas are helpful or harmful demonstrates that a lack of knowledge still exists and the interaction between MSCs and sarcomas is still somewhat ill-defined. Limitations of the aforementioned studies include the use of immunodeficient murine models, which may not be translatable to human patients. However, perhaps the greatest limitation to the work that has

been done thus far in determining the influence and potential safety of using MSCs in a sarcoma patient is that all of the aforementioned studies utilize MSCs in the presence of gross tumors or prior to establishment of the primary tumor. The influence and safety of MSC use in patients following tumor excision remains unclear, and yet this would be the most clinically-relevant scenario. In nearly all clinical cases, MSCs would be used to enhance bone healing *following* primary tumor resection. The disease burden at such a time would be at its smallest, limited to microscopic pulmonary disease and possibly, at worst, microscopic residual disease at the surgical site. Therefore, further research is needed to elucidate the interaction between MSCs and tumor growth and metastatic behavior, particularly in the post-resection setting.

REFERENCES

1. Agarwal M, Anchan C, Shah M, Puri A, Pai S. Limb salvage surgery for osteosarcoma: effective low-cost treatment. *Clin Orthop Relat Res*. 2007;459:82-91.
2. Aguilar S, Nye E, Chan J, Loebinger M, Spencer-Dene B, Fisk N, Stamp G, Bonnet D, Janes SM. Murine but Not Human Mesenchymal Stem Cells Generate Osteosarcoma-Like Lesions in the Lung. *Stem Cells*. 2007;25:1586-1594.
3. Arinzeh TL, Peter SJ, Archambault MP, van den Bos C, Gordon S, Kraus K, Smith A, Sudha K. Allogeneic Mesenchymal Stem Cells Regenerate Bone in a Critical-Sized Canine Segmental Defect. *The Journal of Bone and Joint Surgery (American)*. 2003;85:1927-1935.
4. Arthur A, Zannettino A, Gronthos S. The therapeutic applications of multipotential mesenchymal/stromal stem cells in skeletal tissue repair. *Journal of Cellular Physiology*. 2009;218:237-245.
5. Baksh D, Yao R, Tuan RS. Comparison of Proliferative and Multilineage Differentiation Potential of Human Mesenchymal Stem Cells Derived from Umbilical Cord and Bone Marrow. *Stem Cells*. 2007;25:1384-1392.
6. Barti-Juhasz H, Mihalik R, Nagy K, Grisendi G, Dominici M, Petak I. Bone marrow derived mesenchymal stem/stromal cells transduced with full length human TRAIL repress the growth of rhabdomyosarcoma cells in vitro. *Haematologica*. 2011;96:e21-e22.
7. Basu-Roy U, Basilico C, Mansukhani A. Perspectives on cancer stem cells in osteosarcoma. *Cancer Lett*. 2012.
8. Bayat MG, Iqbal SA, A. Exploring the application of mesenchymal stem cells in bone repair and regeneration. *Journal of Bone & Joint Surgery, British Volume*. 2012;93-B:427-434.
9. Bensaid W, Oudina K, Viateau V, Potier E, Bousson V, Blanchat C, Sedel L, Guillemain G, Petite H. De novo reconstruction of functional bone by tissue engineering in the metatarsal sheep model. *Tissue Engineering*. 2005;11:814-824.
10. Bernardo ME, Zaffaroni N, Novara F, Cometa AM, Avanzini MA, Moretta A, Montagna D, Maccario R, Villa R, Daidone MG, Zuffardi O, Locatelli F. Human Bone Marrow-Derived Mesenchymal Stem Cells Do Not Undergo Transformation after Long-term In vitro Culture and Do Not Exhibit Telomere Maintenance Mechanisms. *Cancer Research*. 2007;67:9142-9149.
11. Bian Z-Y, Fan Q-M, Li G, Xu W-T, Tang T-T. Human mesenchymal stem cells promote growth of osteosarcoma: Involvement of interleukin-6 in the interaction between human mesenchymal stem cells and Saos-2. *Cancer Science*. 2010;101:2554-2560.
12. Bonab M, Alimoghaddam K, Talebian F, Ghaffari S, Ghavamzadeh A, Nikbin B. Aging of mesenchymal stem cell in vitro. *BMC Cell Biology*. 2006;7:14-14.
13. Brune JC, Tormin A, Johansson MC, Rissler P, Brosjö O, Löfvenberg R, von Steyern FV, Mertens F, Rydholm A, Scheduling S. Mesenchymal stromal cells from primary osteosarcoma are non-malignant and strikingly similar to their bone marrow counterparts. *International Journal of Cancer*. 2011;129:319-330.
14. Bruno S, Collino F, Iavello A, Camussi G. Effects of Mesenchymal Stromal Cell-Derived Extracellular Vesicles on Tumor Growth. *Frontiers in Immunology*. 2014;5:382.
15. Burns JS, Abdallah BM, Schroder HD, Kassem M. The histopathology of a human mesenchymal stem cell experimental tumor model: support for an hMSC origin for Ewing's sarcoma? *Histol Histopathol*. 2008;23:1229-1240.
16. Caplan AI. Mesenchymal stem cells. *Journal of Orthopaedic Research*. 1991;9:641-650.

17. Castellero-Trejo Y, Eliazar S, Xiang L, Richardson JA, Ilaria RL. Expression of the EWS/FLI-1 Oncogene in Murine Primary Bone-Derived Cells Results in EWS/FLI-1-Dependent, Ewing Sarcoma-Like Tumors. *Cancer Research*. 2005;65:8698-8705.
18. Centeno CJ, Schultz JR, Cheever M, Robinson B, Freeman M, Marasco W. Safety and Complications Reporting on the Re-implantation of Culture-Expanded Mesenchymal Stem Cells using Autologous Platelet Lysate Technique. *Current Stem Cell Research & Therapy*. 2010;5:81-93.
19. Chanda D, Kumar S, Ponnazhagan S. Therapeutic potential of adult bone marrow-derived mesenchymal stem cells in diseases of the skeleton. *Journal of Cellular Biochemistry*. 2010;111:249-257.
20. Choi HJ, Kim JM, Kwon E, Che J-H, Lee J-I, Cho S-R, Kang SK, Ra JC, Kang B-C. Establishment of Efficacy and Safety Assessment of Human Adipose Tissue-Derived Mesenchymal Stem Cells (hATMSCs) in a Nude Rat Femoral Segmental Defect Model. *J Korean Med Sci*. 2011;26:482-491.
21. Coathup MJ, Kalia P, Konan S, Mirza K, Blunn GW. A comparison of allogeneic and autologous mesenchymal stromal cells and osteoprogenitor cells in augmenting bone formation around massive bone tumor prostheses. *Journal of Biomedical Materials Research Part A*. 2013;101A:2210-2218.
22. Coomer A, Farese J, Milner R, Liptak J, Bacon N, Lurie D. Radiation therapy for canine appendicular osteosarcoma. *Vet Comp Oncol*. 2009;7:15-27.
23. Corcoran KE, Trzaska KA, Fernandes H, Bryan M, Taborga M, Srinivas V, Packman K, Patel PS, Rameshwar P. Mesenchymal Stem Cells in Early Entry of Breast Cancer into Bone Marrow. *PLoS ONE*. 2008;3:e2563-e2563.
24. Cui L, Liu B, Liu G, Zhang W, Cen L, Sun J, Yin S, Liu W, Cao Y. Repair of cranial bone defects with adipose derived stem cells and coral scaffold in a canine model. *Biomaterials*. 2007;28:5477-5486.
25. Cuomo A, Virk M, Petrigliano F, Morgan E, Lieberman J. Mesenchymal Stem Cell Concentration and Bone Repair: Potential Pitfalls from Bench to Bedside. *J Bone Joint Surg Am*. 2009;91-A:1073.
26. Dalerba P, Cho RW, Clarke MF. Cancer Stem Cells: Models and Concepts. *Annual Review of Medicine*. 2007;58:267-284.
27. De Kok IJ, Drapeau SJ, Young R, Cooper LF. Evaluation of mesenchymal stem cells following implantation in alveolar sockets: a canine safety study. *The International journal of oral & maxillofacial implants*. 2005;20:511-518.
28. Di Bella C, Aldini NN, Lucarelli E, Dozza B, Frisoni T, Martini L, Fini M, Donati D. Osteogenic Protein-1 Associated with Mesenchymal Stem Cells Promote Bone Allograft Integration. *Tissue Engineering Part A*. 2010;16:2967-2976.
29. Dominici M, Le Blanc K, Mueller I, Slaper-Cortenbach I, Marini F, Krause D, Deans R, Keating A, Prockop D, Horwitz E. Minimal criteria for defining multipotent mesenchymal stromal cells. The International Society for Cellular Therapy position statement. *Cytotherapy*. 2006;8:315-317.
30. Dupont KM, Sharma K, Stevens HY, Boerckel JD, García AJ, Guldberg RE. Human stem cell delivery for treatment of large segmental bone defects. *Proceedings of the National Academy of Sciences of the United States of America*. 2010;107:3305-3310.
31. Fong ELS, Chan CK, Goodman SB. Stem cell homing in musculoskeletal injury. *Biomaterials*. 2011;32:395-409.
32. Friedenstein AJ, Petrakova KV, Kurolesova AI, Frolova GP. Heterotopic of bone marrow. Analysis of precursor cells for osteogenic and hematopoietic tissues. *Transplantation*. 1968;6:230-247.

33. Frohlich M, Grayson WL, Marolt D, Gimble JM, Kregar-Velikonja N, Vunjak-Novakovic G. Bone grafts engineered from human adipose-derived stem cells in perfusion bioreactor culture. *Tissue engineering. Part A*. 2010;16:179-189.
34. Gao Z, Zhang L, Hu J, Sun Y. Mesenchymal stem cells: a potential targeted-delivery vehicle for anti-cancer drug, loaded nanoparticles. *Nanomedicine: Nanotechnology, Biology and Medicine*.
35. Garcia S, Martín MC, de la Fuente R, Cigudosa JC, Garcia-Castro J, Bernad A. Pitfalls in spontaneous in vitro transformation of human mesenchymal stem cells. *Experimental Cell Research*. 2010;316:1648-1650.
36. Giannoni P, Mastrogiacomo M, Alini M, Pearce SG, Corsi A, Santolini F, Muraglia A, Bianco P, Cancedda R. Regeneration of large bone defects in sheep using bone marrow stromal cells. *Journal of Tissue Engineering and Regenerative Medicine*. 2008;2:253-262.
37. Gibbs C, Levings P, Ghivizzani S. Evidence for the osteosarcoma stem cell. *Current Orthopaedic Practice*. 2011;22:322-326.
38. Gibbs CP, Kukekov VG, Reith JD, Tchigrinova O, Suslov ON, Scott EW, Ghivizzani SC, Ignatova TN, Steindler DA. Stem-Like Cells in Bone Sarcomas: Implications for Tumorigenesis. *Neoplasia*. 2005;7:967-976.
39. Gimble JM, Katz AJ, Bunnell BA. Adipose-Derived Stem Cells for Regenerative Medicine. *Circulation Research*. 2007;100:1249-1260.
40. Gou S, Wang C, Liu T, Wu H, Xiong J, Zhou F, Zhao G. Spontaneous Differentiation of Murine Bone Marrow-Derived Mesenchymal Stem Cells into Adipocytes without Malignant Transformation after Long-Term Culture. *Cells Tissues Organs*. 2010;191:185-192.
41. Goujon E. Recherches experimentales sur les proprietes physiologiques de la moelle des os. *Journal of Anatomy and Physiology*. 1869;6:399-412.
42. Granero-Moltó F, Weis JA, Miga MI, Landis B, Myers TJ, O'Rear L, Longobardi L, Jansen ED, Mortlock DP, Spagnoli A. Regenerative Effects of Transplanted Mesenchymal Stem Cells in Fracture Healing. *Stem cells (Dayton, Ohio)*. 2009;27:1887-1898.
43. Grassi Rici RE, Alcântara D, Fratini P, Wenceslau CV, Ambrósio CE, Miglino MA, Maria DA. Mesenchymal stem cells with rhBMP-2 inhibits the growth of canine osteosarcoma cells. *BMC Veterinary Research*. 2012;8:17-17.
44. Grayson WL, Frohlich M, Yeager K, Bhumiratana S, Chan ME, Cannizzaro C, Wan LQ, Liu XS, Guo XE, Vunjak-Novakovic G. Regenerative Medicine Special Feature: Engineering anatomically shaped human bone grafts. *Proceedings of the National Academy of Sciences*. 2009;107:3299-3304.
45. Kalia P, Bhalla A, Coathup MJ, Miller J, Goodship AE, Blunn GW. Augmentation of massive implant fixation using mesenchymal stem cells. *Journal of Bone & Joint Surgery, British Volume*. 2006;88-B:392.
46. Karnoub AE, Dash AB, Vo AP, Sullivan A, Brooks MW, Bell GW, Richardson AL, Polyak K, Tubo R, Weinberg RA. Mesenchymal stem cells within tumour stroma promote breast cancer metastasis. *Nature*. 2007;449:557-563.
47. Keibl C, Fügl A, Zanoni G, Tangl S, Wolbank S, Redl H, van Griensven M. Human adipose derived stem cells reduce callus volume upon BMP-2 administration in bone regeneration. *Injury*. 2011;42:814-820.
48. Khakoo AY, Pati S, Anderson SA, Reid W, Elshal MF, Rovira II, Nguyen AT, Malide D, Combs CA, Hall G, Zhang J, Raffeld M, Rogers TB, Stetler-Stevenson W, Frank JA, Reitz M, Finkel T. Human mesenchymal stem cells exert potent antitumorigenic effects in a model of Kaposi's sarcoma. *The Journal of Experimental Medicine*. 2006;203:1235-1247.

49. Kim HJ, Kim UJ, Vunjak-Novakovic G, Min BH, Kaplan DL. Influence of macroporous protein scaffolds on bone tissue engineering from bone marrow stem cells. *Biomaterials*. 2005;26:4442-4452.
50. Ko EK, Jeong SI, Rim NG, Lee YM, Shin H, Lee B-K. In Vitro Osteogenic Differentiation of Human Mesenchymal Stem Cells and In Vivo Bone Formation in Composite Nanofiber Meshes. *Tissue Engineering Part A*. 2008;14:2105-2119.
51. Lee S-W, Padmanabhan P, Ray P, Gambhir SS, Doyle T, Contag C, Goodman SB, Biswal S. Stem cell-mediated accelerated bone healing observed with in vivo molecular and small animal imaging technologies in a model of skeletal injury. *Journal of Orthopaedic Research*. 2009;27:295-302.
52. Li N, Yang R, Zhang W, Dorfman H, Rao P, Gorlick R. Genetically transforming human mesenchymal stem cells to sarcomas. *Cancer*. 2009;115:4795-4806.
53. Liu S, Ginestier C, Ou SJ, Clouthier SG, Patel SH, Monville F, Korkaya H, Heath A, Dutcher J, Kleer CG, Jung Y, Dontu G, Taichman R, Wicha MS. Breast Cancer Stem Cells Are Regulated by Mesenchymal Stem Cells through Cytokine Networks. *Cancer Research*. 2011;71:614-624.
54. Liu X, Li X, Fan Y, Zhang G, Li D, Dong W, Sha Z, Yu X, Feng Q, Cui F, Watari F. Repairing goat tibia segmental bone defect using scaffold cultured with mesenchymal stem cells. *Journal of Biomedical Materials Research Part B: Applied Biomaterials*. 2010;94B:44-52.
55. Maijenburg MW, van der Schoot CE, Voermans C. Mesenchymal Stromal Cell Migration: Possibilities to Improve Cellular Therapy. *Stem Cells and Development*. 2011.
56. Mirabello L, Troisi RJ, Savage SA. International osteosarcoma incidence patterns in children and adolescents, middle ages, and elderly persons. *International journal of cancer. Journal international du cancer*. 2009;125:229-234.
57. Miura M, Miura Y, Padilla-Nash HM, Molinolo AA, Fu B, Patel V, Seo BM, Sonoyama W, Zheng JJ, Baker CC, Chen W, Ried T, Shi S. Accumulated chromosomal instability in murine bone marrow mesenchymal stem cells leads to malignant transformation. *Stem Cells*. 2006;24:1095-1103.
58. Miyagawa Y, Okita H, Nakaijima H, Horiuchi Y, Sato B, Taguchi T, Toyoda M, Katagiri YU, Fujimoto J, Hata J-i, Umezawa A, Kiyokawa N. Inducible Expression of Chimeric EWS/ETS Proteins Confers Ewing's Family Tumor-Like Phenotypes to Human Mesenchymal Progenitor Cells. *Molecular and Cellular Biology*. 2008;28:2125-2137.
59. Mohseny AB, Szuhai K, Romeo S, Buddingh EP, Briaire-de Bruijn I, de Jong D, van Pel M, Cleton-Jansen A-M, Hogendoorn PCW. Osteosarcoma originates from mesenchymal stem cells in consequence of aneuploidization and genomic loss of Cdkn2. *The Journal of Pathology*. 2009;219:294-305.
60. Morozov A, Downey RJ, Healey J, Moreira AL, Lou E, Franceschino A, Dogan Y, Leung R, Edgar M, LaQuaglia M, Maki RG, Moore MAS. Benign Mesenchymal Stromal Cells in Human Sarcomas. *Clinical Cancer Research*. 2010;16:5630-5640.
61. Muehlberg FL, Song Y-H, Krohn A, Pinilla SP, Droll LH, Leng X, Seidensticker M, Ricke J, Altman AM, Devarajan E, Liu W, Arlinghaus RB, Alt EU. Tissue-resident stem cells promote breast cancer growth and metastasis. *Carcinogenesis*. 2009;30:589-597.
62. Mueller F, Fuchs B, Kaser-Hotz B. Comparative Biology of Human and Canine Osteosarcoma. *Anticancer Research*. 2007;27:155-164.
63. Perrot P, Rousseau J, Bouffaut A-L, Rédini F, Cassagnau E, Deschaseaux F, Heymann M-F, Heymann D, Duteille F, Trichet V, Gouin F. Safety Concern between Autologous Fat Graft, Mesenchymal Stem Cell and Osteosarcoma Recurrence. *PLoS ONE*. 2010;5:e10999-e10999.
64. Picci P. Osteosarcoma (Osteogenic sarcoma). *Orphanet Journal of Rare Diseases*. 2007;2:6.

65. Picci P, Sieberova G, Alberghini M, Balladelli A, Vanel D, Hogendoorn PCW, Mercuri M. Late sarcoma development after curettage and bone grafting of benign bone tumors. *European Journal of Radiology*. 2011;77:19-25.
66. Pittenger MF. Multilineage Potential of Adult Human Mesenchymal Stem Cells. *Science*. 1999;284:143-147.
67. Porter JR, Henson A, Ryan S, Popat KC. Biocompatibility and Mesenchymal Stem Cell Response to Poly(ϵ -Caprolactone) Nanowire Surfaces for Orthopedic Tissue Engineering. *Tissue Engineering Part A*. 2009;15:2547-2559.
68. Ra JC, Shin IS, Kim SH, Kang SK, Kang BC, Lee HY, Kim YJ, Jo JY, Yoon EJ, Choi HJ, Kwon E. Safety of Intravenous Infusion of Human Adipose Tissue-Derived Mesenchymal Stem Cells in Animals and Humans. *Stem Cells and Development*. 2011.
69. Ren Y-X, Finckenstein FG, Abdueva DA, Shahbazian V, Chung B, Weinberg KI, Triche TJ, Shimada H, Anderson MJ. Mouse Mesenchymal Stem Cells Expressing PAX-FKHR Form Alveolar Rhabdomyosarcomas by Cooperating with Secondary Mutations. *Cancer Research*. 2008;68:6587-6597.
70. Riggi N, Suvà M-L, Suvà D, Cironi L, Provero P, Tercier S, Joseph J-M, Stehle J-C, Baumer K, Kindler V, Stamenkovic I. EWS-FLI-1 Expression Triggers a Ewing's Sarcoma Initiation Program in Primary Human Mesenchymal Stem Cells. *Cancer Research*. 2008;68:2176-2185.
71. Rodriguez R, Rubio R, Gutierrez-Aranda I, Melen GJ, Elosua C, García-Castro J, Menendez P. FUS-CHOP Fusion Protein Expression Coupled to p53 Deficiency Induces Liposarcoma in Mouse but Not in Human Adipose-Derived Mesenchymal Stem/Stromal Cells. *Stem Cells*. 2011;29:179-192.
72. Roodhart Jeanine ML, Daenen Laura GM, Stigter Edwin CA, Prins H-J, Gerrits J, Houthuijzen Julia M, Gerritsen Marije G, Schipper Henk S, Backer Marieke JG, van Amersfoort M, Vermaat Joost SP, Moerer P, Ishihara K, Kalkhoven E, Beijnen Jos H, Derksen Patrick WB, Medema Rene H, Martens Anton C, Brenkman Arjan B, Voest Emile E. Mesenchymal Stem Cells Induce Resistance to Chemotherapy through the Release of Platinum-Induced Fatty Acids. *Cancer Cell*. 2011;20:370-383.
73. Rosland GV, Svendsen A, Torsvik A, Sobala E, McCormack E, Immervoll H, Mysliwicz J, Tonn JC, Goldbrunner R, Lonning PE, Bjerkvig R, Schichor C. Long-term cultures of bone marrow-derived human mesenchymal stem cells frequently undergo spontaneous malignant transformation. *Cancer Res*. 2009;69:5331-5339.
74. Rubio D, Garcia-Castro J, Martín MC, de la Fuente R, Cigudosa JC, Lloyd AC, Bernad A. Spontaneous human adult stem cell transformation. *Cancer research*. 2005;65:3035-3035.
75. Rubio R, García-Castro J, Gutiérrez-Aranda I, Paramio J, Santos M, Catalina P, Leone PE, Menendez P, Rodríguez R. Deficiency in p53 but not Retinoblastoma Induces the Transformation of Mesenchymal Stem Cells In vitro and Initiates Leiomyosarcoma In vivo. *Cancer Research*. 2010;70:4185-4194.
76. Savage SA, Mirabello L. Using epidemiology and genomics to understand osteosarcoma etiology. *Sarcoma*. 2011;2011:548151.
77. Shimizu T, Ishikawa T, Sugihara E, Kuninaka S, Miyamoto T, Mabuchi Y, Matsuzaki Y, Tsunoda T, Miya F, Morioka H, Nakayama R, Kobayashi E, Toyama Y, Kawai A, Ichikawa H, Hasegawa T, Okada S, Ito T, Ikeda Y, Suda T, Saya H. c-MYC overexpression with loss of Ink4a/Arf transforms bone marrow stromal cells into osteosarcoma accompanied by loss of adipogenesis. *Oncogene*. 2010;29:5687-5699.
78. Siclari VA, Qin L. Targeting the osteosarcoma cancer stem cell. *Journal of Orthopaedic Surgery and Research*. 2010;5:78-78.

79. Suvà M-L, Riggi N, Stehle J-C, Baumer K, Tercier S, Joseph J-M, Suvà D, Clément V, Provero P, Cironi L, Osterheld M-C, Guillou L, Stamenkovic I. Identification of Cancer Stem Cells in Ewing's Sarcoma. *Cancer Research*. 2009;69:1776-1781.
80. Ta HT, Dass CR, Choong PFM, Dunstan DE. Osteosarcoma treatment: state of the art. *Cancer and Metastasis Reviews*. 2009;28:247-263.
81. Tang N, Song W-X, Luo J, Haydon RC, He T-C. Osteosarcoma Development and Stem Cell Differentiation. *Clinical Orthopaedics and Related Research*. 2008;466:2114-2130.
82. Tasso R, Augello A, Carida' M, Postiglione F, Tibiletti MG, Bernasconi B, Astigiano S, Fais F, Truini M, Cancedda R, Pennesi G. Development of sarcomas in mice implanted with mesenchymal stem cells seeded onto bioscaffolds. *Carcinogenesis*. 2009;30:150-157.
83. Tirino V, Desiderio V, Paino F, De Rosa A, Papaccio F, Fazioli F, Pirozzi G, Papaccio G. Human primary bone sarcomas contain CD133+ cancer stem cells displaying high tumorigenicity in vivo. *The FASEB Journal*. 2011;25:2022-2030.
84. Tolar J, Nauta AJ, Osborn MJ, Panoskaltsis Mortari A, McElmurry RT, Bell S, Xia L, Zhou N, Riddle M, Schroeder TM, Westendorf JJ, McIvor RS, Hogendoorn PCW, Szuhai K, Oseth L, Hirsch B, Yant SR, Kay MA, Peister A, Prockop DJ, Fibbe WE, Blazar BR. Sarcoma Derived from Cultured Mesenchymal Stem Cells. *Stem Cells*. 2007;25:371-379.
85. Torsvik A, Røslund GV, Svendsen A, Molven A, Immervoll H, McCormack E, Lønning PE, Primon M, Sobala E, Tonn J-C, Goldbrunner R, Schichor C, Mysliwicz J, Lah TT, Motaln H, Knappskog S, Bjerkvig R. Spontaneous Malignant Transformation of Human Mesenchymal Stem Cells Reflects Cross-Contamination: Putting the Research Field on Track – Letter. *Cancer Research*. 2010;70:6393-6396.
86. Tsukamoto S, Honoki K, Fujii H, Tohma Y, Kido A, Mori T, Tsujiuchi T, Tanaka Y. Mesenchymal stem cells promote tumor engraftment and metastatic colonization in rat osteosarcoma model. *International journal of oncology*. 2012;40:163-169.
87. Wakitani S, Okabe T, Horibe S, Mitsuoka T, Saito M, Koyama T, Nawata M, Tensho K, Kato H, Uematsu K, Kuroda R, Kurosaka M, Yoshiya S, Hattori K, Ohgushi H. Safety of autologous bone marrow-derived mesenchymal stem cell transplantation for cartilage repair in 41 patients with 45 joints followed for up to 11 years and 5 months. *Journal of Tissue Engineering and Regenerative Medicine*. 2011;5:146-150.
88. Wang Y, Huso DL, Harrington J, Kellner J, Jeong DK, Turney J, McNiece IK. Outgrowth of a transformed cell population derived from normal human BM mesenchymal stem cell culture. *Cytotherapy*. 2005;7:509-519.
89. Wilson H, Huelsmeyer M, Chun R, Young KM, Friedrichs K, Argyle DJ. Isolation and characterisation of cancer stem cells from canine osteosarcoma. *The Veterinary Journal*. 2008;175:69-75.
90. Withrow SJ, Powers BE, Straw RC, Wilkins RM. Comparative aspects of osteosarcoma. Dog versus man. *Clin Orthop Relat Res*. 1991:159-168.
91. Withrow SJ, Vail D. *Withrow and MacEwen's Small Animal Clinical Oncology*: Elsevier Health Sciences; 2007.
92. Withrow SJ, Wilkins RM. Cross talk from pets to people: translational osteosarcoma treatments. *ILAR journal / National Research Council, Institute of Laboratory Animal Resources*. 2010;51:208-213.
93. Xu W-t, Bian Z-y, Fan Q-m, Li G, Tang T-t. Human mesenchymal stem cells (hMSCs) target osteosarcoma and promote its growth and pulmonary metastasis. *Cancer Letters*. 2009;281:32-41.
94. Yarmish G, Klein MJ, Landa J, Lefkowitz RA, Hwang S. Imaging Characteristics of Primary Osteosarcoma: Nonconventional Subtypes. *RadioGraphics*. 2010;30:1653-1672.

95. Yuan J, Zhang WJ, Liu G, Wei M, Qi ZL, Liu W, Cui L, Cao YL. Repair of Canine Mandibular Bone Defects with Bone Marrow Stromal Cells and Coral. *Tissue Engineering Part A*. 2010;16:1385-1394.
96. Zhou Z, Lafleur EA, Koshkina NV, Worth LL, Lester MS, Kleinerman ES. Interleukin-12 Up-Regulates Fas Expression in Human Osteosarcoma and Ewing's Sarcoma Cells by Enhancing Its Promoter Activity. *Molecular Cancer Research*. 2005;3:685-692.
97. Zhu L, Liu W, Cui L, Cao Y. Tissue-engineered bone repair of goat-femur defects with osteogenically induced bone marrow stromal cells. *Tissue Engineering*. 2006;12:423-433.
98. Zuk P, Chou Y-F, Mussano F, Benhaim P, Wu BM. Adipose-derived Stem cells and BMP2: Part 2. BMP2 may not influence the osteogenic fate of human adipose-derived stem cells. *Connective Tissue Research*. 2011;52:119-132.

Chapter 3: Development of a Luciferase expressing OSA Cell Line, In Vivo Model Development and Validation of MSC-Tumor Interaction

3.1 Introduction

Animal models have often been used to study disease progression and characteristics [2, 14, 19, 32, 35]. In many instances, athymic murine models are preferred because human tissues can be utilized without activation of the immune response. However, syngeneic models of disease can be more accurate with respect to immune system activation, cellular interaction, and observation of disease progression. This accuracy can translate to more clinically-relevant results.

In order to study the behavior of mesenchymal stromal cells in a clinically-relevant minimal residual disease setting, a traceable [11], orthotopic [17] model of murine osteosarcoma needed to be developed. Building on the prior work of Sottnik [28], two new models of minimal residual OS disease were developed- a pulmonary minimal residual disease model and a surgical site minimal residual disease model. Below, the development and validation of these models are described in detail. These models were utilized throughout the experiments to address the hypotheses and specific aims previously described.

3.2 Preliminary Experiment 1 – Development of Cell Line and Validation of Primary Tumor Establishment Methods

3.2.1 Introduction

Dunn and Andervont first discovered the Dunn osteogenic sarcoma line in a wild mouse colony at the National Cancer Institute in 1963 [13]. The line was passaged through the lungs 8 times and an LM8 line was established [3]. Further work with this line has been completed, including transfection with the luciferase gene here at the Flint Animal Cancer Center [28]. This luc-transfected DLM8 cell line did not maintain stable luciferase transfection and therefore we

developed a new DLM8-origin cell line with consistent luciferase expression, rapid primary tumor growth, and spontaneous metastatic disease.

3.2.2 Materials and Methods

3.2.2.1 Cell Line

Murine DLM8 osteosarcoma cells, originally developed from wild mice [13], were obtained from the Animal Cancer Center at Colorado State University (Fort Collins, CO, USA) and cultured in MEM supplemented with 10% FBS, MEM vitamin solution, non-essential amino acids, sodium pyruvate solution, and antibiotic-antimycotic (Appendix A) and incubated in a humidified atmosphere at 37°C with 5% CO₂. Cells were passaged after being washed with HBSS and detached with 0.25% trypsin supplemented with 2.21 mM EDTA. Cells were treated with Baytril (25µg/mL) for a period of 8 days in complete media to ensure no mycoplasma were present when cryopreserved cells were cultured.

3.2.2.2 Luciferase Transfection

Transfection of the parent DLM8 line provided by Dr. Douglas Thamm at the Flint Animal Cancer Center, Colorado State University was previously achieved using electroporation [28], but there were issues with long term stability of expression, and it was concluded that a new method may enhance the permanence of the transfection. Therefore, both the luciferase reporter vector (Promega) and the neo mammalian expression vector (Promega) were inserted into the DLM8 cells using a dendrimer-mediated cell transfection method (Appendix A). DLM8 cells were plated using a concentration of 1×10^5 cells/mL on a 60 mm dish. Vectors were added to the samples using Superfect Transfection Reagent (Qiagen) and the cells were allowed to incubate for 3 hours in a humidified atmosphere at 37°C with 5% CO₂. Cells were washed, given fresh media, and placed into the incubation chamber for 48 hours. After this time point, G-418 was added to the media and cells were cultured until colonies appeared.

3.2.2.3 In Vitro Cell Clone Selection

To select cells with the brightest and most consistent bioluminescent expression, a two-fold serial dilution assay was conducted on the newly-transfected cells. Assays were performed in two 96-well microtiter plates (Corning, Manassas, VA), each well in the first column receiving 100 μ l of either 2×10^5 or 5×10^5 DLM8 cells in complete media. Serial dilutions of 1:2 were completed throughout the length of the plate. In conjunction with this, cells were also seeded in 60 mm dishes and colonies with strong luciferase expression levels were selected using 0.25% trypsin supplemented with 2.21 mM EDTA and plated in new dishes to allow for further cell propagation. These two methods were continued until two highly expressing lines were chosen, one from each selection type.

3.2.2.4 Animals

All animal studies were performed with approval of the Institutional Animal Care and Use Committee. Female 8-10 week old C3H mice were obtained from Charles River and housed under standard conditions. Tumor inoculation sites were prepared by shaving the fur, followed by cleaning the site with chlorhexidine and 70% alcohol. Pain control was achieved through an intraperitoneal injection of 0.1 mg/kg buprenorphine-HCl before injection of tumor cells and as needed in consultation with a veterinarian.

3.2.2.5 Bioluminescent Imaging

Bioluminescent (BL) imaging (In Vivo Imaging System 100 (IVIS), Perkin Elmer, Waltham, USA) was utilized to confirm cells carried the luciferase gene and to track tumor development *in vivo*. To activate the luc gene, D-luciferin was reconstituted in PBS (30 mg/mL) and 50 – 100 μ L was utilized for each culture dish. Cells were exposed for five minutes before being imaged (Appendix A). Mice were injected intraperitoneally (IP) with 100 μ L luciferin (30 mg/mL) and remained ambulatory for five minutes before being anesthetized with isoflurane and imaged (Appendix A). Mice recovered under monitoring in their cages post-imaging.

3.2.2.6 Radiographic Tumor Assessment

In order to track tumor growth, in addition to bioluminescent imaging, radiographs were also collected once a week. Intraoral radiography (Heliodont^{PLUS}, Sirona, Bensheim, Germany) was tried digitally as well as on film at a setting of 0.10 KVP, although there was no oral aspect and the machine was positioned over the distal aspect of the mouse in order to image pelvis and both distal limbs. Conventional radiography and computerized radiography using settings of 75, 55, and 50 kV at 1 mAs, 2.8 mAs and 2.0 mAs was tested.

3.2.2.7 *In Vivo* Cell Selection and Primary Tumor Establishment

Luciferase expression stability of the newly transfected DLM8-Luc cells *in vivo* was tested by injecting three different DLM8-Luc cell clone lines into either the femur or mammary pads. Cells were washed with HBSS and detached with 0.25% trypsin supplemented with 2.21 mM EDTA. After three rinses, three mice were inoculated using a 22 G needle with 1×10^6 DLM8-Luc cells in 25 μ L of MEM through the greater trochanteric notch and into the mid-femur. One mouse was injected with 1×10^6 DLM8-Luc cells in 50 μ L of MEM into the left mammary pad along with 1×10^6 DLM8-Luc cells in 50 μ L of MEM into the right mammary pad. Bioluminescent imaging was completed on all mice and radiographs of the femur were followed for one month to ascertain if bioluminescence would persist.

In order to optimize location for orthotopic tumor formation, three mice were inoculated with one of two different DLM8-Luc cell clones in one of three regions – through the greater trochanteric notch into the mid-femur (clone 1, n=1), the distal femur (clone 1, n=1), or the tibial crest (clone 2; n=1). Each mouse received 1×10^6 DLM8-Luc cells in 25 μ L of media. Mice were imaged and followed with BLI and/or radiographs for up to 2.5 weeks before being sacrificed.

Selection of the highest BLI expressing DLM8-Luc cell clone between two clones was completed through inoculation of six mice, three with clone 1 and three with clone 2, all with $1 \times$

10⁵ cells in 50µL of MEM into the right proximal tibia via the tibial plateau (**Figure 3.2– 1**).

Bioluminescent images were obtained every 2-3 days and radiographs to supplement results were obtained weekly. At one week, two weeks, and three weeks, one mouse from each cell clone was euthanized by deep isoflurane anesthesia, followed by a cervical dislocation.

3.2.3 Results

3.2.3.1 Transfection and *In Vitro* Cell Clone Selection

Multiple luciferase transfected cell colonies appeared and were selected through BLI. As propagation of the cell lines continued, some clones only had moderate BLI expression and growth and were discarded, while other clones continued to have high levels of luciferase expression. Two DLM8-Luc cell clones were selected for further analysis – one from the serial dilution and one from the plate culture. Both clones quickly propagated in culture and maintained high luc BLI expression over time. The clones were cultured for further use *in vivo* in complete growth media.

3.2.3.2 *In Vivo* Cell Selection and Primary Tumor Establishment

Tumor inoculation into the femoral greater trochanteric notch resulted in no immediate evidence of luc-expression or tumor growth by either BLI or radiographs at one month post-injection. Immediately after injection into the mammary pads, however, both clones expressed luciferase. However, by three and a half weeks, only one cell clone had detectable luc expression in the mammary fat pad. At sacrifice, tumor tissue was present in the right ovary and both mammary pads.

Tumor inoculation into the mid-femur, resulted in no immediate luc expression within the femur but one week post injection the animal was euthanized due to extensive macroscopic metastatic disease in liver, ovarian, and lung tissue. No gross evidence of primary tumor in the mid-femur was seen at sacrifice. Macroscopic metastatic disease at the time of sacrifice was not

bioluminescent. Tumor inoculation into the proximal tibia resulted in consistent expression of luciferase at the inoculation site (**Figure 3.2– 2**). At euthanasia, this animal had luciferase expression evident in the tibia, the liver, and the lungs. Tumor was also evident grossly within the tibia and soft tissue surrounding the tibia. Radiographic imaging was inconsistent in showing changes consistent with tumor formation despite clear gross evidence of orthotopic tumor formation at sacrifice.

Of the six mice inoculated into the proximal tibia, mice euthanized one week post-injection did not express luciferase or have any evidence of tumor growth. Two weeks post-injection, both mice with clone 2 had luciferase evidence of tumor cells at the primary site and one of the two mice injected with clone 1 had BLI expression at the primary site. In the mice inoculated with clone 2, *ex vivo* lung tissue displayed BLI evidence of tumor cells, possibly indicative of metastatic disease. There was no other evidence of metastatic disease at that time point. At three weeks post-injection, both remaining mice had BL evidence of tumor cells at the primary site. At euthanasia, lung tissue from the mouse inoculated with clone 2 had evidence of tumor cells and a sample of the tissue was collected to harvest the tumor cells.

3.2.4 Conclusions and Discussion

Initially, the plan was to create a primary orthotopic tumor in the mid-femur; however, we were unsuccessful at creating a femur model. The femoral canal presented little resistance after the needle was inserted, cells were injected but had no way to attach and establish a tumor in the site. The conclusion was that the femoral injection acted like an intravenous injection –cells were injected into the marrow space and immediately taken up by the blood stream and dispersed throughout the body. The widespread metastatic disease seen at one week supported the conclusion that in this pilot, all the cells immediately went systemic. In contrast, the tibial injection sites provided consistent tumor formation with the ability to detect luciferase

and primary tumor formation. Metastatic disease was noted as expected with luciferase expression.

Radiographic analysis of the tumor was an inconsistent method to monitor local tumor progression, presumably due to the small size and limited spatial resolution of the radiographic equipment utilized. However, previous work [9] has shown this method to be an alternative to luciferase or fluorescent protein tracking modalities. *In vivo* microCT would be a more sensitive means to detect the bony changes associated with primary tumor progression.

Based on the results of this experiment, the DLM8-Luc clone 2 line was chosen to use for future experiments. These data also suggested that pulmonary metastatic disease remained at a microscopic (clinically undetectable) level for approximately 3 weeks when DLM8 cells were injected into the proximal tibia. The presence of luciferase-expressing tumor cells in the lungs suggested that an M1 clone could be harvested that might be more likely to preferentially metastasize to the pulmonary tissue and therefore lung tissue containing the luciferase-expressing metastatic nodules was collected at the conclusion of the experiment.

FIGURES



Figure 3.2 – 1: Injection of DLM8-Luc-M1 tumor cells into the proximal tibia of a C3H mouse.

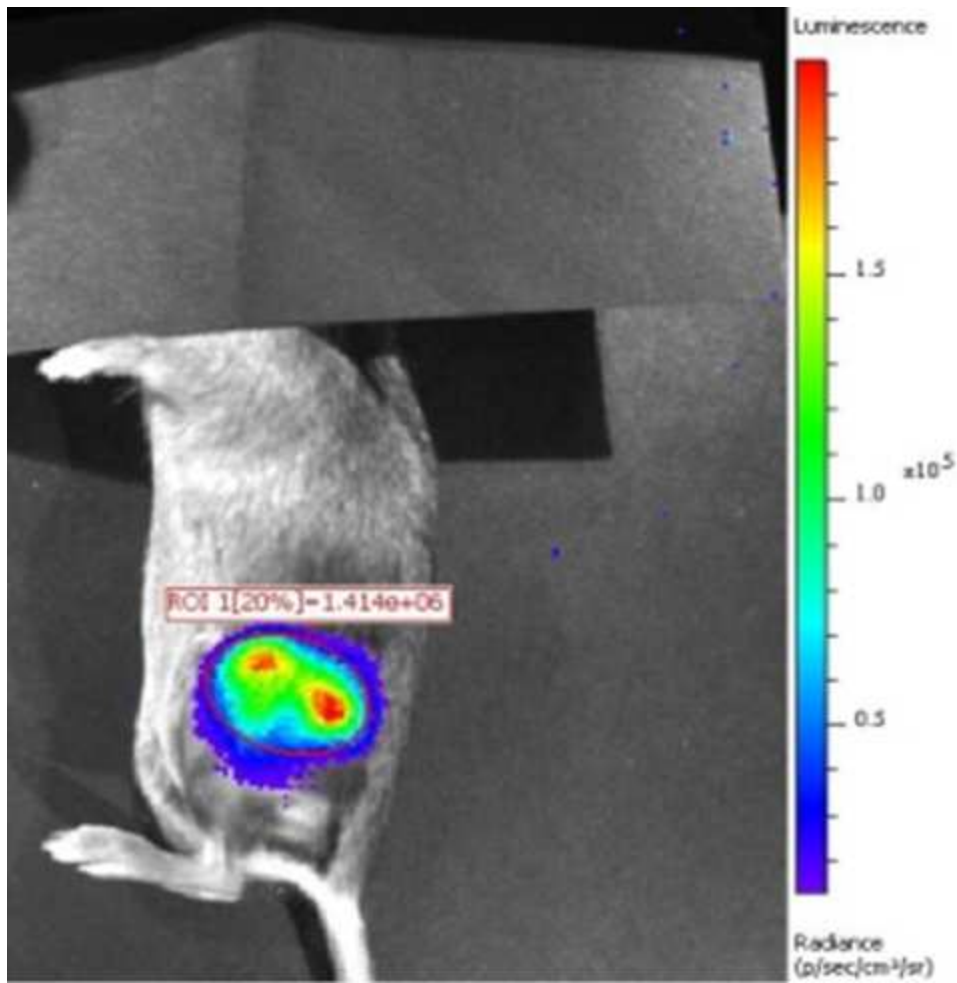


Figure 3.2 – 2: Following injection of tumor cells, formation of the primary tumor was tracked using bioluminescent imaging on an IVIS 100 imaging system.

3.3 Preliminary Experiment 2 –Optimal Cell Line Selection, Validation of Primary Tumor Growth Behavior, and Timing of Amputation to Obtain Minimal Residual Pulmonary Disease

3.3.1 Introduction

Animal models have often been used to study disease progression and characteristics [2, 14, 19, 32, 35]. In many instances, athymic mouse models are considered ideal because human cell lines can be utilized without rejection. However, syngeneic models of disease may be a more accurate representation of the clinical scenario and therefore provide more accurate data from which to translate to human or pet populations.

Our next goal was to optimize the metastatic behavior of the DLM8-Luc cell clone selected in the previous pilot study.

3.3.2 Materials and Methods

3.3.2.1 Cell Line

Tumor cells from the lung tissue of the mouse described previously were collected and a Fiddler selection was performed to select cells for the remaining experiments. (Appendix A). Lung tissue was minced and rinsed three times with HBSS. It was exposed to collagenase and Elastase (Worthington Biochemicals) for 2 hours and then filtered with a 70 μm mesh. The resulting complex was centrifuged, washed, and resuspended in media before being plated. Cells were cultured for 48 hours before the media was changed. Cells were cultured in media and detached as described in section 3.2.2.1. Cells selected were named “DLM8-Luc-M1”.

A second Fiddler selection, with the same method as described above, was completed on cells obtained from the lungs of a mouse with a primary tumor created from the DLM8-Luc-M1 cell line. As before, cells were cultured in the same manner and once confluent, cells were washed

with HBSS and detached with 0.25% trypsin supplemented with 2.21 mM EDTA. Cells selected from this selection were named “DLM8-Luc-M2”.

Both cell lines were maintained in culture media consisting of MEM supplemented with 10% FBS, MEM vitamin solution, non-essential amino acids, G-418 (700ng/mL concentration), sodium pyruvate solution, and antibiotic-antimycotic for the duration of the study. Cells were passaged at 80-90% confluence.

3.3.2.2 *In Vitro* Cell Clone Selection

To select cells with the brightest and most consistent bioluminescent expression, cells were seeded in 60 mm dishes and 25 mL flasks and colonies with strong expression levels were selected using 0.25% trypsin supplemented with 2.21 mM EDTA and plated in new dishes or flasks to allow for further cell propagation. Cell colonies were continually selected and propagated until clones with luc expression and fast propagation were consistent and sustainable. These methods were applied to both the DLM8-Luc-M1 and DLM8-Luc-M2 cell lines. Cells from both lines were cryopreserved for future studies.

3.3.2.3 Animals

All animal studies were performed with approval of the Institutional Animal Care and Use Committee. Female 8-10 week old C3H mice were obtained from Charles River and housed under standard conditions. Animals were prepared for injection as described in section 3.2.2.4. Mice were euthanized according to the scoring assessment, upon the advice of a veterinarian, or at an end-point of 24 (DLM8-Luc-M1 compared to DLM8-Luc-M2 experiment), 45, 52 or 58 (DLM8-Luc-M1 compared to DLM8-Luc experiment) days post-tumor inoculation. Two mice inoculated with DLM8-Luc-M2 cells with lung metastasis evidence by BLI were sacrificed for lung metastatic cell collection at day 7 or day 13 post tumor inoculation. Two mice inoculated

with DLM8-Luc-M2 cells were euthanized at day 15 post tumor inoculation but no tissues were collected.

3.3.2.4 Primary Tumor Establishment

Osteosarcoma cells were washed with HBSS and detached with 0.25% trypsin supplemented with 2.21 mM EDTA. After three rinses, 1×10^6 cells from either the DLM8-Luc clone (n=6) or the DLM8-Luc-M1 clone (n=6) in 25 μ L of MEM were injected as described in section 3.2.2.7.

Injections comparing the DLM8-Luc to DLM8-Luc-M1 cell lines took place over a three week period with 2 mice from each group injected each week to assess timing of tumor development. To evaluate the ability of the DLM8-Luc-M1 and DLM8-Luc-M2 cell lines to form primary and metastatic pulmonary tumors, 1×10^6 cells in 25 μ L of MEM were injected into the proximal tibias of 8-10 week old C3H female mice (n=4 per cell line). Mice were assessed for tumor establishment and growth in the proximal tibia using bioluminescent imaging and radiographs.

3.3.2.5 Surgical Procedures

Coxo-femoral amputations were completed at time points of 14, 21, and 28 days after tumor cell exposure for both of the DLM8-Luc and DLM8-Luc-M1 cell lines and monitored for metastatic disease progression in order to determine the optimal time line for amputation to ensure micro-metastatic pulmonary disease at the time of amputation. A second experiment was performed comparing the DLM8-Luc-M1 and DLM8-Luc-M2 cell lines in which coxo-femoral amputations were completed at 14 days in mice receiving the DLM8-Luc-M1 to compare the metastatic progression between the two cell lines. Amputation was performed using an elliptical incision around the upper thigh; muscles were dissected to the coxofemoral joint. Major vessels were cauterized using electrocautery. The coxofemoral joint was disarticulated and the tumor bearing limb was removed. A splash block of 2% Lidocaine HCL (Hospira, Inc, Lake Forest, IL) was applied to the surgical site prior to closure. The surgical site was closed with 5-0 Biosyn suture (Covidien, Mansfield, MA) in two layers and surgical wound clips (ez clips, Stoelting, Wood

Dale, IL) were used on top of skin sutures to protect the wound. Mice were monitored during recovery in a heated cage. Mice were given buprenorphine every 8 hours for the first 72 hours following surgery. Mice were imaged every 3 days and scored for pain and function using a scoring assessment for post-operative limb surgery (Appendix B) to track pulmonary metastasis.

3.3.2.6 Bioluminescent Imaging

Bioluminescent (BL) imaging (In Vivo Imaging System 100 (IVIS), Perkin Elmer, Waltham, USA) was utilized to confirm cells expressed luciferase and to track tumor development *in vivo*. Mice were imaged as previously described in section 3.2.2.5.

3.3.2.7 Radiographic Tumor Assessment

In order to track tumor growth, in addition to bioluminescent imaging, radiographs were also collected once a week. Intraoral digital and film radiography (Heliodont^{PLUS}, Sirona, Bensheim, Germany) was tried at a setting of 0.10 KVP, and the machine was positioned over the distal aspect of the mouse in order to image pelvis and both distal limbs. Conventional radiography and computerized radiography using settings of 75, 55, and 50 kV at 1 mAs, 2.8 mAs and 2.0 mAs was tested.

3.3.3 Results

3.3.3.1 *In Vitro* Cell Clone Selection

Colony selection was completed and a new line, “DLM8-Luc-M1” was selected which represented both a high proliferation rate and sustained bioluminescent expression. These cells were injected into a mouse and the resultant lung metastases were harvested. Cells were isolated from tissue and colony selection was completed. A new line, “DLM8-Luc-M2” was selected from colonies with high proliferation rates and sustained bioluminescent expression.

3.3.3.2 In Vivo Modeling

Of the twelve mice inoculated with either the DLM8-Luc or DLM8-Luc-M1 cells, four developed a primary tumor - two inoculated with the DLM8-Luc clone and two with the DLM8-Luc-M1 clone. However, only the mice with the DLM8-Luc-M1 cell line developed lung metastases.

Mice inoculated with DLM8-M2 developed metastasis to ovaries and liver, but no pulmonary metastasis was detectable at the time of euthanasia. The best time-point appeared to be 14 days of primary tumor growth before amputation, followed by 31 days of monitoring for metastasis. Mice inoculated with DLM8-Luc-M2 cells developed metastatic disease within 1 week and had to be euthanized at early time-points based on illness. Mice inoculated with the DLM8-Luc-M1 line all had bioluminescent evidence of lung metastasis at euthanasia. In mice inoculated with DLM8-Luc-M1, the optimal time-point appeared to be 14 days of primary tumor growth before amputation, followed by 31 days of monitoring for metastasis. The DLM8-Luc-M1 cell line was chosen for future experiments.

3.3.4 Conclusions and Discussion

A DLM8-Luc-M1 cell line was established that exhibited reliable primary tumor growth and spontaneous metastasis with stable luciferase expression when injected into the proximal tibia. The DLM8-Luc-M2 cells, when inoculated into the proximal tibia, also formed lung metastases. The DLM8-Luc line was rejected as a suitable cell line to continue with as it did not consistently metastasize to the lungs and the DLM8-Luc-M2 line was rejected as the cells caused rapid metastasis to abdominal organs, resulting in early morbidity. At 14 days following tumor inoculation of the DLM8-Luc-M1 clone into the proximal tibia, a primary tumor was present, with no evidence of gross pulmonary metastasis. However, following removal of the tumor-bearing limb at 14 days, detection of luciferase-expressing pulmonary metastasis was confirmed in all mice by 31 days, thereby validating the model of pulmonary micrometastasis at the time of primary tumor removal.

3.4 Preliminary Experiment 3 – *In Vitro* Osteosarcoma – Chemotherapy Interactions

3.4.1 Materials and Methods

DLM8-Luc-M1 cells were cultured in media consisting of DMEM supplemented with 10% FBS, and antibiotic-antimycotic and sustained in a humidified atmosphere at 37°C with 5% CO₂.

Cells at passage 15-22 were washed with HBSS and detached with a cell scraper into complete media for the cytotoxicity assay and into DMEM without supplements for injections (Appendix A).

Cytotoxicity assays were performed in 96-well microtiter plates (Corning Life Sciences, Manassas, VA), each well receiving 200 µl of culture medium with 2×10^4 DLM8-Luc-M1 clone cells (P16-22). After 24 hours, the medium was removed from all wells and replaced by 200 µl of fresh medium. Once the cells reached at least 50% confluence in all wells, medium was removed from all wells and fresh medium was added to all columns except for those in the first column. Medium containing the highest drug concentration was added to wells of the first column. Serial drug dilutions were prepared by transferring the dilution factor volume from wells of the first column to wells of the second column. After gentle mixing, the dilution factor volume from the second column was transferred to the third column, and so on. The highest concentration for the cisplatin compound was 50 µM and the highest concentration of drug for methotrexate was 15 mM. To test the difference in cell clone response to cisplatin, twelve 2-fold dilutions were used, covering a range from 50 µM to 0.024 µM. Each drug was tested in triplicate.

To assess the response of the cells to methotrexate, twelve 3-fold dilutions were used, covering a range from 15 mM to 8.47×10^{-5} mM. After 72 hours of incubation the plates were inspected under an inverted microscope to assure growth of the controls and sterile conditions. Drug was removed and fresh media (100 µl) was added to every well, along with 10 µl of Alamar Blue (12.5 mg resazurin dissolved in 100 ml distilled water) and the plates were incubated for 2 hours

at 37° C. Assays were run in triplicate. The plates were read on a Spectramax Gemini XS microplate fluorometer (Molecular Devices Cooperation, Sunnyvale, CA, USA) using an excitation wave length of 536 nm and an emission wave length of 588 nm. IC50 values were determined using Prism 6.0 (GraphPad, La Jolla, CA) to graph concentrations and slope measurements were used to determine the inhibition value at 50%.

3.4.2 Results

An average of three assays resulted in a cisplatin IC50 value of $13.17 \pm 5.94 \mu\text{M}$ and a methotrexate IC50 value of $4.64 \pm 1.17 \text{ mM}$ (**Figures 3.4 – 1 and 3.4 – 2**).

3.4.3 Conclusions and Discussion

From the results, we concluded that DLM8-Luc-M1 cells are susceptible to both cisplatin and methotrexate, although the IC50 for methotrexate is 100 times higher than cisplatin, indicating a greater resistance of DLM8-Luc-M1 cells to methotrexate compared to the cisplatin. The IC50 values for cisplatin and methotrexate were within a range found in the literature of other osteosarcoma lines [10, 24]. Osteosarcoma is highly resistant to methotrexate and this was also the case in our assay in which a high dose of the drug was needed to kill 50% of the cells.

FIGURES

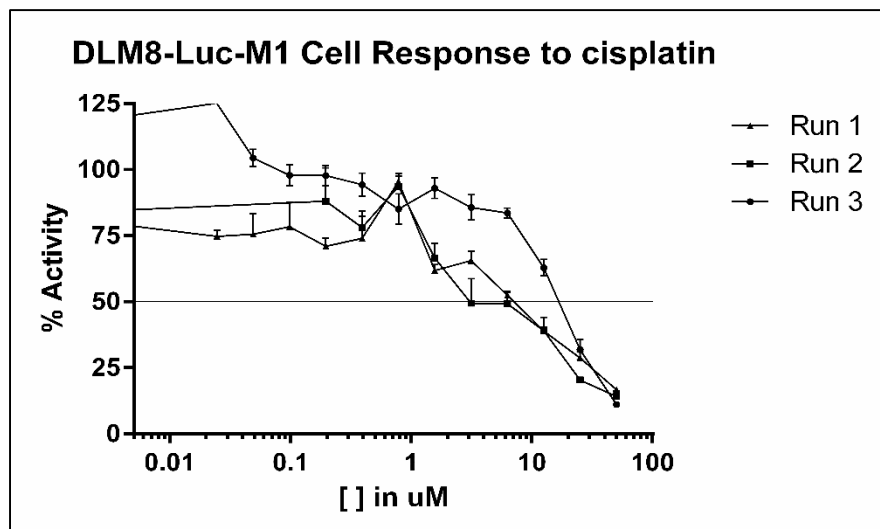


Figure 3.4 – 1: IC₅₀ values of DLM8-Luc-M1 cell sensitivity to cisplatin were calculated using a growth inhibition assay.

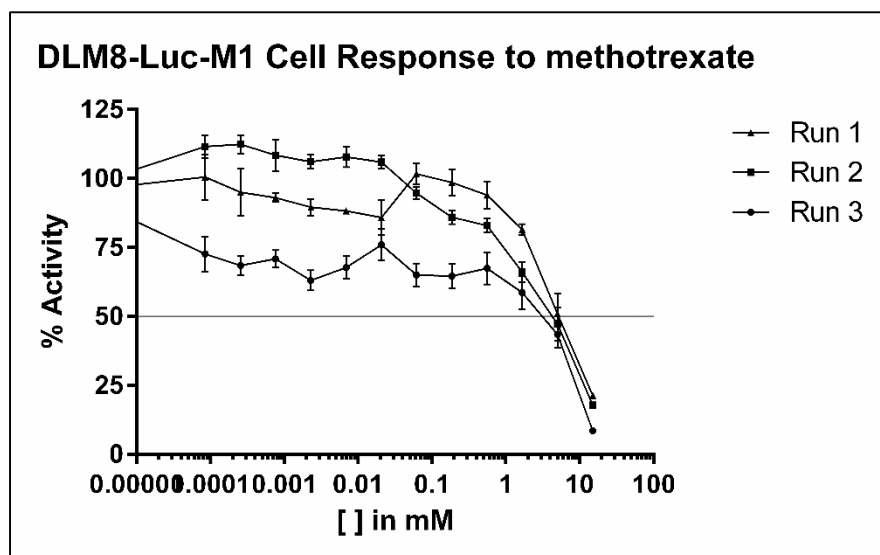


Figure 3.4 – 2: IC₅₀ values of DLM8-Luc-M1 cell sensitivity to methotrexate were calculated using a growth inhibition assay.

3.5 Preliminary Experiment 4 – Treatment with Mesenchymal Stromal Cell Influence on Osteosarcoma Primary Tumor Growth

3.5.1 Introduction

Numerous studies have demonstrated the interaction of MSCs with OSA cells *in vitro* or *in vivo* [5, 25, 32, 33]. However, these studies have investigated sarcoma responses when either a primary tumor was present or when MSCs were co-injected with sarcoma cells. We have developed a clinically relevant model that allows us to study the influence of MSCs in conjunction other treatments in a minimal residual disease setting. The projects described below addressed preliminary work to determine optimization of variables to allow us to assess the use of MSCs in a microscopic tumor environment after surgical removal of the primary tumor.

3.5.2 Materials and Methods

3.5.2.1 Cell Lines

DLM8-Luc-M1 cells were prepared for injection as described in section 3.4.1.

Adipose was harvested from C3H mice in a sterile environment for collection of adipose derived mesenchymal stromal cells (AD-MSCs). In brief, the tissue was collected using sterile instrumentation, washed in HBSS, and minced mechanically using #10 blades. It was then moved into a 25-mL Erlenmeyer flask with a stir bar and enzymatically digested in 1 mg/mL Type I collagenase for 30 minutes at 37 °C on a stir plate. The digested tissue was transferred to a 50-mL conical tube, combined with DMEM (low glucose; Corning) and antibiotic-antimycotic, and centrifuged at 2000 rpm for 5 minutes, gently agitated, and spun again for 5 minutes at 2000 rpm. The supernatant was discarded and the pellet was plated with culture media consisting of DMEM, low glucose supplemented with 15% FBS, antibiotic-antimycotic, MEM vitamins (Corning), and MEM nonessential amino acids (Corning). Cells were allowed to grow for 4 days after which they were fed with fresh media and from then on were passaged

when cells reached 75% to 80% confluence. Cells were washed with HBSS and detached with 0.25% trypsin supplemented with 2.21 mM EDTA for subculturing or injection.

3.5.2.2 Animals

All animal studies were performed with approval of the Institutional Animal Care and Use Committee. Female 8-10 week old C3H mice were obtained from National Institute of Health (NIH) and housed under standard conditions. Injection sites were prepared as described in section 3.2.2.4. Mice were euthanized at day 28 by deep isoflurane anesthesia followed by a cervical dislocation. At necropsy, tissue was collected from the primary tumor and lungs and preserved in formalin.

3.5.2.3 Primary Tumor Establishment

DLM8-Luc-M1 tumor cells were washed twice before being resuspended in sterile HBSS to a final concentration of 2×10^7 cells/mL. Cells were enumerated and viability assessed using trypan blue staining. All cells used for the experiment were at least 90% viable. A volume of 50 μ L (1×10^6 cells) was injected. Mice were prepared as described above, the needle was inserted through the cortex of the tibial crest oriented proximal to distal, and tumor cells were slowly injected. Mice were assessed for tumor establishment and growth in the proximal tibia using bioluminescent imaging (n=9).

3.5.2.4 Mesenchymal Stromal Cell Injections

AD-MSCs were washed with HBSS and detached with 0.25% trypsin supplemented with 2.21 mM EDTA. After three rinses, cells from passage 3 were prepared for injection in a 10% heparin and PBS solution at a volume of 5×10^5 cells in 50 μ L and injected into the site of tumor inoculation on day 5 (n=5). Four animals served as controls and received no AD-MSCs

3.5.2.5 Bioluminescent Imaging

Mice were imaged every 2-3 days using IVIS to assess primary tumor growth as well as presence of metastatic disease using the protocol described in section 3.2.2.5. Mice recovered under monitoring in their cages post-imaging. Images were also obtained immediately before euthanasia as well as *ex vivo* of tumor sites post euthanasia.

3.5.2.6 Tumor Burden

Caliper measurements of the tumor inoculation site were obtained once weekly and at euthanasia. Measurements were taken in the cranial-caudal and medial-lateral dimensions based on location of the initial tumor injection site and palpation of tumor edges. Volume was estimated using a formula from Comstock, et al.[11]

$$Tumor\ Volume = \frac{(long\ dimension) * (short\ dimension)^2}{2}$$

3.5.2.7 Statistical Analysis

A comparison of the bioluminescent intensity of the primary tumor throughout the study was analyzed using ANOVA. A p-value of less than 0.05 was considered statistically significant. Tumor volume sample size was too small to assess statistically significant differences between groups as this was a pilot study.

3.5.3 Results

All mice had primary tumor luciferase expression detectible on the IVIS camera by day 5. There were no complications from MSC injections and all mice recovered. By week 4, mice injected with MSCs had significantly higher bioluminescent expression ($p = 0.046$) than those without MSC treatment (**Figure 3.5 – 1**). Three MSC treated mice and two control mice developed microscopic lung metastases, visible using bioluminescent imaging, by 28 days. Hind limb measurements taken at the femur indicated a trend toward MSC-treated mice having higher tumor volumes; however this did not reach statistical significance.

3.5.4 Conclusions and Discussion

Mice receiving MSCs had significantly higher luciferase expression by 4 weeks indicating greater tumor volume in mice treated with MSCs. Hind limb circumference and caliper measurements of gross tumor at sacrifice could not confirm this; however, these measurements did not prove to be a reliable or repeatable means of comparing tumor volume between treatment groups. No difference was seen between groups with respect to the onset of metastasis disease. We conclude that AD-MSCs, when injected in the presence of a DLM8-Luc-M1 primary tibial tumor, promote primary tumor progression as evidenced by significantly increased BLI in the MSC treated-mice as compared to controls.

This pilot study was designed to determine whether MSCs would influence primary tumor growth as well as timing of metastatic disease presence on bioluminescent images. Our results agreed with other investigators who have shown that MSCs promote primary tumor progression when injected in the presence of a primary tumor. Bioluminescent imaging of the primary tumor allowed for tracking and measurement between treatment groups at weekly time-points. Using these data values, there was an increase in expression levels of mice treated with MSCs compared to controls at weeks 2 and 4, although only week 4 was significantly different. Intensity of bioluminescence is a semi-quantitative indication of tumor volume [16]. Direct measurement of tumor volume was attempted but tumor formation was not spherical or uniform in location and therefore the measurements were difficult to standardize and therefore not reproducible from one time to another and one individual person performing the measurements to another.

FIGURES

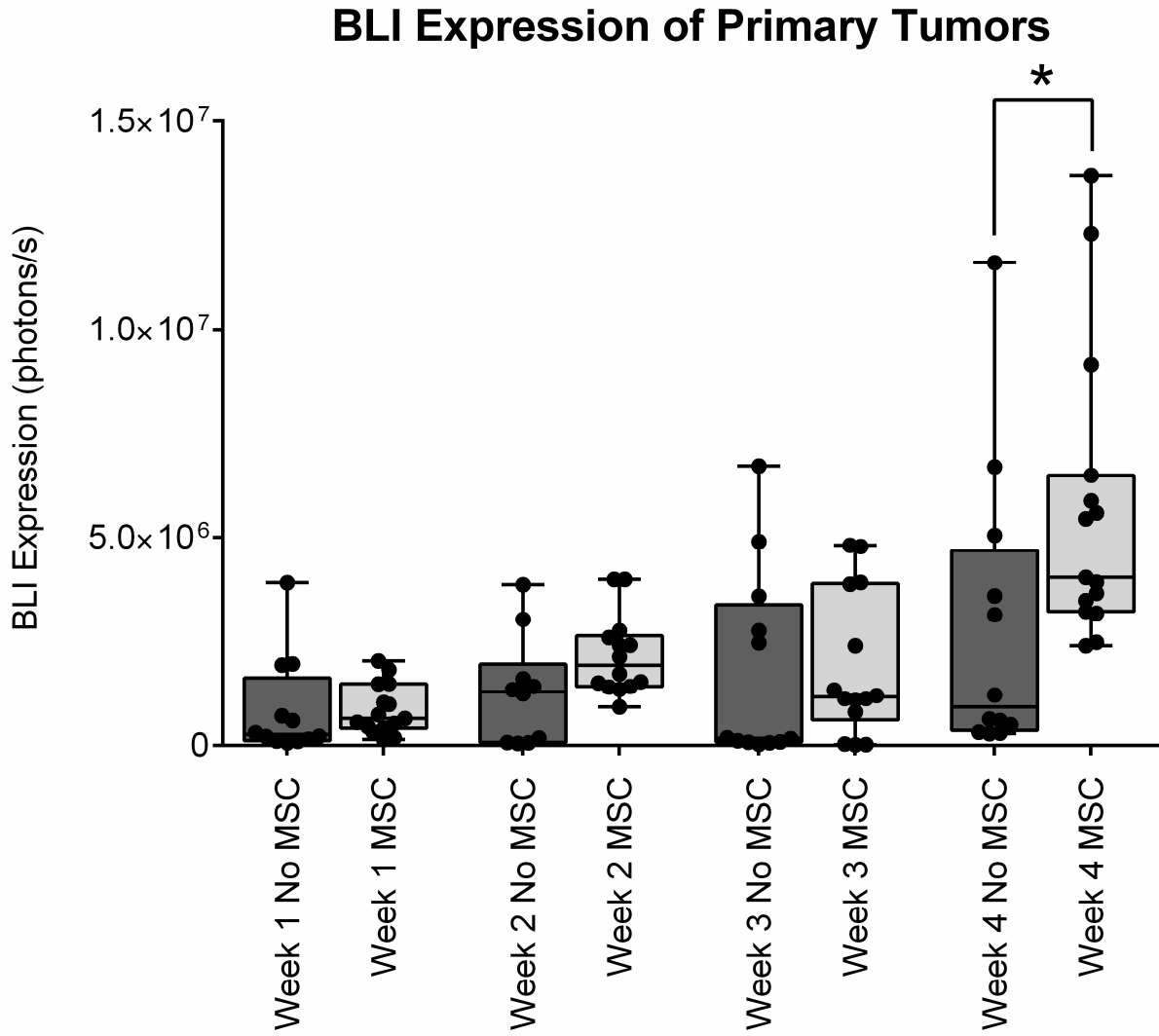


Figure 3.5 – 1: Mice injected with MSCs had significantly higher bioluminescent expression at week 4 (“*”; $p = 0.046$) than those without MSC treatment. ANOVA test was used for analysis.

3.6 Preliminary Experiment 5 –Confirmation of MSCs Homing to DLM8-Luc-M1

Osteosarcoma Primary Tumors

3.6.1 Materials and Methods

3.6.1.1 Cell Line

DLM8-Luc-M1 cells and AD-MSCs were prepared as previously described in sections 3.4.1 and 3.5.2.1. Cells were cultured in complete media, trypsinized, and washed three times before being resuspended in PBS for injection. AD-MSCs were used upon reaching passage 3 *in vitro*.

3.6.1.2 Quantum Dot Labeling

AD-MSCs were harvested, counted, and labeled using a standard protocol for the QDot 655 Kit (Life Sciences) (Appendix A). In brief, cells were exposed to the quantum dots in media and incubated for 1 hour. The compound was vortexed and cells were washed three times. A final concentration of 4×10^5 cells in 50 μL of 10% heparin and PBS was prepared for injection. Quantum dot uptake was verified on a fluorescent confocal microscope using a *TRITC* (tetramethylrhodamine isothiocyanate) filter (Nikon Eclipse, Nikon Instruments, Americas).

3.6.1.3 Animal Procedures

Five C3H mice were given 100 μL of luciferin and 0.06 mg/kg of Buprenorphine SR subcutaneously and anesthetized. Mice were inoculated with 1×10^6 DLM8-Luc-M1 tumor cells in the lumbar subcutaneous tissue and immediately imaged using the IVIS camera to determine whether the cells were visible. Imaging was repeated at days 1, 5, 7, 9, 12 and 14. Fourteen days after tumor inoculation, mice were injected with QD-labeled MSCs either intravenously through the tail vein ($n=2$) or at the site of tumor injection ($n=2$). One mouse served as a control and received no MSC injection ($n=1$). Mice were sacrificed at day 16. Prior to euthanasia, mice were imaged to assess primary tumor burden as well as metastases.

3.6.1.4 Bioluminescent Imaging

Bioluminescent (BL) imaging (In Vivo Imaging System 100 (IVIS), Perkin Elmer, Waltham, USA) was utilized to track tumor development *in vivo* utilizing the methods outlined in 3.2.2.5.

3.6.1.5 Tissue Collection and Histology

The primary tumor was removed en bloc, bisected, and placed in optimal cutting temperature (OCT) compound and were immediately frozen in liquid nitrogen. The samples were then sliced on a microtome to a thickness of 5 μm and examined using a *TRITC* (tetramethylrhodamine isothiocyanate) filter on a fluorescent microscope (Nikon Eclipse, Nikon Instruments, Americas) to assess for quantum dots. The same image was then examined in bright light to determine whether the quantum dots visible were within MSCs.

3.6.2 Results

All mice had bioluminescent expression of tumor cells in the site of primary inoculation. Gross tumor was also present at euthanasia. Quantum dot uptake in MSCs was verified microscopically. Frozen samples from mice receiving both intravenous injection of MSCs and local injection of MSCs had quantum dot labeled MSCs that were visualized histologically within the primary tumor (**Figure 3.6 – 1**).

3.6.3 Conclusions and Discussion

We concluded that AD-MSCs can be labeled with quantum dots and when injected intravenously, they will home to osteosarcoma. In particular, this experiment validated that exogenous C3H AD-MSCs will home to DLM8-Luc-M1 primary tumors 24 hours after intravenous injection. These results are in line with other published literature that MSCs will home to the site of a large primary tumor *in vivo* [15, 18, 20].

FIGURES

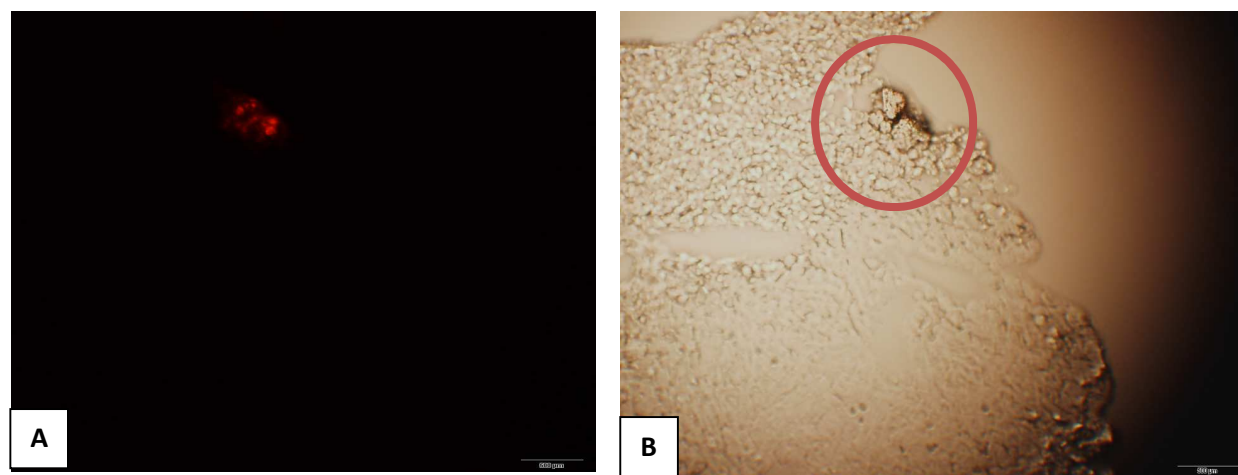


Figure 3.6 – 1: Quantum dots are visible (A) in MSCs located within primary DLM8 tumor tissue (B). The presence of the Q-dots means the cells have tracked to the primary tumor after being injected intravenously.

3.7 Preliminary Experiment 6 –Development and Quantification of Pulmonary Disease in a Minimal Residual Murine Osteosarcoma Model

3.7.1 Materials and Methods

3.7.1.1 Cell Line

DLM8-Luc-M1 cells were cultured in media consisting of DMEM supplemented with 10% FBS, and antibiotic-antimycotic (Appendix A) and sustained in a humidified atmosphere at 37°C with 5% CO₂. Once confluent, cells were washed with HBSS and detached with 0.25% trypsin supplemented with 2.21 mM EDTA.

3.7.1.2 Animals

All animal studies were performed with approval of the Institutional Animal Care and Use Committee. Female 8-10 week old C3H mice were obtained from NIH and housed under standard conditions. Surgical and injection sites were prepared by shaving the fur, followed by cleaning the site with chlorohexidine and 70% alcohol. A subcutaneous injection of sustained-release buprenorphine (0.6 mg/kg; ZooPharm, Fort Collins, USA) was given immediately before the procedures. Anesthesia was induced and maintained using a 3% isoflurane - oxygen mixture. Post-operative care included subcutaneous saline for hydration and recovery in a clean cage on a warming pad until ambulatory. Mice were monitored following procedures daily for 3 days and then at least three times weekly for evidence of morbidity related to the primary tumor or metastases.

3.7.1.3 Establishment of primary tumor

DLM8-Luc-M1 tumor cells were prepared for injection as previously described in section 3.5.2.3 and 1 x 10⁶ cells were inoculated into the proximal tibia.

3.7.1.4 Surgical Procedures

Coxo-femoral amputations were performed at 14 days (n=28) after primary tumor inoculation as previously described in section 3.3.2.5.

3.7.1.5 Bioluminescent Imaging

Bioluminescent imaging was performed as previously described in section 3.2.2.5. Mice recovered in cages under supervision. Images were analyzed using Living Image Software (Living Image 4.2; PerkinElmer, Waltham, USA) for luciferase activity and image analysis was repeated at days 4, 7, and 10. Following removal of the primary tumor, images were obtained every 3-4 days post inoculation to track development and progression of pulmonary metastatic disease. Mice were euthanized after a final image at 24 days.

3.7.1.6 Histology

At the time of amputation, primary tumor bearing limbs were formalin fixed followed by decalcification for 48 hours. One to two longitudinal sections, 20 μ m apart, were paraffin-embedded and stained with hematoxylin and eosin (H&E). After euthanasia, lungs were removed. Lobes were separated and individually placed dorsal aspect down in the same cassette. Tissues were formalin-fixed, paraffin-embedded, sectioned, and stained with H&E. Two coronal plane lung sections 20 μ m apart, from ventral to dorsal surface, were utilized for analysis.

3.7.1.7 Primary and Pulmonary Disease Burden Analysis

Primary tumor growth immediately pre-amputation was documented by bioluminescence imaging of the inoculated limb and confirmation of primary osteosarcoma tumor growth was made by histological analysis following amputation. Only mice with documented primary tumor establishment and histological confirmation were included in pulmonary metastatic data analyzed.

Slides were assessed for the presence of pulmonary metastasis and primary tumor formation. Pulmonary nodules larger than 5 cells in a cluster were quantified and the mean numbers of nodules was quantified (**Figure 3.7 – 1**). Additionally, tumor area relative to total lung area measurements were completed utilizing Bioquant (Bioquant Osteo 2012 Version 12.1.6; Bioquant Image Analysis Corp, Nashville, TN, USA) software. In brief, slides were scanned and converted to picture files and read into the software. Using software tools, the area of each lobe of the lung was obtained. A similar tool was then used to outline and quantify only the area of the nodules previously identified (**Figure 3.7 – 2**). The area of the nodules was summed and a percentage of tumor area to total lung area was computed (Appendix A).

3.7.2 Results

Twenty-four mice (86%) of mice developed a primary tumor. Out of the mice which developed a primary tumor, 17 developed pulmonary metastatic nodules (71%). The mean number of nodules was 7.16 ± 11.70 and the mean relative pulmonary metastatic area to total lung area was $0.62 \% \pm 1.73 \%$.

3.7.3 Conclusions and Discussion

The purpose of this project was to develop a model of spontaneous pulmonary metastatic disease following removal of the primary tumor. We found that after two weeks of primary tumor cell injection into an orthotopic location, 71% of mice injected with the DLM8-Luc-M1 cell line developed histologically quantifiable pulmonary disease. We were able to track both primary tumor growth as well as pulmonary disease development throughout the study using bioluminescent imaging and nodules were large enough to be visible on histology. The use of area measurements, while a unique quantifier, allowed us to determine the clinical impact of the disease burden – in other words, in this model, we could calculate both how many nodules are present as well as how destructive they were to the pulmonary tissues. This model validated the choice of the DLM8-Luc-M1 cell line and demonstrated the ability to obtain pulmonary

disease formation within a short time period following primary tumor removal. However, the size of nodules was small across most samples at 24 days with only 71% developing pulmonary metastatic disease. We therefore elected to extend future studies for one additional week to enhance the opportunity for pulmonary disease formation and make nodule identification easier.

FIGURES

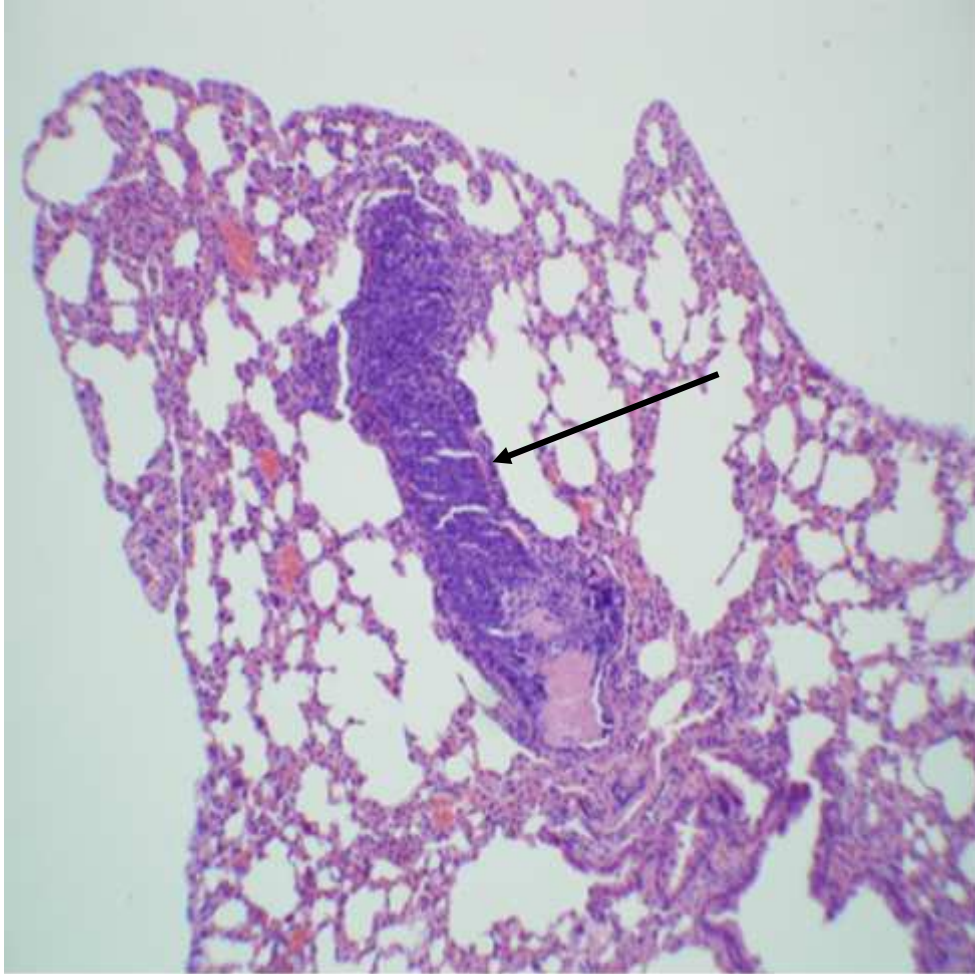


Figure 3.7 – 1: Representative sample of a pulmonary metastatic nodule in the caudal lung lobe of a C3H mouse. Sample has been stained with H&E and is at 2X magnification.

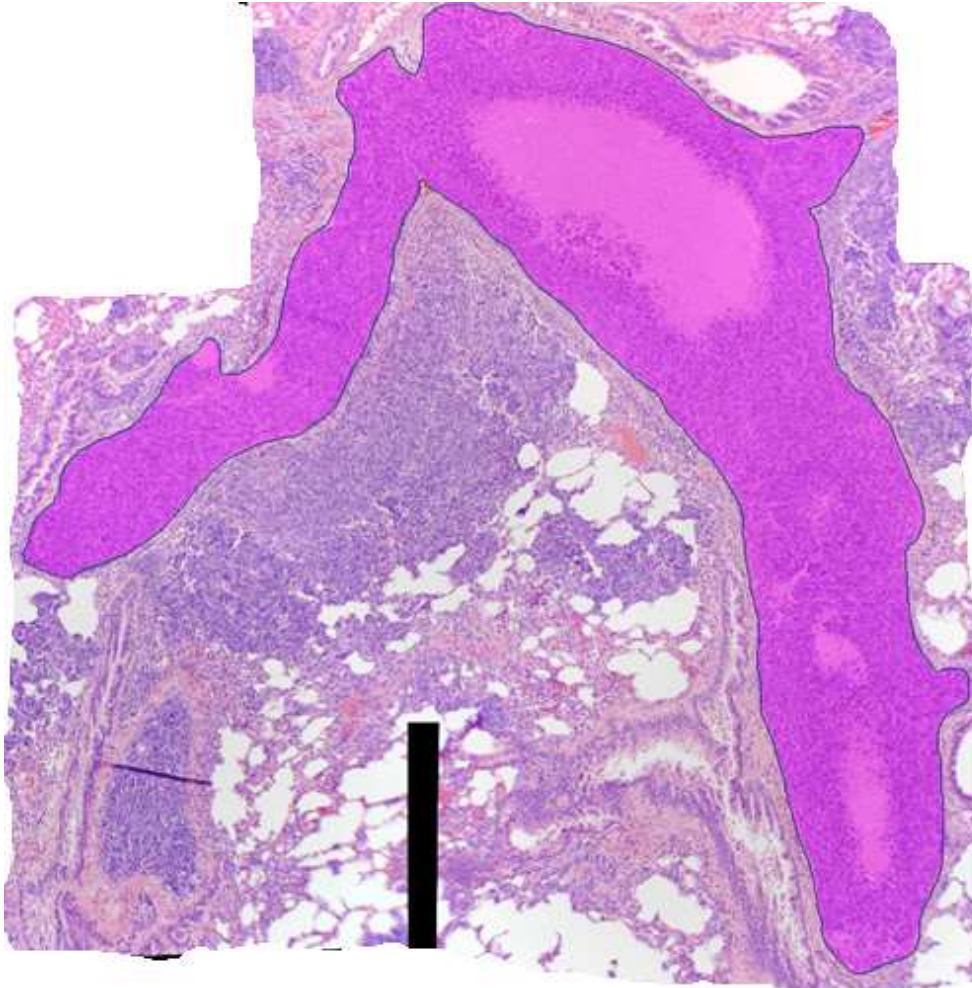


Figure 3.7 – 2: Using Bioquant Osteo software, the area of a metastatic nodule could be isolated and measured. The image above was scanned at 10X and stitched together before analysis so the entire nodule would be visible in one viewing window. Every nodule was individually measured and values were added together for each slide and each slide was averaged together to obtain one value per mouse.

3.8 Preliminary Experiment 7 – Development of a Local Recurrence Model of Osteosarcoma

3.8.1 Introduction

Osteosarcoma (OS) metastasizes to the lungs and axial skeleton [29]. Micrometastasis is typically present at initial diagnosis, although confirmation is difficult until the metastatic lesions become visible using current imaging modalities [7]. Survival rates are 55-75% if no gross metastatic disease is present at diagnosis [21, 27]; whereas the survival rate drops to 30% when disease is present in a second site [26].

Surgical removal of the primary tumor involves amputation or limb sparing, with the latter method requiring reconstruction and bone healing [23, 31]. Amputation leaves patients with a lifelong need for prosthetic limbs. Complications arising from amputation include limited mobility, residual limb or phantom pain, infection, and other concerns [23]. Consequently, approximately 85% of human patients with OS have limb reconstruction surgery [12, 30]. The nature of limb reconstruction dictates that neurovascular structures be spared to preserve function thereby requiring a narrow margin resection and increasing the risk residual microscopic disease in the surgical wound. Residual microscopic tumor is associated with an increase of local recurrence [4]. Over 30% of OS patients will experience disease relapse before 5 years [4, 8] and up to 14% of these relapses can be attributed to local recurrence [4, 6, 22]. When local recurrence is identified, the patient must undergo either an amputation or additional ablative surgery [1, 34]. Limb reconstruction techniques have high complication rates, often necessitating intervention to accelerate healing or treat non-union. When microscopic residual tumor is present in the surgical wound, interventions aimed at promoting normal tissue healing can also promote tumor growth. Therefore, animal models of post-operative local tumor recurrence resulting from microscopic residual tumor are needed.

The purpose of this project was to develop a syngeneic murine model of bioluminescent osteosarcoma local recurrence. Removal of the primary tumor was completed with a narrow margin rather than a wide margin to ensure microscopic disease would remain behind. The model mimics the clinical situation of a limb reconstruction following primary tumor removal when microscopic disease remains in the compartment in an animal recipient with an intact immune system.

3.8.2 Materials and Methods

3.8.2.1 Cell Line

DLM8-Luc-M1 cells were cultured as previously described in section 3.7.1.1.

3.8.2.2 Animals

Animal care and use was approved by the local Institute for Animal Care and Use Committee. Female 8-10 week old C3H mice (National Institutes of Health, Bethesda, MD, USA) were housed under standard laboratory animal conditions. Surgical and injection sites were prepared as previously described in section 3.7.1.2. Post-operative care consisted of recovery in a warm cage and a subcutaneous injection of 1.0 mL sterile saline. Mice were monitored following procedures daily for 3 days, then three times weekly to assess for evidence of primary tumor formation as well as local recurrence and metastatic disease.

3.8.2.3 Primary Tumor Formation

DLM8-luc-M1 cells were prepared for injection as previously described in section 3.5.2.3. Mice were anesthetized using inhalation of 3% isoflurane balanced with oxygen for the procedure. A concentration of 1×10^6 DLM8-luc-M1 cells in 30ul HBSS were injected into the medullary cavity of the tibia over a period of 30 seconds. A total of 8 mice were injected with primary tumor cells.

3.8.2.4 Characterization of primary tumor

In order to track the growth of the primary tumor, mice were imaged as previously described in section 3.2.2.5 with an IVIS 100 imaging system 24 hours following tumor cell injection and then twice weekly until amputation. A region of interest was obtained and compared using Living Image software to evaluate tumor growth over time.

3.8.2.5 Surgical Procedure

To determine the optimal time to remove the primary tumor, mice underwent a narrow margin removal of the primary tumor at either 10 days (n=4) or 14 days (n=4). Mice were prepared as described above; anesthesia was induced and maintained using a 3% isoflurane - oxygen mixture. Amputation of tumor bearing limbs was undertaken with a circumferential incision of the skin, just proximal to the palpable tumor. A partial limb amputation was performed with sharp dissection through the soft tissues and bone with a #15 blade (Stainless Steel, Aspen Surgical, Caledonia, MI, USA) just outside of the visible tumor capsule. Care was taken to remove all gross evidence of tumor but a margin of normal tissue was purposely not obtained. Muscle, subcutaneous tissue and skin was closed in standard fashion using 5-0 Biosyn suture (Covidien, Mansfield, MA).

3.8.2.6 Characterization of Local Recurrence and Metastasis

Mice were assessed 4 hours after amputation using bioluminescent imaging to determine whether there was expression in the residual limb. They were imaged weekly for a total of six images of residual limbs to evaluate local recurrence. During imaging, mice were also assessed for development of metastatic disease outside of the surgical site. All animals were subjected to a final bioluminescent image immediately prior to euthanasia.

3.8.2.7 Histology

Primary tumor bearing limbs were harvested at the time of amputation, formalin fixed, decalcified, paraffin embedded, and stained for histological evaluation. Following euthanasia at 5 weeks post tumor inoculation, the femur, hemipelvis and surgical stump site were harvested, formalin fixed, decalcified, paraffin embedded, and stained for histological evaluation.

Specimens from the primary site and residual surgical site were sliced longitudinally and one to two sections, 20 μ m apart, were stained with hematoxylin and eosin and examined for the presence of primary and local tumor recurrence. Slides were examined on a fluorescent microscope (Olympus VS120-S5, Center Valley, PA) and evaluated for presence or absence of local recurrence.

3.8.3 Results

Six mice had evidence of primary tumor growth (75%) leaving 4 mice in the 10 day amputation group and 2 mice in the 14 day amputation group. Local recurrence was histologically evident in five of these mice (83%), 3 in the 10 day amputation group and 2 in the 14 day amputation group. Four mice developed local recurrence by day 35 (n=1 from 14 day amputation group; n=3 from 10 day amputation group) and one mouse developed local recurrence by day 38 (14 day amputation group) (**Figure 3.8 – 1**). Of the group amputated at 14 days, metastatic disease development occurred before or co-currently with local recurrence. The group amputated at 10 days had local recurrence in 75% of mice and only one had evidence of metastatic disease.

3.8.4 Conclusions and Discussion

We concluded that we could expect a 75% local recurrence rate at 35 days when mice were amputated at 10 days using the narrow margin amputation technique. This model was chosen for all subsequent local tumor recurrence studies.

We developed a local recurrence model using an orthotopically implanted osteosarcoma cell line in an immune-competent recipient. The model is a novel way to assess narrow margin removal of primary osteosarcoma. Although the numbers were small, local recurrence was evident histologically at study end-points. Further, the time-point of 10 days between primary tumor cell injection and amputation appeared to be better as mice in this group were more likely to develop local recurrence without metastatic disease burden. This innovative model of local osteosarcoma recurrence is an important tool to test effects of treatment in the site of a surgical bed following removal of primary osteosarcoma when microscopic residual disease is present.

Local recurrence models have important utility as it recapitulates primary tumor development, surgical intervention and local recurrence. Although a relatively small population of human and canine OS patients will develop local recurrence, the development of a new tumor at the previous surgery site is both devastating and prognostically significant.

FIGURES



Figure 3.8 – 1: Gross local recurrence in the surgical site of a mouse following a narrow margin excision of primary tibial osteosarcoma.

REFERENCES

1. Ahlmann ER, Menendez LR, Kermani C, Gotha H. Survivorship and clinical outcome of modular endoprosthetic reconstruction for neoplastic disease of the lower limb. *J Bone Joint Surg Br.* 2006;88:790-795.
2. Arinze TL, Peter SJ, Archambault MP, van den Bos C, Gordon S, Kraus K, Smith A, Sudha K. Allogeneic Mesenchymal Stem Cells Regenerate Bone in a Critical-Sized Canine Segmental Defect. *The Journal of Bone and Joint Surgery (American).* 2003;85:1927-1935.
3. Asai T, Ueda T, Itoh K, Yoshioka K, Aoki Y, Mori S, Yoshikawa H. Establishment and characterization of a murine osteosarcoma cell line (LM8) with high metastatic potential to the lung. *International Journal of Cancer.* 1998;76:418-422.
4. Bacci G, Forni C, Longhi A, Ferrari S, Mercuri M, Bertoni F, Serra M, Briccoli A, Balladelli A, Picci P. Local recurrence and local control of non-metastatic osteosarcoma of the extremities: A 27-year experience in a single institution. *Journal of Surgical Oncology.* 2007;96:118-123.
5. Bian Z-Y, Fan Q-M, Li G, Xu W-T, Tang T-T. Human mesenchymal stem cells promote growth of osteosarcoma: Involvement of interleukin-6 in the interaction between human mesenchymal stem cells and Saos-2. *Cancer Science.* 2010;101:2554-2560.
6. Bramer JA, Abudu AA, Grimer RJ, Carter SR, Tillman RM. Do pathological fractures influence survival and local recurrence rate in bony sarcomas? *Eur J Cancer.* 2007;43:1944-1951.
7. Bruland ØS, Høifødt H, Sæter G, Smeland S, Fodstad Ø. Hematogenous Micrometastases in Osteosarcoma Patients. *Clinical Cancer Research.* 2005;11:4666-4673.
8. Bruland OS, Pihl A. On the current management of osteosarcoma. A critical evaluation and a proposal for a modified treatment strategy. *Eur J Cancer.* 1997;33:1725-1731.
9. Cole HA, Ichikawa J, Colvin DC, O'Rear L, Schoenecker JG. Quantifying intra-osseous growth of osteosarcoma in a murine model with radiographic analysis. *Journal of Orthopaedic Research.* 2011;29:1957-1962.
10. Cole PD, Smith AK, Kamen BA. Osteosarcoma cells, resistant to methotrexate due to nucleoside and nucleobase salvage, are sensitive to nucleoside analogs. *Cancer chemotherapy and pharmacology.* 2002;50:111-116.
11. Comstock KE, Hall CL, Daignault S, Mandlebaum SA, Yu C, Keller ET. A bioluminescent orthotopic mouse model of human osteosarcoma that allows sensitive and rapid evaluation of new therapeutic agents In vivo. *In vivo.* 2009;23:661-668.
12. DiCaprio MR, Friedlaender GE. Malignant Bone Tumors: Limb Sparing Versus Amputation. *Journal of the American Academy of Orthopaedic Surgeons.* 2003;11:25-37.
13. Dunn TB, Andervont HB. Histology of Some Neoplasms and Non-Neo-plastic Lesions Found in Wild Mice Maintained Under Laboratory Conditions. *Journal of the National Cancer Institute.* 1963;31:873-901.
14. Giannoni P, Mastrogiacomo M, Alini M, Pearce SG, Corsi A, Santolini F, Muraglia A, Bianco P, Cancedda R. Regeneration of large bone defects in sheep using bone marrow stromal cells. *Journal of Tissue Engineering and Regenerative Medicine.* 2008;2:253-262.
15. Hung S-C, Deng W-P, Yang WK, Liu R-S, Lee C-C, Su T-C, Lin R-J, Yang D-M, Chang C-W, Chen W-H, Wei H-J, Gelovani JG. Mesenchymal Stem Cell Targeting of Microscopic Tumors and Tumor Stroma Development Monitored by Noninvasive In vivo Positron Emission Tomography Imaging. *Clinical Cancer Research.* 2005;11:7749-7756.

16. Jenkins DE, Oei Y, Hornig YS, Yu SF, Dusich J, Purchio T, Contag PR. Bioluminescent imaging (BLI) to improve and refine traditional murine models of tumor growth and metastasis. *Clin Exp Metastasis*. 2003;20:733-744.
17. Khanna C, Prehn J, Yeung C, Caylor J, Tsokos M, Helman L. An orthotopic model of murine osteosarcoma with clonally related variants differing in pulmonary metastatic potential. *Clin Exp Metastasis*. 2000;18:261-271.
18. Kidd S, Spaeth E, Dembinski JL, Dietrich M, Watson K, Klopp A, Battula VL, Weil M, Andreeff M, Marini FC. Direct Evidence of Mesenchymal Stem Cell Tropism for Tumor and Wounding Microenvironments Using In Vivo Bioluminescent Imaging. *Stem Cells*. 2009;27:2614-2623.
19. Li GC, Ye QH, Xue YH, Sun HJ, Zhou HJ, Ren N, Jia HL, Shi J, Wu JC, Dai C, Dong QZ, Qin LX. Human mesenchymal stem cells inhibit metastasis of a hepatocellular carcinoma model using the MHCC97 - H cell line. *Cancer Science*. 2010;101:2546-2553.
20. Loebinger MR, Kyrtatos PG, Turmaine M, Price AN, Pankhurst Q, Lythgoe MF, Janes SM. Magnetic Resonance Imaging of Mesenchymal Stem Cells Homing to Pulmonary Metastases Using Biocompatible Magnetic Nanoparticles. *Cancer Research*. 2009;69:8862-8867.
21. Mirabello L, Troisi RJ, Savage SA. International osteosarcoma incidence patterns in children and adolescents, middle ages, and elderly persons. *International journal of cancer. Journal international du cancer*. 2009;125:229-234.
22. Nathan SS, Gorlick R, Bukata S, Chou A, Morris CD, Boland PJ, Huvos AG, Meyers PA, Healey JH. Treatment algorithm for locally recurrent osteosarcoma based on local disease-free interval and the presence of lung metastasis. *Cancer*. 2006;107:1607-1616.
23. Ottaviani G, Robert RS, Huh WW, Jaffe N. Functional, Psychosocial and Professional Outcomes in Long-Term Survivors of Lower-Extremity Osteosarcomas: Amputation Versus Limb Salvage Pediatric and Adolescent Osteosarcoma. In: Jaffe N, Bruland OS, Bielack S, ed.: Springer US; 2010:421-436.
24. Pasello M, Michelacci F, Scionti I, Hattinger CM, Zuntini M, Caccuri AM, Scotlandi K, Picci P, Serra M. Overcoming glutathione S-transferase P1-related cisplatin resistance in osteosarcoma. *Cancer Res*. 2008;68:6661-6668.
25. Perrot P, Rousseau J, Bouffaut A-L, Rédini F, Cassagnau E, Deschaseaux F, Heymann M-F, Heymann D, Duteille F, Trichet V, Gouin F. Safety Concern between Autologous Fat Graft, Mesenchymal Stem Cell and Osteosarcoma Recurrence. *PLoS ONE*. 2010;5:e10999-e10999.
26. Picci P. Osteosarcoma (Osteogenic sarcoma). *Orphanet Journal of Rare Diseases*. 2007;2:6.
27. Savage SA, Mirabello L. Using epidemiology and genomics to understand osteosarcoma etiology. *Sarcoma*. 2011;2011:548151.
28. Sottnik JL, Duval DL, J. Ehrhart E, Thamm DH. An orthotopic, postsurgical model of luciferase transfected murine osteosarcoma with spontaneous metastasis. *Clinical & Experimental Metastasis*. 2010;27:151-160.
29. Ta HT, Dass CR, Choong PFM, Dunstan DE. Osteosarcoma treatment: state of the art. *Cancer and Metastasis Reviews*. 2009;28:247-263.
30. Tan PX, Yong BC, Wang J, Huang G, Yin JQ, Zou CY, Xie XB, Tang QL, Shen JN. Analysis of the efficacy and prognosis of limb-salvage surgery for osteosarcoma around the knee. *European Journal of Surgical Oncology (EJSO)*. 2012;38:1171-1177.
31. Withrow SJ, Wilkins RM. Cross talk from pets to people: translational osteosarcoma treatments. *ILAR journal / National Research Council, Institute of Laboratory Animal Resources*. 2010;51:208-213.
32. Xu W-t, Bian Z-y, Fan Q-m, Li G, Tang T-t. Human mesenchymal stem cells (hMSCs) target osteosarcoma and promote its growth and pulmonary metastasis. *Cancer Letters*. 2009;281:32-41.

33. Yu FX, Hu WJ, He B, Zheng YH, Zhang QY, Chen L. Bone marrow mesenchymal stem cells promote osteosarcoma cell proliferation and invasion. *World journal of surgical oncology*. 2015;13:465.
34. Zhang Y, Yang Z, Li X, Chen Y, Zhang S, Du M, Li J. Custom prosthetic reconstruction for proximal tibial osteosarcoma with proximal tibiofibular joint involved. *Surg Oncol*. 2008;17:87-95.
35. Zhu L, Liu W, Cui L, Cao Y. Tissue-engineered bone repair of goat-femur defects with osteogenically induced bone marrow stromal cells. *Tissue Engineering*. 2006;12:423-433.

Chapter 4: Do Mesenchymal Stromal Cells Delivered Intravenously or into a Surgical Site Promote Osteosarcoma Pulmonary Metastases?

4.1 Introduction

Osteosarcoma is the second most common cause of cancer-related deaths in children and adolescents. It arises most frequently as a bone-producing sarcoma of the appendicular skeleton [20] and pulmonary micrometastases are presumed to be present at initial diagnosis [16]. Wide resection with limb salvage is currently the standard approach to eradicating the primary tumor when possible; however, large-segment bone reconstruction presents many challenges for the surgeon because it is associated with a high complication rate and frequent need for revision procedures arising from allograft failure, infection, local recurrence, and wound healing [17, 18, 21].

Mesenchymal stromal cells (MSCs) have been shown to improve bone integration between native tissue and allograft or endoprosthetics such as are used in limb reconstruction [8] [3] [5]. As well, MSCs have been shown to aid in healing of damaged tissue in several preclinical studies and have great potential for therapeutic use in limb salvage after massive bone loss resulting from trauma or tumor resection [6, 7, 12]. However, MSCs have also been shown to promote primary tumor and pulmonary metastatic tumor growth when injected either locally near existing gross tumor or co-injected with sarcoma cells in rodent models [2, 9, 23, 25]. Although these results raise concerns about the safety of using MSCs in patients with sarcoma, MSCs are unlikely to be used in a clinical setting when gross tumor is present. Instead, they are potentially useful in combination with other treatments for improvement of bone healing and integration of an endoprosthesis and/or allograft after limb reconstruction. What remains unclear, however, is whether MSCs are safe to use in a microscopic residual disease setting. To our knowledge, no previous studies have explored the influence of mesenchymal stromal cells on progression of pulmonary micrometastasis following surgical removal of the primary

osteosarcoma tumor.

Several rodent models of osteosarcoma have been developed to study pulmonary metastasis [1, 4, 11, 13, 14, 22]. These models vary widely from scenarios where the primary tumor remains in situ throughout the study to others where the primary tumor is resected before analyzing metastatic growth to models where cell lines are injected into the right ventricle to seed lungs directly. These different models make it difficult to compare results between studies [4, 11, 13, 14, 22]. Orthotopic tumor models with spontaneous metastasis are thought to most accurately recapitulate tumor-stroma interactions in the tumor microenvironment [4, 22]. MSCs are known to exist in both the stromal tissues and the circulating blood [10].

The purpose of this study was to use the pulmonary metastatic model developed above to determine whether the administration of adipose-derived MSCs (AD-MSCs) would promote pulmonary metastatic osteosarcoma progression after primary tumor removal. We hypothesized that AD-MSCs, injected either locally at the surgical site or intravenously after a wide margin amputation for tibial osteosarcoma, would not influence pulmonary metastatic disease progression after primary tumor resection.

4.2 Materials and Methods

4.2.1 Cell Lines

DLM8-Luc-M1 cells were prepared for injection as previously described in section 3.4.1 of Chapter 3 and resuspended in DMEM media without supplements for injection.

AD-MSCs harvested from C3H mice as previously described in section 3.5.2.1 of Chapter 3 were utilized for the experiment. Cells were resuspended in PBS with 10% heparin for injection.

4.2.2 Animals

All animal studies were performed as previously described in section 3.7.1.2 of Chapter 3. Mice were monitored following procedures daily for 3 days and then at least three times weekly for evidence of morbidity related to the primary tumor or metastases.

4.2.3 Establishment of primary tumor

DLM8-Luc-M1 tumor cells were prepared as described in section 3.5.2.3 of Chapter 3. Mice were prepared as described above and the needle was inserted through the cortex of the tibial crest. A total of n=74 mice were inoculated with tumor cells.

4.2.4 Surgical Procedures

Coxo-femoral amputations were completed at 10 days (n=67) after primary tumor inoculation as previously described in section 3.3.2.5 of Chapter 3. Amputated limbs were collected for histology. Mice were monitored during recovery on room air in a clean cage on a warming pad until ambulatory and were given buprenorphine every 8 hours for the first 72 hours following surgery.

4.2.5 Mesenchymal Stromal Cell Treatment

Twenty-four hours after the removal of the primary tumor, mice were randomly assigned to either an injection of AD-MSCs into the surgical site, an injection of AD-MSCs intravenously (IV) through the tail vein, or an untreated control group. Mice in the AD-MSC treatment groups (n=45) received one injection of 5×10^5 AD-MSCs in sterile PBS (+ 100 units/mL Heparin for IV group) through a 29 ½ G insulin needle (Becton Dickinson, East Rutherford, USA) and were allowed to recover at room temperature in a clean cage.

4.2.6 Bioluminescent Imaging

Bioluminescent imaging was performed as previously described in section 3.2.2.5 of Chapter 3. Mice recovered in cages under supervision. Images were analyzed using Living Image

Software (Living Image 4.2; PerkinElmer, Waltham, USA) for luciferase activity and image analysis was repeated at days 4, 7, and 10. Following removal of the primary tumor, images were obtained every 3-4 days post inoculation to track development and progression of pulmonary metastatic disease. Mice were euthanized after a final image at 31 days (n = 67). The mean time to first detection of metastasis as determined by bioluminescence imaging in each MSC treatment group was compared.

4.2.7 Histology

Primary tumor-bearing limbs were formalin fixed immediately after amputation and decalcified for 48 hours. Tissues were paraffin-embedded; one to two longitudinal sections, 20 μm apart were cut and stained with hematoxylin and eosin (H&E). Following the in life portion of the study mice were euthanized and lungs were collected. Lobes were separated and individually placed dorsal aspect down in the same cassette. Pulmonary tissues were formalin-fixed, paraffin-embedded, sectioned, and stained with H&E. Two coronal plane lung sections, 20 μm apart, from ventral to dorsal surface, were utilized for analysis.

4.2.8 Primary and Pulmonary Disease Burden Analysis

Primary tumor growth pre-amputation was documented by bioluminescence imaging of the inoculated limb and confirmation of primary osteosarcoma tumor growth was made by histological analysis following amputation. Only mice with documented primary tumor establishment and histological confirmation were included in data analyzed.

Slides were assessed for the presence of pulmonary metastasis and primary tumor formation using the same criteria as in the model development in section 3.7.1. The mean number of nodules between treatment groups was compared. Additionally, pulmonary metastatic area relative to total lung area measurements was calculated utilizing the techniques described in the model development project in section 3.7.1. Metastatic area was summed and a percentage of

tumor area to total lung area was computed. Mean metastatic area was compared between treatment groups.

4.2.9 Statistical Analysis

Before beginning this study, a power calculation was performed based on the number of nodules in the preliminary experiment 6 ($\sigma_1 = 17.1$, $\sigma_2 = 3.9$, $\delta = 7.85$, $\alpha = 0.05$). The study below was designed to detect a difference in the number of metastatic nodules using 26 animals per treatment group at 60% power.

Results were expressed as means \pm SD per treatment group. Presence of disease was analyzed using Fisher's Exact Test. The number of nodules and percentage of tumor area was compared using ANOVA. Welch's test was used to compare the time to first detectable pulmonary disease using BLI. A t-test was used for all pairwise comparisons (GraphPad, La Jolla, CA). For all tests, a p-value of less than 0.05 was considered statistically significant.

4.3 Results

Seven mice were lost to the study before amputation. Sixty-five mice developed a primary tumor (97%). These were randomized into one of three treatment groups. No MSCs (n=22), surgical site injection MSCs (n=23), and intravenous MSCs (n=20). Only mice with a primary tumor were used for the data analysis below.

At euthanasia, 64% of untreated mice, 70% of surgical site MSC treated mice, and 70% of intravenous MSC treated mice had pulmonary metastases; there was no difference in treatment groups ($p=0.893$). Mean number of days until first BL detectable metastasis in the intravenous group (12.93 ± 1.90 days) was significantly shorter when compared to the surgical site injection group (16.94 ± 6.78 days) and untreated group (15.93 ± 4.55 days) ($p=0.022$) (**Figure 4.3 – 1**).

The mean number of nodules was not different between treatment groups (50.28 ± 85.04 intravenous MSC group, 24.04 ± 61.9 surgical site injection group, 34.23 ± 76.77 untreated

group; $p=0.52$) (**Figure 4.3 – 2**). The percentage of pulmonary metastatic area relative to total lung area was not different between treatment groups ($4.62 \pm 7.20\%$ intravenous MSC group, $2.26 \pm 4.98\%$ surgical site injection group, $3.95 \pm 9.33\%$ untreated group; $p=0.55$) (**Figure 4.3 – 3**).

4.4 Conclusions and Discussion

The purpose of this study was to investigate whether MSCs would affect pulmonary metastatic burden following removal of the primary tumor with wide margins. Pulmonary disease burden was assessed by four measures – the time to first BLI detectable metastatic disease, presence of disease in lung tissue, number of nodules in the average of two step sections, and percentage of pulmonary tumor area to total pulmonary area. We concluded that pulmonary disease is detectable faster in mice treated with intravenous MSCs compared to other groups, but there was no difference in the number of metastatic nodules or percentage of tumor area.

While only one measure was significantly different, the variation between mice was high in all assessments and this variability contributed to a statistical power that may have led to a type II statistical error. Posteriori analysis using percentage of tumor area indicated many of the outcome measures were greatly underpowered ($\sigma_1 = 7.2$, $\sigma_2 = 4.98$, $\delta = 2.36$, $\alpha = 0.05$). The variation within treatment groups was high and a larger sample size ($n=110$) would be required for 80% power. However, even with these sample size and variance issues, there were concerning trends showing intravenous delivery of MSCs in a microscopic pulmonary metastasis environment may be contraindicated and result in undesirable clinical ramifications. In all measures, intravenously delivered MSCs caused trends toward faster detection of metastasis, higher mean number of pulmonary nodules and higher mean metastatic area when compared to no MSC treatment or MSCs delivered into the surgical site. Further study is required before MSCs are intravenously delivered to patients with a history of osteosarcoma.

Pulmonary metastatic development occurrence following MSCs injected locally into the surgical site was not different compared to mice untreated with MSCs.

Animal models that recapitulate the natural disease progression as closely as possible are of paramount importance for translation of these models to human populations. This study utilized a novel murine osteosarcoma model that included spontaneous pulmonary micrometastasis to study the influence of MSC administration on pulmonary disease development following primary tumor removal.

The use of MSCs to augment bone healing in limb salvage patients following sarcoma resection holds significant therapeutic promise [8], but the safety of MSC use in sarcoma patients remains unknown [2]. It has been well-established that pulmonary micrometastases exist early in the course of osteosarcoma and many patients have microscopic pulmonary disease at the time of diagnosis [13, 23, 24]. Thus, the use of mesenchymal stromal cells as part of a post-operative treatment plan needs to be validated as safe as well as effective in a model of pulmonary osteosarcoma following primary tumor removal.

Previous investigators have shown that MSCs promote both primary and metastatic tumor growth when co-injected in the presence of established primary osteosarcoma or concurrently with osteosarcoma cell lines [2, 19, 23]. This effect of MSCs has been shown with other tumor types as well [9, 15]. It has been recently theorized that the homing and subsequent tumor-promoting effects of MSCs in the presence of primary osteosarcoma may be due to non-specific chemokine receptor interactions and the influence of growth factors such as VEGF [26]. Nonetheless, the influence of MSCs on primary tumor growth and metastatic disease may differ depending on the degree of tumor burden (microscopic or gross) and other *in vivo* factors.

FIGURES

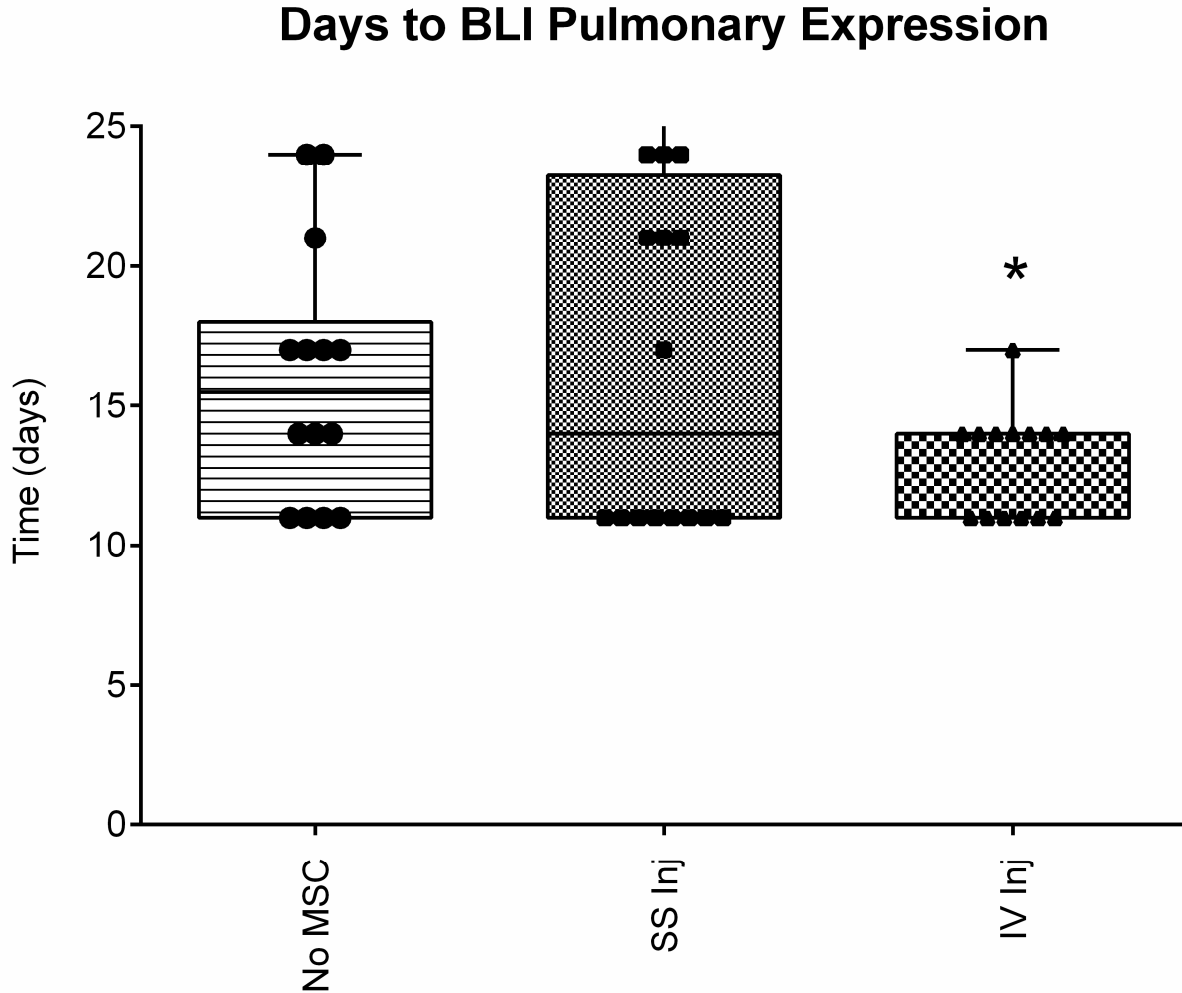


Figure 4.3 – 1: The time to first detection of pulmonary disease using bioluminescent (BLI) imaging after amputation of the primary tumor was measured and compared across treatment groups. Mice were treated with either an injection of MSCs in the surgical site, an injection of MSCs in the tail vein, or received no treatment. There was a significantly shorter time to detection in the intravenous treatment group compared to the surgical site group and no MSC group (“*”; $p=0.022$) using Welch’s test.

Mean Number of Pulmonary Metastatic Nodules

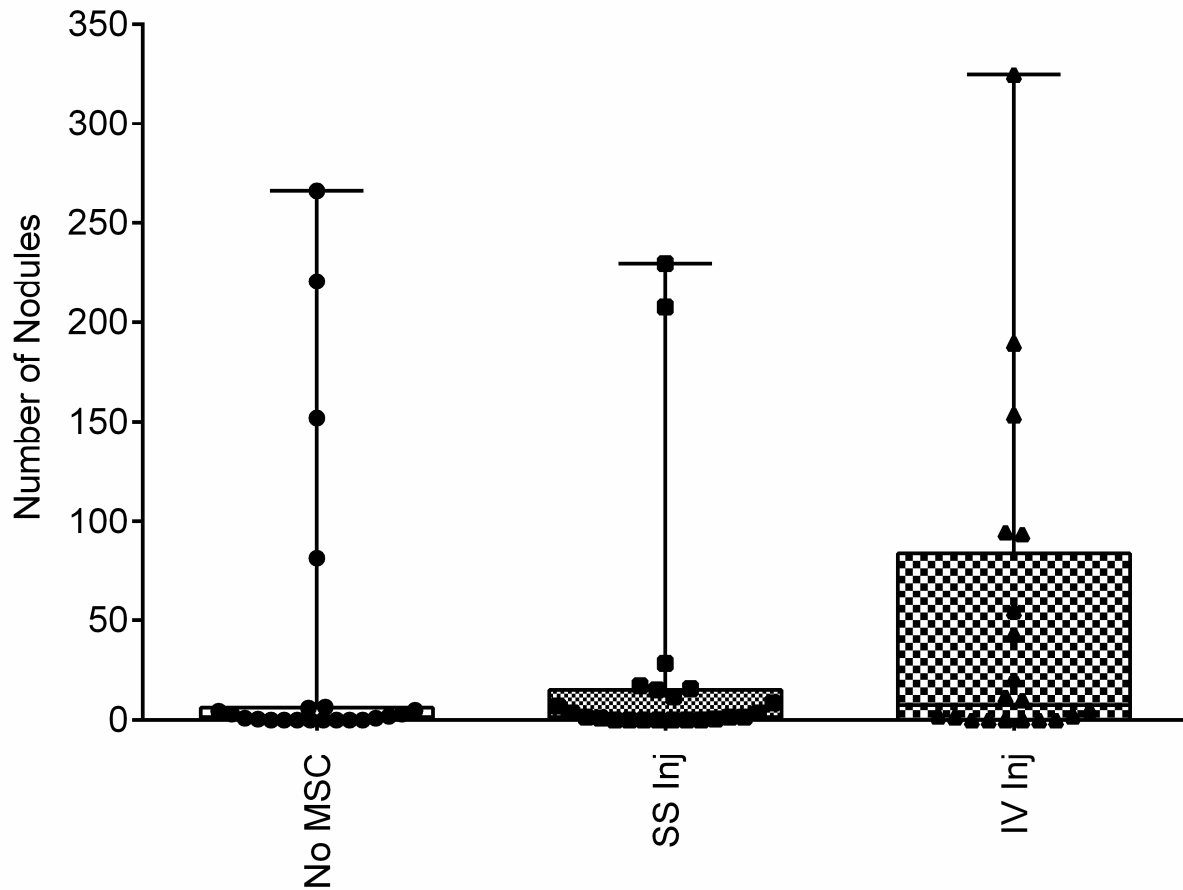


Figure 4.3 – 2: Mean number of pulmonary metastatic nodules versus treatment groups for all mice. Mice were treated with either an injection of MSCs in the surgical site, an injection of MSCs in the tail vein, or received no treatment. There was no difference between groups ($p=0.52$) using ANOVA test.

Pulmonary Metastatic Tumor Area as a Percentage of Total Lung Area

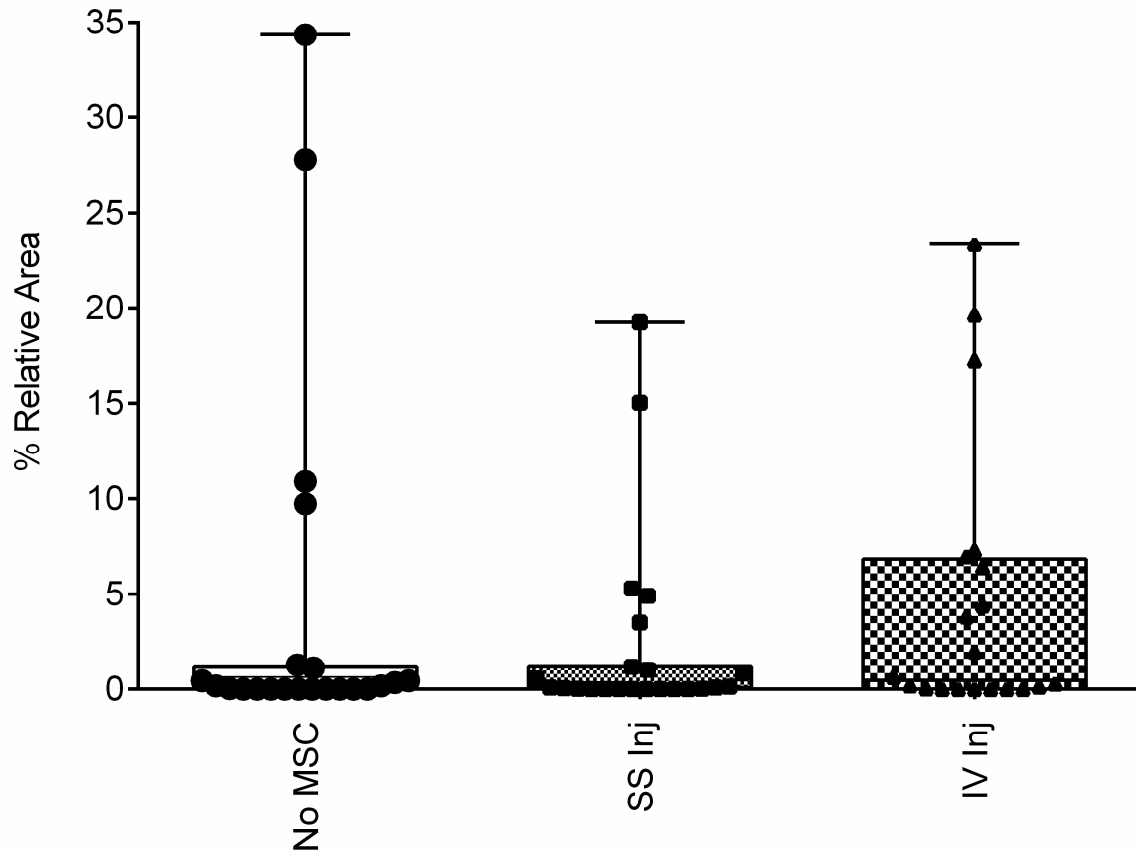


Figure 4.3 – 3: The area of each pulmonary nodule from mice was measured and combined. This value was then compared against the total lung area for each lobe to determine what percentage of the lung was tumor for each treatment group. Mice were treated with either an injection of MSCs in the surgical site, an injection of MSCs in the tail vein, or received no treatment. There was no difference between groups ($p=0.55$) using ANOVA test.

REFERENCES

1. Berlin O, Samid D, Donthineni-Rao R, Akeson W, Amiel D, Woods VL, Jr. Development of a novel spontaneous metastasis model of human osteosarcoma transplanted orthotopically into bone of athymic mice. *Cancer Res.* 1993;53:4890-4895.
2. Bian Z-Y, Fan Q-M, Li G, Xu W-T, Tang T-T. Human mesenchymal stem cells promote growth of osteosarcoma: Involvement of interleukin-6 in the interaction between human mesenchymal stem cells and Saos-2. *Cancer Science.* 2010;101:2554-2560.
3. Coathup MJ, Kalia P, Konan S, Mirza K, Blunn GW. A comparison of allogeneic and autologous mesenchymal stromal cells and osteoprogenitor cells in augmenting bone formation around massive bone tumor prostheses. *Journal of Biomedical Materials Research Part A.* 2013;101A:2210-2218.
4. Comstock KE, Hall CL, Daignault S, Mandlebaum SA, Yu C, Keller ET. A bioluminescent orthotopic mouse model of human osteosarcoma that allows sensitive and rapid evaluation of new therapeutic agents *In vivo.* *In vivo.* 2009;23:661-668.
5. Di Bella C, Aldini NN, Lucarelli E, Dozza B, Frisoni T, Martini L, Fini M, Donati D. Osteogenic Protein-1 Associated with Mesenchymal Stem Cells Promote Bone Allograft Integration. *Tissue Engineering Part A.* 2010;16:2967-2976.
6. Dupont KM, Sharma K, Stevens HY, Boerckel JD, García AJ, Guldberg RE. Human stem cell delivery for treatment of large segmental bone defects. *Proceedings of the National Academy of Sciences of the United States of America.* 2010;107:3305-3310.
7. Granero-Moltó F, Weis JA, Miga MI, Landis B, Myers TJ, O'Rear L, Longobardi L, Jansen ED, Mortlock DP, Spagnoli A. Regenerative Effects of Transplanted Mesenchymal Stem Cells in Fracture Healing. *Stem cells (Dayton, Ohio).* 2009;27:1887-1898.
8. Kalia P, Bhalla A, Coathup MJ, Miller J, Goodship AE, Blunn GW. Augmentation of massive implant fixation using mesenchymal stem cells. *Journal of Bone & Joint Surgery, British Volume.* 2006;88-B:392.
9. Karnoub AE, Dash AB, Vo AP, Sullivan A, Brooks MW, Bell GW, Richardson AL, Polyak K, Tubo R, Weinberg RA. Mesenchymal stem cells within tumour stroma promote breast cancer metastasis. *Nature.* 2007;449:557-563.
10. Keibl C, Fögl A, Zanoni G, Tangl S, Wolbank S, Redl H, van Griensven M. Human adipose derived stem cells reduce callus volume upon BMP-2 administration in bone regeneration. *Injury.* 2011;42:814-820.
11. Khanna C, Prehn J, Yeung C, Caylor J, Tsokos M, Helman L. An orthotopic model of murine osteosarcoma with clonally related variants differing in pulmonary metastatic potential. *Clin Exp Metastasis.* 2000;18:261-271.
12. Liu X, Li X, Fan Y, Zhang G, Li D, Dong W, Sha Z, Yu X, Feng Q, Cui F, Watari F. Repairing goat tibia segmental bone defect using scaffold cultured with mesenchymal stem cells. *Journal of Biomedical Materials Research Part B: Applied Biomaterials.* 2010;94B:44-52.
13. Luu HH, Kang Q, Park JK, Si W, Luo Q, Jiang W, Yin H, Montag AG, Simon MA, Peabody TD, Haydon RC, Rinker-Schaeffer CW, He TC. An orthotopic model of human osteosarcoma growth and spontaneous pulmonary metastasis. *Clin Exp Metastasis.* 2005;22:319-329.
14. Miretti S, Roato I, Tauli R, Ponzetto C, Cilli M, Olivero M, Di Renzo MF, Godio L, Albin A, Buracco P, Ferracini R. A Mouse Model of Pulmonary Metastasis from Spontaneous Osteosarcoma Monitored *In Vivo* by Luciferase Imaging. *PLoS ONE.* 2008;3:e1828.

15. Muehlberg FL, Song Y-H, Krohn A, Pinilla SP, Droll LH, Leng X, Seidensticker M, Ricke J, Altman AM, Devarajan E, Liu W, Arlinghaus RB, Alt EU. Tissue-resident stem cells promote breast cancer growth and metastasis. *Carcinogenesis*. 2009;30:589-597.
16. Mueller F, Fuchs B, Kaser-Hotz B. Comparative Biology of Human and Canine Osteosarcoma. *Anticancer Research*. 2007;27:155-164.
17. Muscolo DL, Ayerza M, Aponte-Tinao L, Farfalli G. Allograft Reconstruction After Sarcoma Resection in Children Younger Than 10 Years Old. *Clinical Orthopaedics and Related Research*. 2008;466:1856-1862.
18. Ogilvie CM, Crawford EA, Hosalkar HS, King JJ, Lackman RD. Long-term results for limb salvage with osteoarticular allograft reconstruction. *Clin Orthop Relat Res*. 2009;467:2685-2690.
19. Perrot P, Rousseau J, Bouffaut A-L, Rédini F, Cassagnau E, Deschaseaux F, Heymann M-F, Heymann D, Duteille F, Trichet V, Gouin F. Safety Concern between Autologous Fat Graft, Mesenchymal Stem Cell and Osteosarcoma Recurrence. *PLoS ONE*. 2010;5:e10999-e10999.
20. Picci P. Osteosarcoma (Osteogenic sarcoma). *Orphanet Journal of Rare Diseases*. 2007;2:6.
21. Ramseier LE, Malinin TI, Temple HT, Mnaymneh WA, Exner GU. Allograft reconstruction for bone sarcoma of the tibia in the growing child. *Journal of Bone & Joint Surgery, British Volume*. 2006;88-B:95-99.
22. Sottnik JL, Duval DL, J. Ehrhart E, Thamm DH. An orthotopic, postsurgical model of luciferase transfected murine osteosarcoma with spontaneous metastasis. *Clinical & Experimental Metastasis*. 2010;27:151-160.
23. Tsukamoto S, Honoki K, Fujii H, Tohma Y, Kido A, Mori T, Tsujiuchi T, Tanaka Y. Mesenchymal stem cells promote tumor engraftment and metastatic colonization in rat osteosarcoma model. *International journal of oncology*. 2012;40:163-169.
24. Withrow SJ, Powers BE, Straw RC, Wilkins RM. Comparative aspects of osteosarcoma. Dog versus man. *Clin Orthop Relat Res*. 1991:159-168.
25. Xu W-t, Bian Z-y, Fan Q-m, Li G, Tang T-t. Human mesenchymal stem cells (hMSCs) target osteosarcoma and promote its growth and pulmonary metastasis. *Cancer Letters*. 2009;281:32-41.
26. Zhang P, Dong L, Yan K, Long H, Yang TT, Dong MQ, Zhou Y, Fan QY, Ma BA. CXCR4-mediated osteosarcoma growth and pulmonary metastasis is promoted by mesenchymal stem cells through VEGF. *Oncol Rep*. 2013;30:1753-1761.

Chapter 5: Influence of Concurrent Treatment of Mesenchymal Stromal Cells and Methotrexate on Long-Term Pulmonary Metastases Following Removal of Primary Osteosarcoma

5.1 Introduction

Chemotherapy treatment in combination with surgical removal of the primary tumor is the standard of care for osteosarcoma [2]. Given the influence of intravenous delivery of MSCs on pulmonary disease burden we found in the previous study, we felt it important to conduct a longer term study to ascertain the influence of intravenously delivered MSCs on the development of pulmonary metastasis, with and without the concurrent treatment of chemotherapy as well as the influence of chemotherapy alone in our model. In this follow-on pilot study, we therefore explored whether chemotherapy would ameliorate the effects of intravenous MSC treatment on pulmonary disease.

Methotrexate (MTX) is a commonly used chemotherapy drug for osteosarcoma metastasis treatment in humans. Therefore, we elected to use MTX in a long-term metastasis study in which we endeavored to determine if the drug would influence the number of pulmonary nodules noted in mice treated with MTX alone, MTX and intravenous MSCs, MSCs alone or no additional treatment following primary tumor removal.

Given our previous findings, we hypothesized that mice treated with MTX chemotherapy would have fewer pulmonary metastatic nodules than mice that did not receive MTX and that mice treated with intravenous MSCs alone would have the highest number of pulmonary nodules compared with mice in other groups.

5.2 Materials and Methods

5.2.1 Cell Lines

DLM8-Luc-M1 cells were as previously described in section 3.4.1 of Chapter 3 and resuspended into DMEM without supplements for injections.

Adipose-derived mesenchymal stromal cells used for the experiment were harvested and cultured as previously described in section 3.5.2.1 of Chapter 3. Cells from passage 2-3 were resuspended in PBS with 10% heparin for injection and utilized for all experiments.

5.2.2 Animals

All animal studies were performed as previously described in section 3.7.1.2 of Chapter 3. Mice were monitored following procedures daily for 72 hours and three to seven times weekly thereafter for evidence of morbidity related to the primary tumor or metastases.

5.2.3 Establishment of primary tumor and surgical methods

DLM8-luc-M1 tumor cells were washed twice before being resuspended in HBSS. Mice (n=20) were prepared and injected as described above in section 3.5.2.3 of Chapter 3.

Ten days following tumor inoculation, mice were prepared for surgery and the tumor bearing limb was amputated by a coxo-femoral disarticulation as described previously in section 3.3.2.5 of Chapter 3. Tumor bearing limbs were collected, formalin fixed, and decalcified for histological evaluation.

5.2.4 Mesenchymal Stromal Cell Treatment

To evaluate the influence of adipose-derived mesenchymal stromal cells (AD-MSC) and chemotherapy on pulmonary metastatic osteosarcoma, twenty-four hours after the removal of the primary tumor, mice were randomly assigned to either an injection of MSCs intravenously through the tail vein (n=12), or a control group with no AD-MSCs (n=8). Mice in the AD-MSC treatment groups received one injection of 5×10^5 AD-MSCs in sterile PBS containing 100 units/mL Heparin and were allowed to recover at room temperature in a clean cage.

5.2.5 Chemotherapy Treatment

To assess the efficacy of chemotherapy treatment when given in the presence of mesenchymal stromal cells, mice in each treatment group were further divided between mice receiving no MSCs or chemotherapy, mice receiving MSCs alone, mice receiving MTX chemotherapy alone, and mice receiving MTX chemotherapy along with MSCs. Methotrexate (Accord Healthcare, Inc, Durham, NC) was adjusted for the weight of each mouse and a clinically relevant dosage (25 mg/kg methotrexate [1]) was delivered intraperitoneally using a 29 ½ G insulin needle within three hours of MSC delivery. A second weight adjusted dosage was delivered one week following the first treatment.

5.2.6 Bioluminescent Imaging

Development of the primary tumor was tracked using bioluminescent imaging on the IVIS 100 system as previously described in section 3.2.2.5 of Chapter 3. Images were analyzed using Living Image Software (Living Image 4.2; PerkinElmer, Waltham, USA) for luciferase activity and image analysis was repeated at days 3 and 7. Following removal of the primary tumor, chest images were obtained weekly as well as on day 31 post inoculation to track development and progression of pulmonary metastatic disease. Mice were euthanized after a final image at 75 days.

5.2.8 Statistical Computations

A Fisher's Exact Test was utilized to assess presence of disease. ANOVA test and unpaired t-test were used to compare quantitative data; mean \pm SD was reported. For all tests, a p-value of less than 0.05 was considered statistically significant.

5.3 Results

A total of 20 mice developed primary tumors and were included in the 75 day analysis. Mice that did not develop primary tumors or died acutely following injection of MSCs were not included.

The final distribution of mice by treatment group was as follows: MSCs alone (n=7), MTX alone (n=5), MTX chemotherapy along with MSCs (n=3), and control (no MSCs or chemotherapy) (n=5).

Mice treated with methotrexate or with methotrexate along with MSCs had no evidence of pulmonary nodules. Forty-three percent of MSC treated mice had pulmonary disease and 40% of untreated control mice had pulmonary disease. A statistical difference was not noted when compared to MSCs alone (p=0.246) or controls with no treatment (p=0.295). There was also no difference in the mean amount of pulmonary nodules present between MTX alone ($\mu=0$), MTX + MSC ($\mu=0$), MSC ($\mu = 12.1, \sigma = 24.2$), or untreated controls ($\mu = 1.1, \sigma = 1.6$) (p=0.44) (**Figure 5.3 – 1**).

5.4 Conclusions and Discussion

In this study, small animal number may have reduced the ability to get significance between groups. Although not significant, the group treated with MSCs alone had the highest number of metastatic nodules. The trend toward higher numbers of pulmonary nodules in mice treated with intravenous MSCs was consistent with the findings in Chapter 4. Interestingly, there were no metastatic nodules in mice receiving MTX treatment, whether or not they received MSCs, indicating that the use of chemotherapy may ameliorate the possible promotional effect of MSCs on pulmonary metastatic disease burden. Using a larger sample size would be of interest to determine whether these results remain consistent when more mice are used. A power calculation shows an n = 34 per group would be needed ($\sigma_1 = 24.18, \sigma_2 = 0, \delta = 12.14, \alpha = 0.05$) to reach 80% power.

If these results are validated using larger animal numbers, biomedical engineers and clinicians may be able to safely use mesenchymal stromal cells in conjunction with standard

chemotherapy treatments such as methotrexate to improve bone healing in patients receiving a limb reconstruction following removal of primary osteosarcoma.

FIGURES

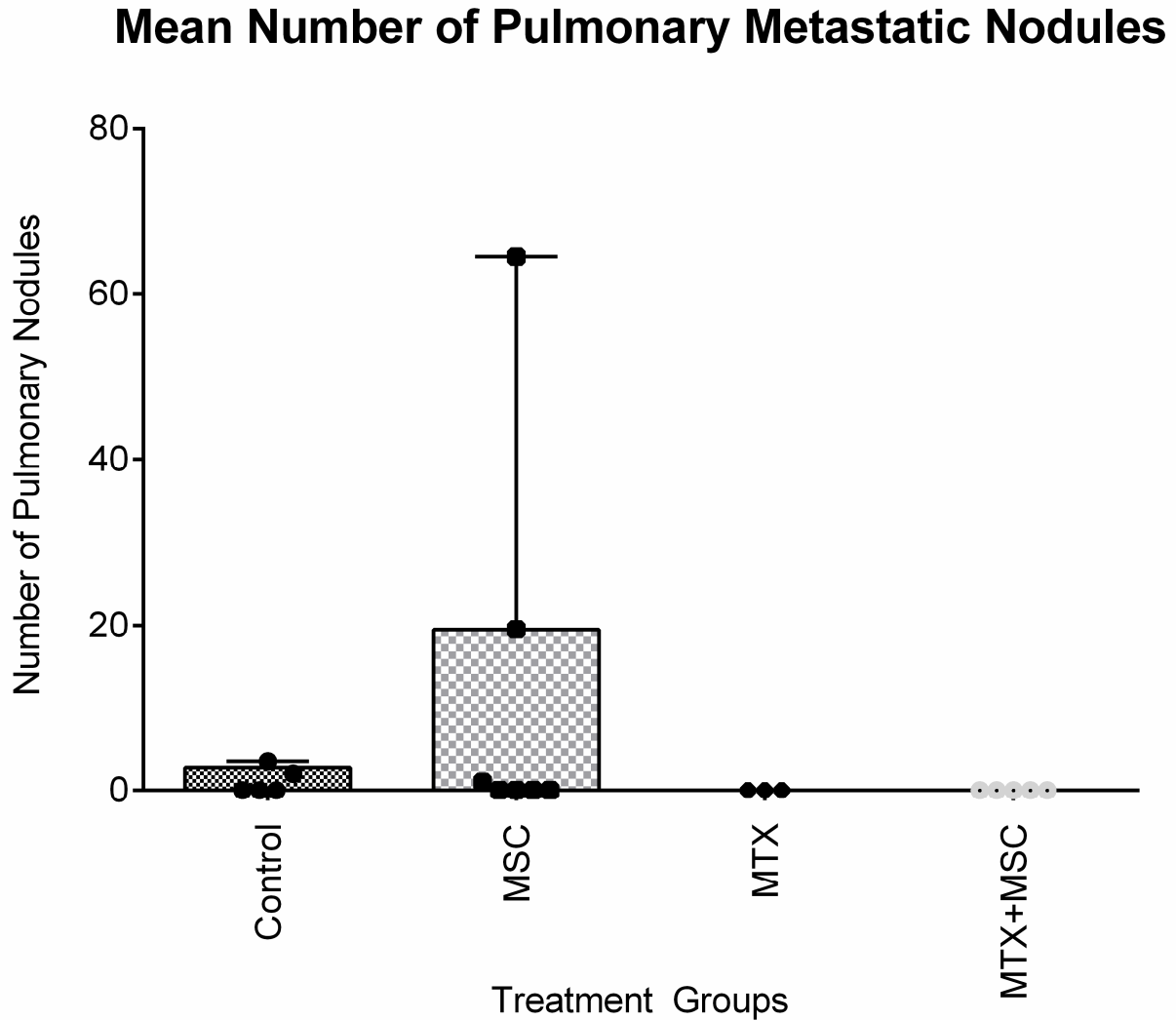


Figure 5.3 – 1: Quantification of mean pulmonary metastatic nodules was not different between mice that had no treatment, mice treated with mesenchymal stromal cells (MSC), mice treated with methotrexate (MTX), or mice treated with a combination of MTX along with MSCs ($p = 0.44$) using ANOVA. Of clinical relevance, however, was the lack of any pulmonary disease in mice treated with MTX.

REFERENCES

1. Huysentruyt LC, Shelton LM, Seyfried TN. Influence of methotrexate and cisplatin on tumor progression and survival in the VM mouse model of systemic metastatic cancer. *Int J Cancer*. 2010;126:65-72.
2. Withrow SJ, Wilkins RM. Cross talk from pets to people: translational osteosarcoma treatments. *ILAR journal / National Research Council, Institute of Laboratory Animal Resources*. 2010;51:208-213.

Chapter 6: Do Mesenchymal Stromal Cells Delivered Intravenously or into a Surgical Site Promote Murine Osteosarcoma Local Recurrence?

6.1 Introduction

Several murine models of osteosarcoma have been developed to aid in understanding the behavior of osteosarcoma [6, 8-10, 13, 15]; however, few have focused on the issue of tumor recurrence at the surgery site. Limitations of current models include the use of athymic strains of mice, site of primary tumor inoculation, tracking mechanisms, and genetic mismatch [1, 5]. Further, to our knowledge, none of these models have addressed the use of mesenchymal stromal cells as a treatment method following removal of the primary tumor.

The purpose of this study was to utilize the newly developed local recurrence model above to determine the influence of mesenchymal stromal cells on residual tumor cells left in the surgical site following a narrow margin amputation of a primary osteosarcoma tumor. The study stimulates the situation in which a patient undergoing limb reconstruction is treated with MSCs during the course of surgery after the primary tumor is removed.

6.2 Materials and Methods

6.2.1 Cell Line

DLM8-Luc-M1 cells were cultured as previously described in section 3.2.2.1 of Chapter 3.

AD-MSCs harvested from C3H mice as previously described were utilized for the experiment.

Cells were cultured as previously described in section 3.5.2.1 of Chapter 3. Passage three cells were resuspended in PBS with 10% heparin for injection.

6.2.2 Animals

Animal care and use was approved by the local Institute for Animal Care and Use Committee.

Female 8-10 week old C3H mice (National Institutes of Health, Bethesda, MD, USA) were housed under standard laboratory animal conditions. Surgical and injection sites were prepared

as previously described in section 3.7.1.2 of Chapter 3. Post-operative care consisted of recovery in a warm cage and a subcutaneous injection of 1.0 mL sterile saline. Mice were monitored following procedures daily for 3 days, then three times weekly to assess for evidence of primary tumor formation as well as local recurrence and metastatic disease.

6.2.3 Primary Tumor Formation

DLM8-luc-M1 cells were prepared as previously described in section 3.5.2.3 of Chapter 3. A total of 1×10^6 DLM8-luc-M1 cells in 30ul HBSS were injected into the medullary cavity of the tibia over a period of 30 seconds.

6.2.4 Characterization of primary tumor

In order to track the growth of the primary tumor, mice were imaged with an IVIS 100 imaging system 24 hours following tumor cell injection and then twice weekly until amputation as previously described in section 3.2.2.5 of Chapter 3. A region of interest was obtained and compared using Living Image software to evaluate tumor growth over time. Primary tumor bearing limbs were harvested at the time of amputation, formalin fixed, decalcified, paraffin embedded, and sectioned for histological evaluation to confirm the presence of a primary tumor and histological evidence of incomplete margins

6.2.5 Surgical Procedure

Ten days after tumor injection, mice underwent a narrow margin amputation of the tumor bearing limb. Mice were prepared as described above in section 3.7.1.2 of Chapter 3; anesthesia was induced and maintained using a 3% isoflurane - oxygen mixture. Narrow-margin amputation of tumor bearing limbs was performed as described in section 3.8.2.5 of Chapter 3 just proximal to the palpable tumor.

6.2.6 Mesenchymal Stromal Cell Treatment

Following narrow-margin amputation, mice were randomized into one of 3 treatment groups: injection of AD-MSCs into the surgical site (n = 14), intravenous (IV) injection of AD-MSCs via the tail vein (n = 17), or a control group receiving no MSCs (n = 16). AD-MSC treated groups received one injection of 5×10^5 AD-MSCs in sterile PBS (+ 100 units/mL Heparin for IV group) twenty-four hours after amputation and were allowed to recover at room temperature in a clean cage.

6.2.6 Characterization of Gross Local Recurrence and Metastasis

Mice were assessed 4 hours after amputation using bioluminescent imaging to determine whether there was expression in the residual limb. They were imaged again at 4 days, 1, 2, 3, and 4 weeks for a total of six images of residual limbs to evaluate local recurrence. All animals were subjected to a final bioluminescent image immediately prior to euthanasia. The surgical site, remaining limb and hemipelves were harvested for histological evaluation, formalin fixed and decalcified. Recurrent tumors were measured using calipers (Absolute Digimatic, Mitutoyo Corp, Kawasaki, Japan) to determine tumor size in the medial-lateral and cranial-caudal dimensions prior to placement in formalin for tissue processing. The longest dimension and the tumor volume were averaged, expressed as means, and compared between treatment groups. Volume was estimated using a formula from Comstock, et al [4].

$$Tumor\ volume = \frac{(Long\ dimension) * (Short\ dimension)^2}{2}$$

6.2.7 Histology

Specimens from the primary site and residual femur were sliced longitudinally and one to two sections, 20 μ m apart, were stained with hematoxylin and eosin and examined for the presence

of primary and local tumor recurrence. Presence or absence of local recurrence was compared between treatment groups.

6.2.8 Statistical Analysis

Presence of disease was analyzed using Fisher's Exact Test. The longest dimension of the tumor was compared using ANOVA test and t-test; results were expressed as means \pm SD per treatment group. Kruskal-Wallis test and Mann-Whitney test were used to compare tumor volume and medians with 95% CI was reported (GraphPad, La Jolla, CA). For all tests, a p-value of less than 0.05 was considered statistically significant.

6.3 Results

6.3.1 Intra-Tibial Injections and Primary Tumor Characterization

Bioluminescent intensity increased in the primary site leading up to amputation. Forty-seven mice (96%) developed primary tumors, completed the in-life portion of the study, and were used for analysis.

6.3.2 Amputation and Characterization of Gross Local Recurrence and Metastasis

Amputation was completed with narrow margins. This anatomical location ranged along the femur from a femoral-tibial disarticulation to a coxo-femoral disarticulation based on tumor size and proximal margins. Twenty-nine mice (62%) had evidence of local recurrence (**Figure 6.3 – 1**). Eighteen mice (38%) exhibited no evidence of local recurrence, defined as gross or microscopic evidence of recurrent tumor. In nineteen mice, the recurrent tumor was located in skeletal muscle surrounding the femur and not within the bone and in ten mice, tumor was located both within portions of femur and within adjacent soft tissue. There was no difference between mice who developed local recurrence and those who didn't with respect to MSC treatment group ($p=0.749$) (**Figure 6.3 – 2**). The mean longest dimension of tumor in mice with gross local recurrence was not different between treatment groups (17.51 ± 7.73 – intravenous

MSC group; 13.90 ± 4.93 – surgical site MSC group; 19.64 ± 4.21 – untreated group; $p=0.221$) but surgical site MSC treated mice had a significantly greater mean longest tumor dimension than mice with no MSCs ($p=0.047$) (**Figure 6.3 – 3**). Median tumor volume was also not different between treatment groups ($1235, 13-3317 \text{ mm}^3$) – intravenous MSC group; $838, 94-2119 \text{ mm}^3$ – surgical site MSC group; $1489, 1289-2162 \text{ mm}^3$ – untreated group; $p=0.584$) (**Figure 6.3 – 4**). Posteriori power calculations using longest dimension values ($\sigma_1 = 7.73, \sigma_2 = 4.21, \delta = 2.14, \alpha = 0.05$) indicated an $n = 108$ mice per group would be needed for 70% power and $n = 135$ for 80% power.

6.4 Conclusions and Discussion

Our results indicate that MSCs do not have a promotive effect on local recurrence in animal residual osteosarcoma setting when administered either intravenously or in the surgical site. We noted a significant difference in the longest dimension of the tumor between mice receiving MSCs into the surgical site and mice not treated with MSCs in that mice receiving MSCs delivered into the surgical site had a smaller mean longest tumor dimension as compared with untreated controls. This suggests that MSCs delivered into the surgical field in the presence of minimal residual disease may have protective effects. Other studies, described in Chapter 2.8, have also found that MSCs exerted an anti-tumor growth effect. The mechanism of action varies from blocking cell cycle progression to arresting cell proliferation to inducing apoptosis [3]. They have also been shown to inhibit Akt activation, which relates to tumor necrosis [7]. In this study, we did not explore the reasons why MSCs may reduce recurrent tumor burden in the surgical site but one of the above effects may have been a factor and further studies to identify the mechanism using larger animal numbers would be of great interest.

Osteosarcoma is the most common primary bone malignancy affecting humans and dogs [12, 14]. Treatment consists of neo-adjuvant chemotherapy and surgical removal of the primary

tumor. Despite successful surgical treatment of the primary tumor, in 4% of patients, local recurrence will result in the need for additional surgery [2, 11]. Accordingly, models of local recurrence that are able to more closely recapitulate the clinical situation are needed to identify novel treatments and evaluate safety of treatments that may be employed in a setting where residual microscopic disease may be present.

We have developed a unique model to explore the safety of therapeutic agents in sarcoma patients with several advantages over previously developed models. There have been other models of local recurrence including ones for *in vivo* tracking [10], syngeneic studies [1], and pulmonary metastasis [16]. Bell et al. [1] used a xenograft of the tumor implanted in the lateral gastrocnemius muscle as their primary tumor. Amputation was performed with microscopic margins remaining. Animals were treated with chemotherapy either pre-operatively, peri-operatively, or post-operatively or were given no chemotherapy as controls. Mice survived for up to 6 months before sacrifice. Limitations of the study were the inability to track tumor growth *in vivo*, the use of a xenograft for primary tumor formation, and the tumor line aggressiveness.

Geller et al. [5] created a human osteosarcoma model to assess the definition of a “wide excision”. The researchers used human tumor lines in SCID mice and after amputation, followed mice for six weeks. Chemotherapy treatment was given over a course of 4 weeks in a second experiment, with six more weeks of observation following. By measuring the exact distance of margins, they were able to determine a minimum distance for “safe” margins. However, their model did not have metastatic disease and was not performed in the presence of an intact immune system.

Limitations in these other models that were addressed in this one included the site of primary tumor inoculation, tracking mechanisms, and genetic mismatch [1, 5]. Disease progression could be tracked over time using bioluminescent imaging and primary tumors were created from

cells injected into an orthotopic site. This model resulted in a recurrence of the disease within 39 days post-tumor inoculation and allowed for the study of treatment effects on local recurrence of osteosarcoma in the surgical site.

The foremost limitation of these experiments was our ability to accurately assess recurrent tumor volume utilizing the measurement equipment on hand. In particular, accurate tumor volume was difficult to measure using calipers due to the irregular shape of the tumor development and differences in initial primary tumor anatomical location compared with a subcutaneous or intramuscular tumor. A more consistent means of measuring tumor volume, such as MR or CT, using 3D volumetric imaging to better assess total volume in non-spherical recurrent tumors, would be advantageous to better assess differences between groups.

Additionally, not all mice developed recurrent tumors and therefore, animal numbers were lower than planned. This loss of numbers could have led to a Type II error and in a larger project, we may have found a difference in treatment groups. Therefore repeating this study using larger numbers would be important to complete to assess whether there is truly no concern of local recurrence with the use of MSCs in the surgical site.

FIGURES

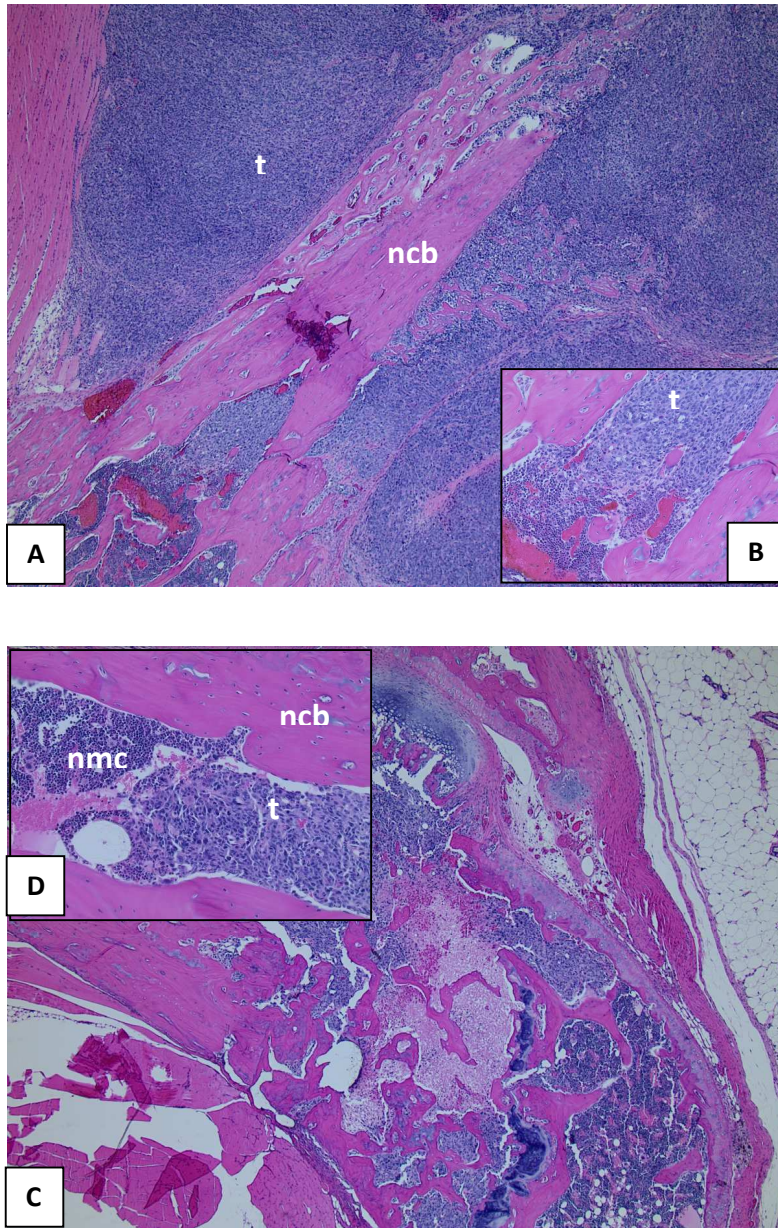
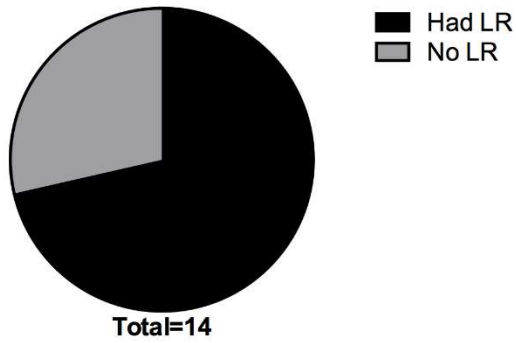
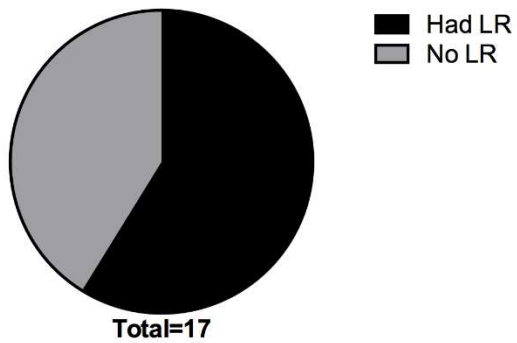


Figure 6.3 – 1: Histological conformation of primary tumor and local recurrence was conducted. (A) Primary tumor in the proximal tibia infiltrated the marrow canal and extended into the soft tissue; (B) close-up of the tumor. (C) Local recurrence was visible in the femoral marrow cavity and extended throughout the distal femur; (D) close-up of the tumor. (Stain, hematoxylin and eosin; original magnification, X2, X10; t = tumor, ncb = normal cortical bone, nmc = normal marrow canal).

Surgical Site MSC Injection



Intravenous MSC Injection



No MSC

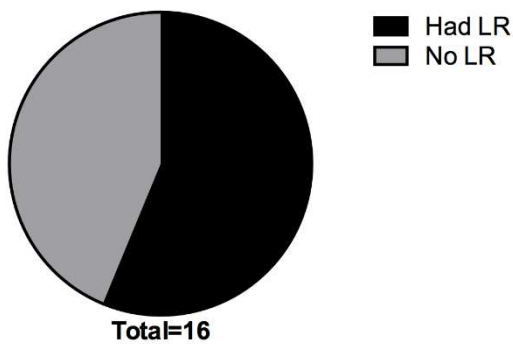


Figure 6.3 – 2: While more than 50% of mice in each group developed local recurrence (LR) of osteosarcoma following a narrow margin amputation, the amount of mice with local recurrence between MSC treatments was not different ($p=0.749$) using Fisher's Exact Test.

Comparison of Local Recurrence: Tumor Diameter

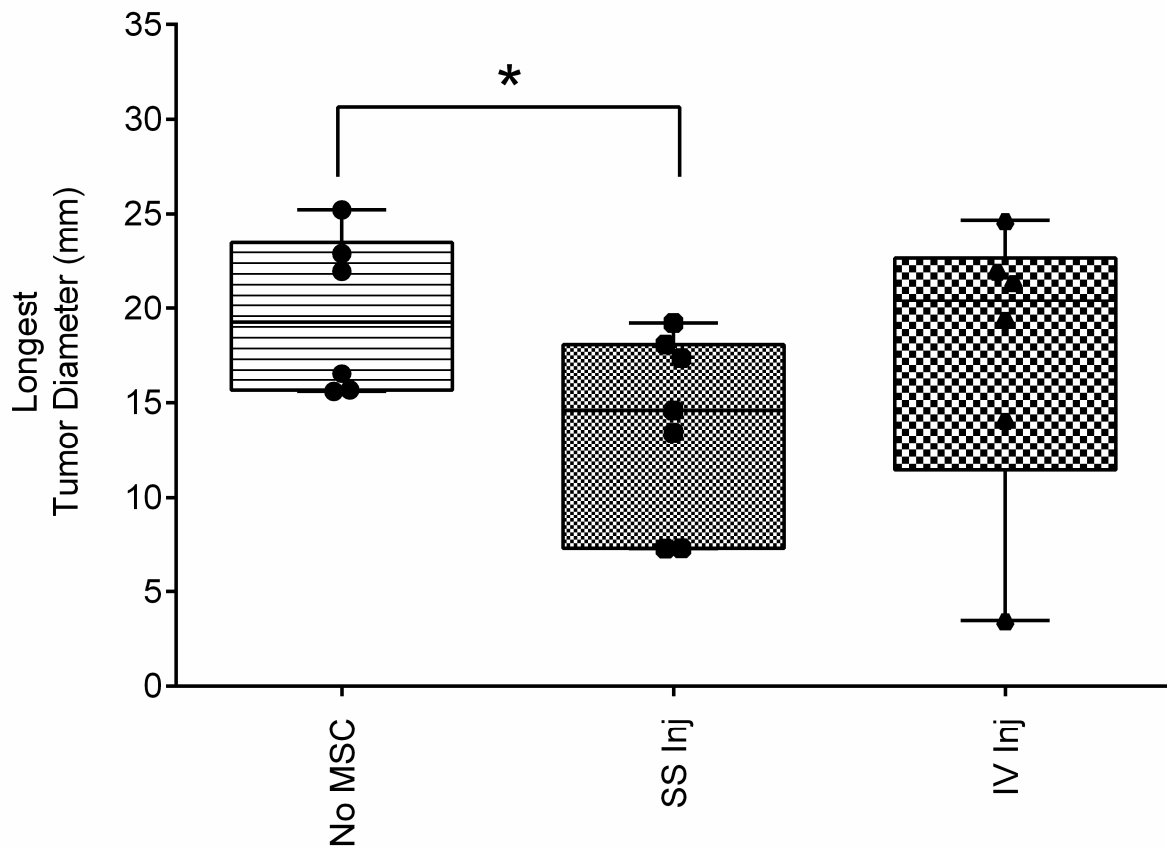


Figure 6.3 – 3: Caliper measurements of gross osteosarcoma local recurrence were completed to assess tumor size. Values were averaged for each treatment of either an injection of MSCs into the surgical site following narrow margin amputation, an injection of MSCs in the tail vein, or an untreated control group and compared. There was no difference in the longest dimension of the tumor between treatments ($p=0.221$). However, there was a difference in pairwise comparisons between the group receiving an injection into the surgical site and the group receiving no MSCs ($p=0.047$). ANOVA and unpaired Student's t-test were used for analysis.

Comparison of Local Recurrence: Tumor Volume

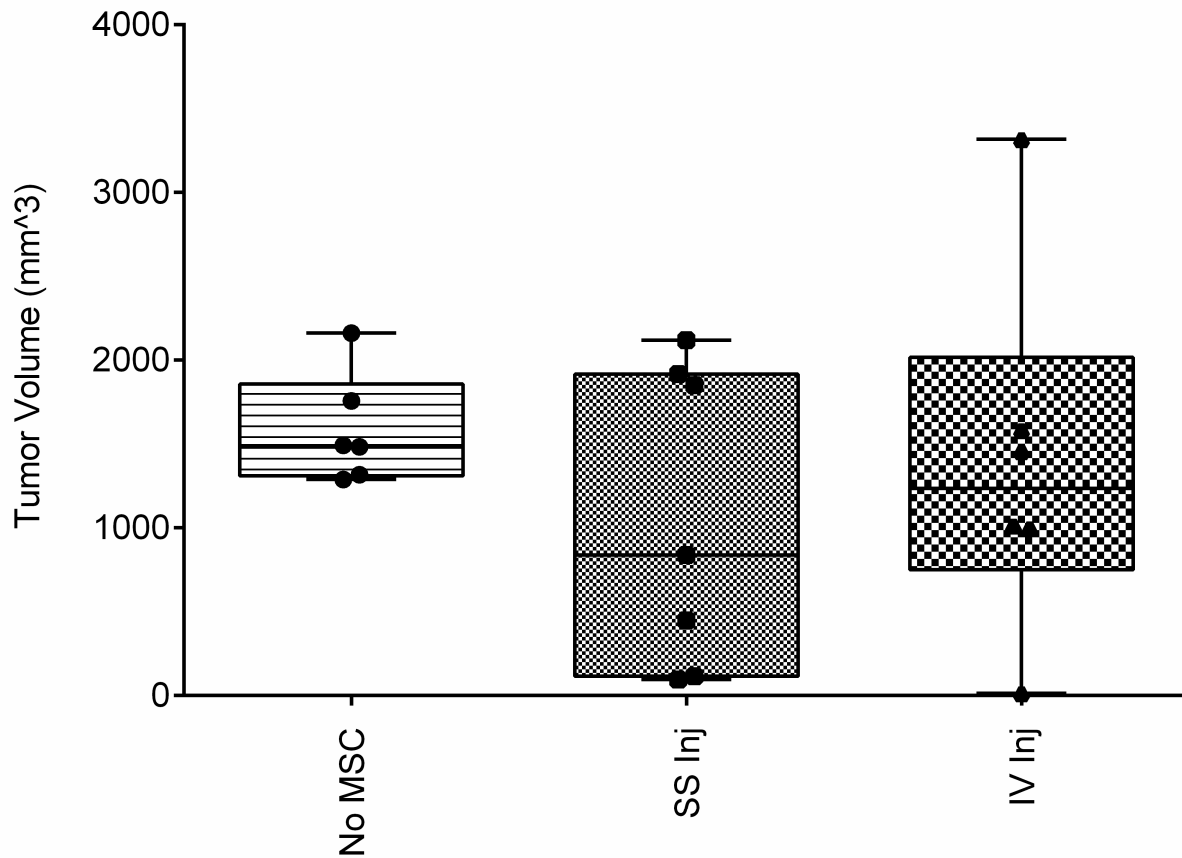


Figure 6.3 – 4: Extrapolation of caliper measurements in two anatomical dimensions into volume was completed through a published formula [4]. Values were averaged and compared for each treatment of either an injection of MSCs into the surgical site following narrow margin amputation, an injection of MSCs in the tail vein, or an untreated control group. There was no difference in the local recurrence tumor volume between treatments ($p=0.584$) using Kruskal Wallis test.

REFERENCES

1. Bell RS, O'Connor G, Bell DF, Jacob J. Effect of doxorubicin on local recurrence following marginal resection in the MGH-OGS murine model. *J Orthop Res.* 1990;8:105-118.
2. Bramer JA, Abudu AA, Grimer RJ, Carter SR, Tillman RM. Do pathological fractures influence survival and local recurrence rate in bony sarcomas? *Eur J Cancer.* 2007;43:1944-1951.
3. Bruno S, Collino F, Iavello A, Camussi G. Effects of Mesenchymal Stromal Cell-Derived Extracellular Vesicles on Tumor Growth. *Frontiers in Immunology.* 2014;5:382.
4. Comstock KE, Hall CL, Daignault S, Mandlebaum SA, Yu C, Keller ET. A bioluminescent orthotopic mouse model of human osteosarcoma that allows sensitive and rapid evaluation of new therapeutic agents In vivo. *In vivo.* 2009;23:661-668.
5. Geller DS, Singh M, Zhang W, Vilanueva-Siles E, Park A, Piperdi S, Gorlick R. Abstract 5034: Quantification of required surgical margins in a xenograft osteosarcoma model with and without single-agent chemotherapy. *Cancer Research.* 2013;73:5034.
6. Jia SF, Worth LL, Kleinerman ES. A nude mouse model of human osteosarcoma lung metastases for evaluating new therapeutic strategies. *Clin Exp Metastasis.* 1999;17:501-506.
7. Khakoo AY, Pati S, Anderson SA, Reid W, Elshal MF, Rovira II, Nguyen AT, Malide D, Combs CA, Hall G, Zhang J, Raffeld M, Rogers TB, Stetler-Stevenson W, Frank JA, Reitz M, Finkel T. Human mesenchymal stem cells exert potent antitumorigenic effects in a model of Kaposi's sarcoma. *The Journal of Experimental Medicine.* 2006;203:1235-1247.
8. Khanna C, Prehn J, Yeung C, Caylor J, Tsokos M, Helman L. An orthotopic model of murine osteosarcoma with clonally related variants differing in pulmonary metastatic potential. *Clin Exp Metastasis.* 2000;18:261-271.
9. Luu HH, Kang Q, Park JK, Si W, Luo Q, Jiang W, Yin H, Montag AG, Simon MA, Peabody TD, Haydon RC, Rinker-Schaeffer CW, He TC. An orthotopic model of human osteosarcoma growth and spontaneous pulmonary metastasis. *Clin Exp Metastasis.* 2005;22:319-329.
10. Miretti S, Roato I, Tauli R, Ponzetto C, Cilli M, Olivero M, Di Renzo MF, Godio L, Albini A, Buracco P, Ferracini R. A Mouse Model of Pulmonary Metastasis from Spontaneous Osteosarcoma Monitored *In Vivo* by Luciferase Imaging. *PLoS ONE.* 2008;3:e1828.
11. Nathan SS, Gorlick R, Bukata S, Chou A, Morris CD, Boland PJ, Huvos AG, Meyers PA, Healey JH. Treatment algorithm for locally recurrent osteosarcoma based on local disease-free interval and the presence of lung metastasis. *Cancer.* 2006;107:1607-1616.
12. Savage SA, Mirabello L. Using epidemiology and genomics to understand osteosarcoma etiology. *Sarcoma.* 2011;2011:548151.
13. Sottnik JL, Duval DL, J. Ehrhart E, Thamm DH. An orthotopic, postsurgical model of luciferase transfected murine osteosarcoma with spontaneous metastasis. *Clinical & Experimental Metastasis.* 2010;27:151-160.
14. Withrow SJ, Powers BE, Straw RC, Wilkins RM. Comparative aspects of osteosarcoma. Dog versus man. *Clin Orthop Relat Res.* 1991:159-168.
15. Yui Y, Itoh K, Yoshioka K, Naka N, Watanabe M, Hiraumi Y, Matsubara H, Watanabe K, Sano K, Nakahata T, Adachi S. Mesenchymal mode of migration participates in pulmonary metastasis of mouse osteosarcoma LM8. *Clin Exp Metastasis.* 2010;27:619-630.
16. Zhang S, Balch C, Chan MW, Lai H-C, Matei D, Schilder JM, Yan PS, Huang TH-M, Nephew KP. Identification and Characterization of Ovarian Cancer-Initiating Cells from Primary Human Tumors. *Cancer Research.* 2008;68:4311-4320.

Chapter 7: Influence of Concurrent Treatment of Mesenchymal Stromal Cells and Cisplatin on Survival Following Removal of Primary Osteosarcoma

7.1 Introduction

Current treatment of osteosarcoma utilizes the combined treatments of chemotherapeutic drugs, surgery, and radiation [2, 7]. In humans, the standard chemotherapy drugs utilized include cisplatin, methotrexate, ifosfamide, and doxorubicin [2]. Standard regimens include both neoadjuvant chemotherapy to target the primary tumor as well as adjuvant treatment to minimize metastases. This multi-modality treatment results in over 76% disease free survival rates at 5 years. [2].

Because of the potential ability of MSCs to aid in healing of large bone defects following tumor resection, the use of MSCs following surgery is attractive. However, as previously discussed in detail in chapter two, worrisome studies in which the interaction between chemotherapy and MSCs led to an increase in pulmonary disease, larger primary tumors and a resistance of the tumor to chemotherapy have been reported [4, 6].

Given our previous results, we elected to conduct a survival study to assess whether the influence of MSCs given intravenously would also translate to decreased survival times using the same residual pulmonary disease model and if the addition of cisplatin chemotherapy would influence survival. Cisplatin was selected as the drug of choice based on the aforementioned work in which it negatively interacted with MSCs as well as the common use of it in human treatment of osteosarcoma. No work has assessed cisplatin use in a minimal residual setting in conjunction with MSCs and a survival study was thought to be the most useful way to assess the concurrent use of cisplatin and MSCs in a model of minimal residual osteosarcoma.

Our hypotheses for the survival study were (1) that there would be no difference in survival between mice regardless of treatment, (2) there would be no difference in survival of untreated control mice and mice receiving cisplatin or cisplatin and MSCs, and (3) there would be no difference in survival of mice receiving MSCs alone compared with mice cisplatin or cisplatin and MSCs.

7.2 Materials and Methods

7.2.1 Cell Lines

DLM8-Luc-M1 cells were cultured as previously described in section 3.4.1 of Chapter 3. Cells at passage 15-22 were resuspended in DMEM without supplements for injections.

Adipose-derived mesenchymal stromal cells used for the experiment were harvested as previously described and expanded as previously described in section 3.5.2.1 of Chapter 3. Cells from passage 2-3 were resuspended in PBS with 10% heparin for injection and utilized for all experiments.

7.2.3 Animals

All animal studies were performed with approval of the Institutional Animal Care and Use Committee. Female 8-10 week old C3H mice were obtained from NIH (National Institutes of Health, Bethesda, MD, USA) and housed under standard laboratory animal conditions. Surgical and injection sites were prepared as previously described in section 3.7.1.2 of Chapter 3. Post-operative care included subcutaneous saline (1.0 mL) for hydration and recovery in a clean cage on a warming pad until ambulatory. Mice were monitored following procedures daily for 72 hours and three to seven times weekly thereafter for evidence of morbidity related to the primary tumor or metastases.

7.2.4 Establishment of primary tumor and surgical methods

DLM8-luc-M1 tumor cells were prepared as described in section 3.5.2.3 of Chapter 3. Mice (n=94) were prepared as described above, the needle was inserted through the cortex of the tibial crest oriented proximal to distal, and 1×10^6 cells in 30 μ L was injected.

Ten days following tumor inoculation, mice were prepared for surgery and the tumor bearing limb was amputated by a coxo-femoral disarticulation as described in section 3.3.2.5 of Chapter 3. Tumor bearing limbs were collected and preserved in formalin for analysis to confirm primary tumor formation.

7.2.5 Mesenchymal Stromal Cell Treatment

To evaluate the influence of adipose-derived mesenchymal stromal cells (AD-MSC) and chemotherapy on survival of metastatic osteosarcoma, twenty-four hours after the removal of the primary tumor, 35 mice were randomly assigned to either an injection of AD-MSCs intravenously through the tail vein (n=17), or a control group with no AD-MSCs (n=18). Mice in the AD-MSC treatment groups received one injection of 5×10^5 AD-MSCs in sterile PBS + 10% Heparin and were allowed to recover at room temperature in a clean cage.

7.2.6 Chemotherapy Treatment

To assess the efficacy of chemotherapy treatment when given in the presence of mesenchymal stromal cells, mice in each treatment group were further divided between those receiving no additional treatment (n=8), mice receiving MSCs alone (n=6), mice receiving cisplatin chemotherapy alone (n=10), and mice treated with both cisplatin chemotherapy and MSCs (n=11). Cisplatin was prepared and calculated by individual mouse weight. A dose of 8 mg/kg cisplatin [1] was delivered intraperitoneally using a 29 $\frac{1}{2}$ G insulin needle within three hours of MSC delivery. A second weight-adjusted dosage of 8 mg/kg was delivered one week following the first treatment.

7.2.7 Bioluminescent Imaging

Development of the primary tumor was tracked using bioluminescent imaging on the IVIS 100 system as previously described in section 3.2.2.5 of Chapter 3.

7.2.8 Survival Scoring Methodology

To determine when mice had become moribund, a scoring system was utilized (Appendix B) and mice were scored every 1-2 days. In brief, appearance, body weight, clinical signs, natural behavior, and provoked behavior were scored from 0-4 by two independent observers. Scores were added; based on the total value (Normal = 0-4, Near Moribund = 5-14, Moribund = 15-20), a plan was determined for each mouse.

7.2.9 Statistical Computations

A Kaplan-Meier survival curve with a Mantel Cox Regression analysis was utilized to determine differences in survival of mice between treatment groups. ANOVA, along with t-test, was used to compare the last score and Kruskal Wallis test, along with Mann-Whitney tests, were used for scores compared over the course of the study. For all tests, a p-value of less than 0.05 was considered statistically significant.

7.3 Results

A total of 35 mice were included in the survival study and all mice had histologic confirmation of primary tumor at the time of amputation.

There was a significant difference in survival scores between groups during the course of the study ($p=0.007$) (**Figure 7.3 – 1**). Additionally, pairwise comparisons on mean scores during the course of the study were significantly different between MSC, Cis, and Cis + MSC treated mice ($p=0.005$) and between Cis and MSC treated mice ($p=0.002$). There was no difference in the last obtained score between groups ($p=0.742$) or in pairwise comparisons (data not shown) (**Figure 7.3 – 2**).

Survival curves were compared between multiple treatment group scenarios. When looking at MSC treatment alone compared to control mice, the survival curves were significantly different ($p=0.036$) (**Figure 7.3 – 3**). A hazard ratio logrank analysis shows a 73% higher chance of death with MSC treatment compared with untreated controls (2.689; 95% CI: 1.248-15.78). Mice treated with MSCs had significantly different survival curves when compared concurrently with cisplatin alone and with cisplatin with MSC treatments ($p<0.001$) (**Figure 7.3 – 4**). Survival curves were significantly different as well when comparing untreated control mice with cisplatin alone and cisplatin with MSC treated mice ($p<0.001$) (**Figure 7.3 – 5**). When all treatment groups were compared together, there was a significant difference in the survival curve ($p<0.001$) (**Figure 7.3 – 5**).

7.4 Conclusions and Discussion

In this experiment, intravenous MSC increased the chance of early death relative to no treatment. Cisplatin therapy and cisplatin therapy plus MSC survival curves were significantly different relative to no treatment. When cisplatin was added to MSC therapy, the survival curves were no different than cisplatin alone indicating that the addition of cisplatin ameliorated the negative influence of intravenously delivered MSCs on survival. This result suggests that it may be possible to reduce the survival impact of MSCs in a patient with a history of cancer if chemotherapy treatment is given.

While we did see a difference in survival scoring throughout the study, this can be explained by the loss of mice – that is, as mice got sicker, scores went up and when they were euthanized, scores went back down in a cyclic pattern. The difference in survival, however, is a more important measure and we did see that mice treated with MSCs alone survived less time than other treatment groups, although the median time was not significantly different, the survival curves were. The important finding was the use of cisplatin in this model negated the reduced survival in MSC groups. In this model, we did not find that MSCs negatively impacted cisplatin

therapy; instead, we found that cisplatin treatment negated early death of mice treated with MSCs alone.

Chemotherapy treatment in combination with surgical removal of the primary tumor is the standard of care for osteosarcoma [7]. If MSCs are to be used in the course of treatment for patients with a history of osteosarcoma, the interaction between the cells and the drugs are important to understand. There are several studies published indicating an adverse interaction between chemotherapy, especially platinum based, and MSCs [4, 6]. Commonly used drugs for osteosarcoma treatment regimens include cisplatin [2, 3] in humans and carboplatin [5] in dogs. The purpose of this project was to gain an understanding of the susceptibility of DLM8-Luc-M1 cells to cisplatin and MSCs concurrently in a survival study. Our previous experiments in Chapter 4 had indicated that intravenous delivery of MSCs resulted in trends toward higher pulmonary disease burden in every outcome measured. While approaching significance, the variability between animals within treatment groups was too high to achieve significance.

Two papers mentioned previously also explored the relationship between MSCs and chemotherapy in a murine model. Roodhart et al. [4] utilized two *in vivo* murine models – one utilizing colon carcinoma and the other utilizing Lewis lung carcinoma. They tested the effects of an IV injection of MSCs immediately prior (< 3 hours) to cisplatin treatment and found that MSCs ameliorated the protective effects of cisplatin. However, if one treatment of MSC conditioned media and two treatments of cisplatin were given, the protective effects of cisplatin were restored. In a study by Tu et al, [6] an *in vitro* assessment of osteosarcoma and MSC interaction was completed to determine whether MSCs had an effect on apoptotic rate when osteosarcoma cells were exposed to cisplatin. The study results indicated that MSCs protected osteosarcoma cells from cytotoxic effects of cisplatin by producing IL-6 *in vitro*. In contrast to these studies, our study changed several variables. First, we removed the primary tumor before treating mice with either MSCs or cisplatin. Second, we used a syngeneic osteosarcoma cell

line *in vivo* for our experiment. Third, like in the second Roodhart et al. study, we treated mice with two rounds of cisplatin. Like them, we saw that cisplatin was able to increase survival time even when utilized concurrently with MSCs when it was given twice compared to one dosage of MSCs. Our study reflected the clinical treatment regimes in which multiple rounds of post-operative chemotherapy are given to patients and not just one single treatment. Further, like in a clinical situation, we removed our primary tumor before treating mice with MSCs.

While the use of MSCs intravenously is still contentious with regards to safe use in patients with a history of osteosarcoma, the use of cisplatin in this model alleviated a decrease in survival time. Further work with larger animal numbers may help to better determine if all unwanted effects from MSC use in a minimal residual tumor environment can be negated by the use of chemotherapy. If this proves to be the case, however, it is promising for engineers and clinicians looking to use mesenchymal stromal cells in conjunction with standard treatment to improve bone healing in patients receiving a limb reconstruction following removal of primary osteosarcoma.

FIGURES

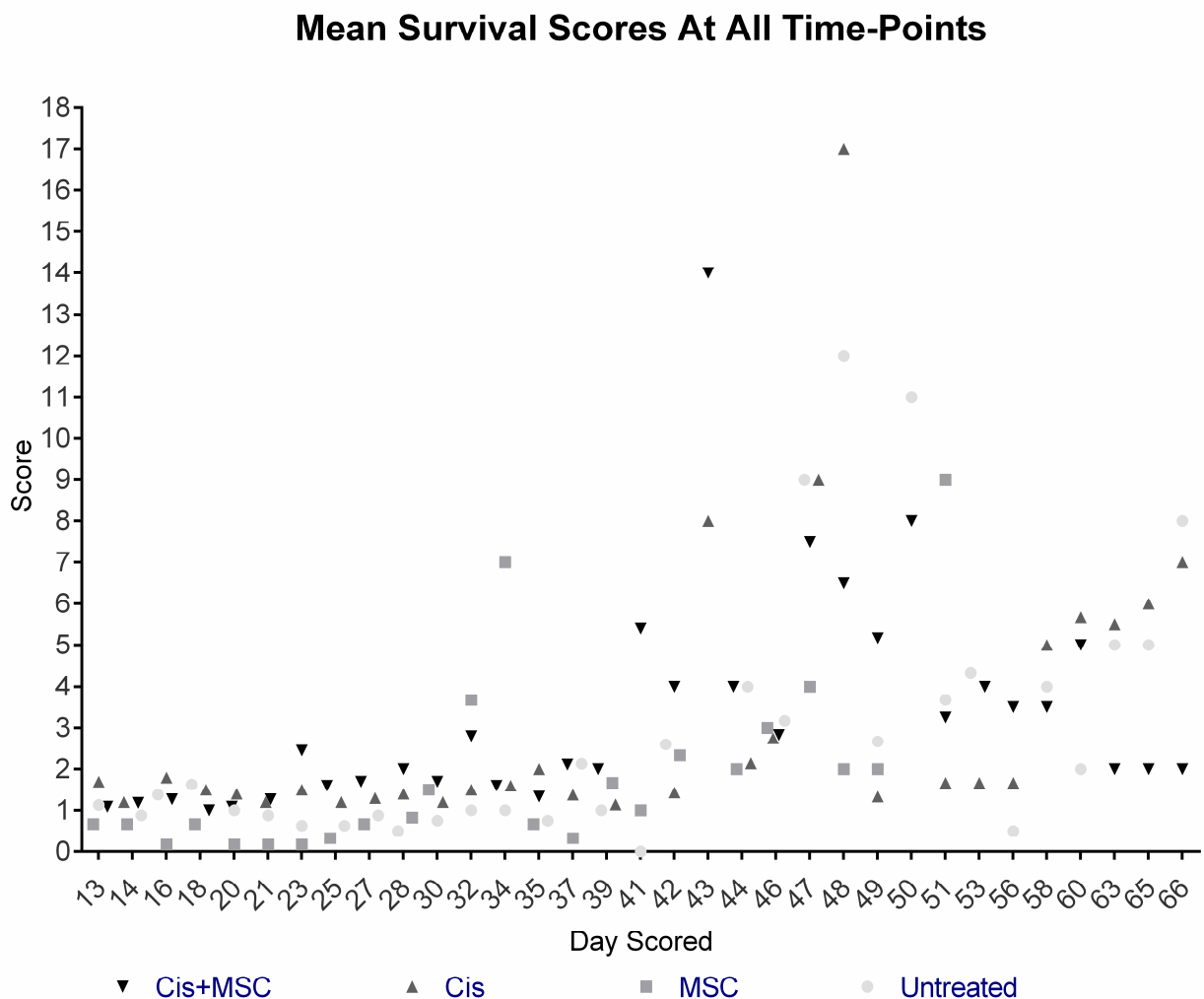


Figure 7.3 – 1: Mice were scored every 1-2 days to assess for tumor burden and determine a euthanasia time-point. The differences in treatment groups (untreated, MSCs alone, Cisplatin alone, Cisplatin + MSCs) was significant ($p=0.005$) using Kruskal Wallis test.

Comparison of Mean Scores at Euthanasia Between Treatment Groups

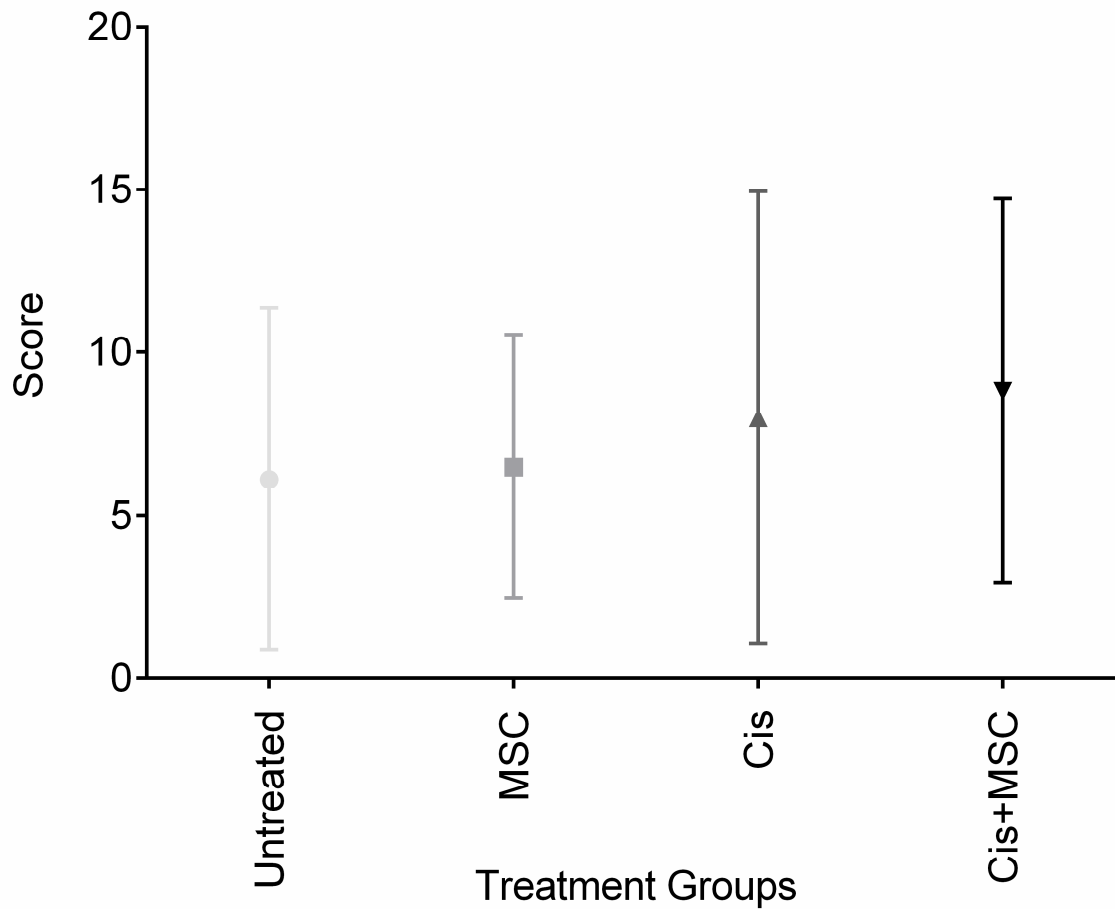


Figure 7.3 – 2: The euthanasia score of each mouse was averaged for each treatment group (untreated controls, mesenchymal stromal cells (MSC), cisplatin (Cis), or Cisplatin and MSCs and mean scores for each group were compared. There was no difference between treatments with respect to euthanasia score ($p=0.742$) using ANOVA test.

Comparison of Survival Estimates: Untreated vs MSC

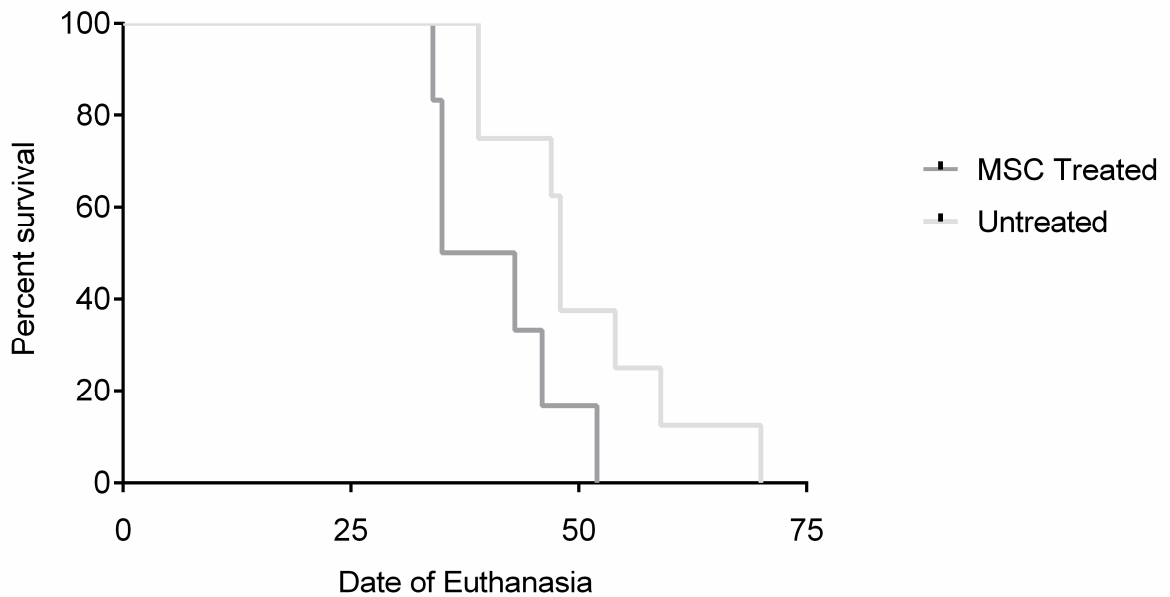


Figure 7.3 – 3: Kaplan Meier survival curves with a Mantel Cox Regression analysis were used to analyze the median survival times between untreated mice (control) compared to mice treated with mesenchymal stromal cells (MSC) alone. The survival curve of MSC alone mice was significantly shorter than control mice ($p=0.036$).

Comparison of Survival Estimates: MSC vs Cis vs Cis + MSC

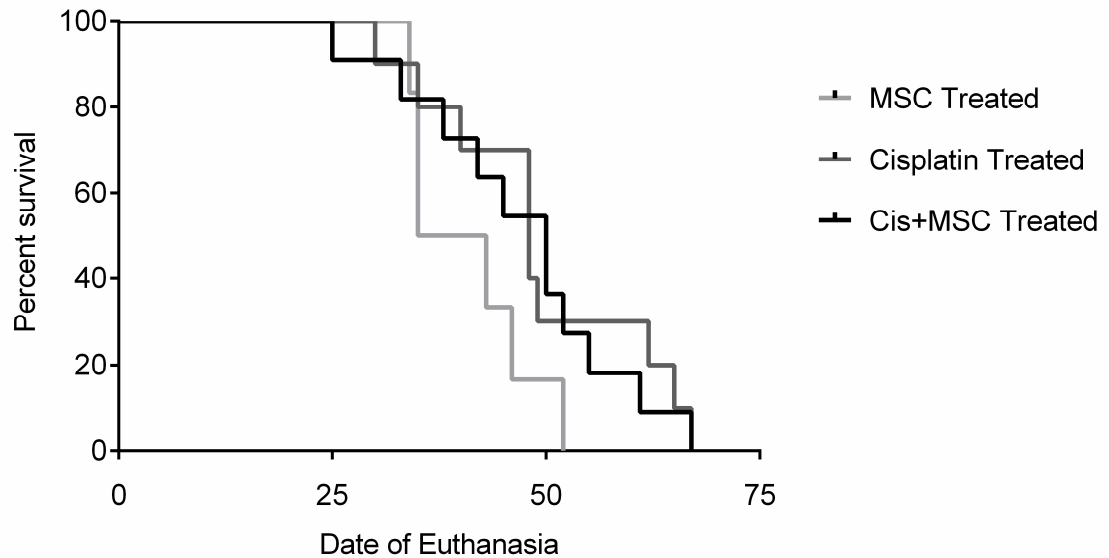


Figure 7.3 – 4: Kaplan Meier survival curves with a Mantel Cox Regression analysis were used to analyze the median survival times between mice treated with mesenchymal stromal cells (MSC) alone, mice treated with cisplatin (Cis), and mice treated with both MSCs and cisplatin. The survival curve of MSC alone mice was significantly shorter than cisplatin or cisplatin and MSC treatment groups ($p < 0.0001$).

Comparison of Survival Estimates: Untreated vs Cis vs Cis+MSC

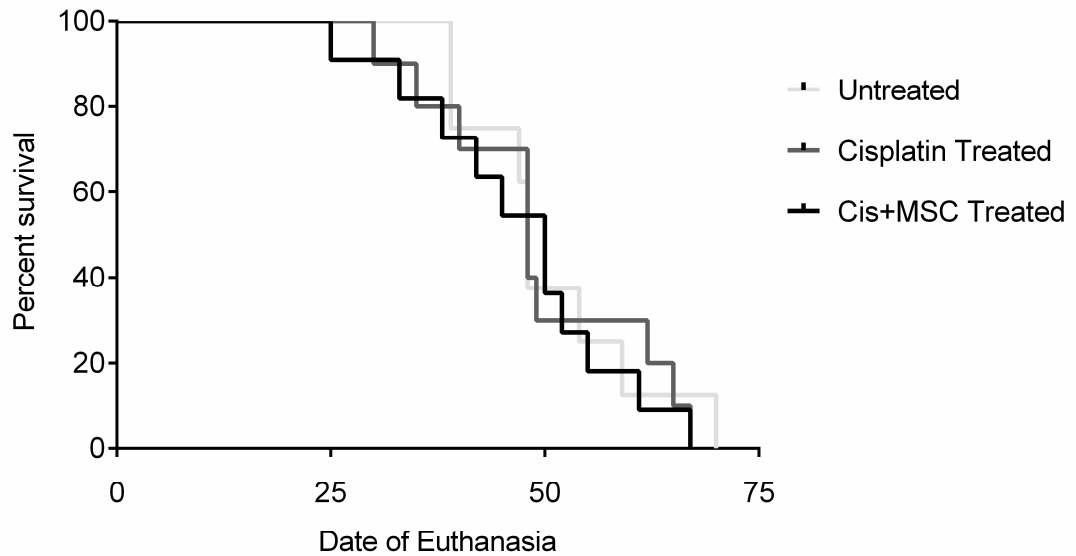


Figure 7.3 – 5: Kaplan Meier survival curves with a Mantel Cox Regression analysis were used to analyze the median survival times between untreated mice (control), mice treated with cisplatin (Cis), and mice treated with both mesenchymal stromal cells (MSC) and cisplatin. The survival curve of untreated control mice was significantly different than cisplatin or cisplatin and MSC treated mice ($p < 0.0001$).

Comparison of Survival Estimates: All Treatment Groups

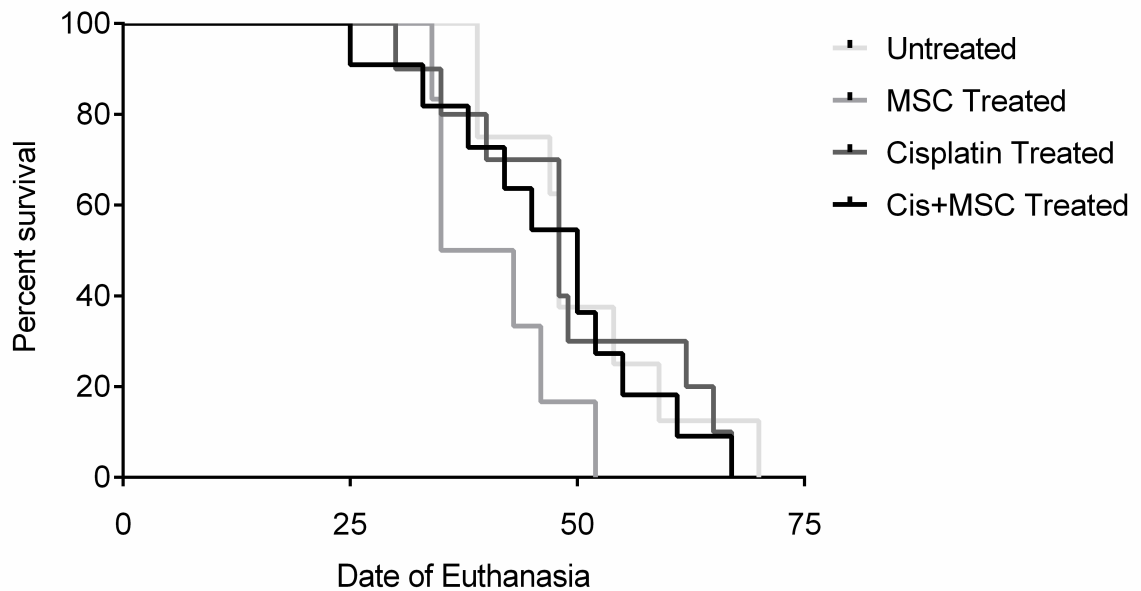


Figure 7.3 – 6: Kaplan Meier survival curves with a Mantel Cox Regression analysis were used to analyze the median survival times between all treatment groups (untreated controls, mesenchymal stromal cells (MSC), cisplatin (Cis), or cisplatin and MSCs). The survival curves were significantly different between groups when all were compared together ($p < 0.001$).

REFERENCES

1. Comstock KE, Hall CL, Daignault S, Mandlebaum SA, Yu C, Keller ET. A bioluminescent orthotopic mouse model of human osteosarcoma that allows sensitive and rapid evaluation of new therapeutic agents *In vivo*. *In vivo*. 2009;23:661-668.
2. Luetke A, Meyers PA, Lewis I, Juergens H. Osteosarcoma treatment – Where do we stand? A state of the art review. *Cancer Treatment Reviews*. 2014;40:523-532.
3. Meyers PA, Schwartz CL, Krailo M, Kleinerman ES, Betcher D, Bernstein ML, Conrad E, Ferguson W, Gebhardt M, Goorin AM, Harris MB, Healey J, Huvos A, Link M, Montebello J, Nadel H, Nieder M, Sato J, Siegal G, Weiner M, Wells R, Wold L, Womer R, Grier H. Osteosarcoma: A Randomized, Prospective Trial of the Addition of Ifosfamide and/or Muramyl Tripeptide to Cisplatin, Doxorubicin, and High-Dose Methotrexate. *Journal of Clinical Oncology*. 2005;23:2004-2011.
4. Roodhart Jeanine ML, Daenen Laura GM, Stigter Edwin CA, Prins H-J, Gerrits J, Houthuijzen Julia M, Gerritsen Marije G, Schipper Henk S, Backer Marieke JG, van Amersfoort M, Vermaat Joost SP, Moerer P, Ishihara K, Kalkhoven E, Beijnen Jos H, Derksen Patrick WB, Medema Rene H, Martens Anton C, Brenkman Arjan B, Voest Emile E. Mesenchymal Stem Cells Induce Resistance to Chemotherapy through the Release of Platinum-Induced Fatty Acids. *Cancer Cell*. 2011;20:370-383.
5. Selmic L, Burton J, Thamm D, Withrow S, Lana S. Comparison of carboplatin and doxorubicin-based chemotherapy protocols in 470. *J Vet Intern Med*. 2014;28:554-563.
6. Tu B, Du L, Fan QM, Tang Z, Tang TT. STAT3 activation by IL-6 from mesenchymal stem cells promotes the proliferation and metastasis of osteosarcoma. *Cancer Lett*. 2012;325:80-88.
7. Withrow SJ, Wilkins RM. Cross talk from pets to people: translational osteosarcoma treatments. *ILAR journal / National Research Council, Institute of Laboratory Animal Resources*. 2010;51:208-213.

Chapter 8: Conclusions and Future Research

8.1 Conclusions

8.1.1 Summary

The projects presented herein explored the interactions between mesenchymal stromal cells (MSC) and minimal residual osteosarcoma disease in a murine model. Through an investigation of the effects of MSCs, their safety in patients with a history of osteosarcoma can be explored. While the use of these cells as agents to improve bone healing following limb reconstruction is already being investigated, the basic question of *should* they be used also needed to be examined. By exploring multiple scenarios including pulmonary metastases, local recurrence, and concurrent use with chemotherapeutic agents, these questions have been addressed. Although models have been created to respond to some of these issues, this work is the first to study all of them in an orthotopic, clinically relevant setting.

Model development began with the creation of a trackable osteosarcoma line using the luc gene. This reduced animal numbers needed compared to serial sacrifices as well as increasing timing reliability for the model. Further, by creating DLM8-Luc-M1 and DLM8-Luc-M2 cell lines, we were able to generate faster, more consistent pulmonary metastases to better recapitulate osteosarcoma clinical behaviors. To create the minimal residual disease setting, we optimized timing of primary tumor removal such that micrometastatic pulmonary disease would be present and would allow a suitable time for treatment before mice became moribund from the disease. Validation of this timing was completed through bioluminescent imaging and histology and we observed evidence of both pulmonary metastatic disease formation as well as recurrence of the disease in the surgical site following model development.

Validation experiments were completed. We confirmed that MSCs harvested fresh from C3H mice “homed” to the primary tumors from our newly developed cell line and, further, these

MSCs influenced the osteosarcoma primary tumor to grow faster *in vivo* when exposed to MSCs. Chemotherapy treatment was applied *in vitro* to assess sensitivity of the DLM8-Luc-M1 line to cisplatin and methotrexate; DLM8-Luc-M1 cells were sensitive to cisplatin and less sensitive to methotrexate.

Subsequent to model development, four studies were completed: 1) Short term pulmonary metastatic development study with MSC treatment; 2) Local recurrence study with MSC treatment; 3) Survival study with cisplatin and MSC treatment; 4) Long term pulmonary metastatic development study with methotrexate and MSC treatment.

The first experiment following model development was completed to determine whether the adipose derived mesenchymal stromal cells harvested from C3H mice would influence osteosarcoma pulmonary disease burden following removal of the primary tumor. We found that when introduced into mice with microscopic pulmonary disease, the cells may be problematic if that introduction is intravenous but do not appear to cause concern if the cells are placed into the surgical site.

The second experiment utilized concurrent MSC and methotrexate treatment in the developed pulmonary disease model to assess whether in a pilot study, chemotherapy would ameliorate the results seen in the first study. Methotrexate is commonly used for treatment of pulmonary osteosarcoma following removal of the primary tumor and thus we wanted to assess whether, when given in combination with MSCs, it would affect pulmonary disease burden development. We found that in this model, the use of methotrexate in combination with MSCs did not increase pulmonary metastatic disease burden in mice. Further studies using this model would be important to determine if the results are still valid with larger animal numbers.

The third experiment was aimed at measuring whether adipose derived mesenchymal stromal cells harvested from C3H mice would influence osteosarcoma recurrence in the surgical site

following narrow margin removal of the primary tumor. We found that when introduced either intravenously or into the surgical site, MSCs do not appear to increase the chances of local recurrence appearance or growth.

The fourth experiment evaluated whether MSCs would influence survival times of mice treated with cisplatin, cisplatin and MSCs, MSCs alone, or no MSCs or cisplatin. Cisplatin is commonly used in treatment of human osteosarcoma and MSCs have been shown to be dangerous when used in combination with cisplatin in some models. The results of our study showed that intravenous MSCs increased the risk of death in mice with microscopic pulmonary disease following primary tumor removal however, two treatments of cisplatin were enough to ameliorate this effect.

The fundamental hypothesis of this project was that adipose-derived mesenchymal stromal cells, delivered either into the surgical site or intravenously after removal of primary osteosarcoma tumor, will, in the presence of microscopic residual disease, influence metastatic pulmonary disease or local tumor regrowth. The results of this work are that, in nearly all situations, we fail to reject the primary hypothesis. In the models studied, mesenchymal stromal cells did influence both pulmonary microscopic residual disease and local recurrence. In the case of pulmonary disease burden, we found that intravenously-delivered MSCs were promotional in influencing time to first detection of metastasis. In the case of local recurrence, we found that surgical site delivery of MSCs resulted in smaller tumor size in locally recurrent tumors.

8.1.2 Implications

This project provides pivotal information that has been previously lacking in the field of osteosarcoma and MSC interaction. The use of MSCs to aid in healing of allografts and endoprosthetics is particularly attractive but the safety of these cells in patients with a history of

cancer must be addressed before physicians should use the new products being developed. This research has provided critical information to begin to address this question. Because pulmonary disease is one of the leading causes of death in canines and humans with osteosarcoma, it was important to determine if MSCs would exacerbate the metastatic nodules and decrease survival rates. The results of this project show that MSCs may be problematic if given intravenously.

Further, this project addressed an additional concern – would MSCs prove to be problematic for narrow margin removal of the osteosarcoma primary tumor, as is the standard surgical method in patients receiving a limb reconstruction? This model addressed this question through the use of a narrow margin “dirty amputation” in which microscopic disease remained in the surgical site. MSCs were then put into close proximity to the tumor cells and it was found that they did not hasten the time to or severity of local recurrence. In fact, in at least one outcome measure, the local administration of MSCs into the surgical site in close proximity to the residual microscopic tumor resulted in smaller recurrent tumors than untreated controls. These results will need to be verified with repeat studies, but provide evidence that MSCS are at least not promotive of tumor recurrence and may possibly be inhibitory.

The work presented herein thus brings engineers and clinicians one step further toward the safe use of MSCs in patients with a history of osteosarcoma. New therapeutic methods involving MSCs in a local delivery mechanism may be a viable way to increase healing of bone in patients following removal of primary osteosarcoma without a concern of causing further harm to the patient.

8.1.3 Limitations

While the implications of this research are promising, there are several limitations of this research which must be acknowledged. The most impactful limitation of this work throughout

every project was the variation seen within and between animals with respect to some of the principle outcome measures. As a result, there were many instances where statistical significance was not achieved but trends were seen. While a priori power analyses were performed to guide each study design, the variation seen resulted in lower than anticipated statistical power for many of our analyses. In certain outcome measures, the finding of “no difference” may have resulted from a Type II error. Increasing animal numbers and performing repeat validation studies would address these limitations.

Another related limitation was the variability of primary and metastatic tumor growth. While clinically relevant, as tumors all behave differently in the real world, this inconsistency was problematic for repeatability and reliability of the work in the laboratory setting. Further testing of injection methods, cell culture optimization, and the choice of osteosarcoma lines could have an impact on the reduction of the variability. As this was unknown going into the project, however, there were subtle changes made instead throughout the work as we learned what was best. One example of this was in changing from detachment of osteosarcoma cells with trypsin to detachment with cell scraping. By changing this method, we reduced the inability of the cells to go into solution and increased reliability of primary tumor formation.

While we chose to use a murine model, these results may not be directly applicable to human medicine. Additionally, we used adipose-derived mesenchymal stromal cells and DLM8 osteosarcoma; the use of other murine osteosarcoma lines or other mesenchymal stromal cells may change the results we found in another study.

Chemotherapy in the clinical setting is utilized both pre-operatively and post-operatively for optimal control over tumors. In the model presented for this work, it was only given post-operatively and only for two rounds. While the results indicate that this was enough to show a difference, the survival times of mice may have increased if further rounds of chemotherapy

were given. Related to this, methotrexate treatment had no statistical effects but the dose given may have been too low as osteosarcoma is highly resistant to this drug when not given in combination with other therapies. Increasing the types of chemotherapy drugs utilized could have better allowed for methotrexate influence to be seen in the data results.

8.2 Future Research

While the results of this work are promising, there are several future projects that could be completed to strengthen the findings and further translate the results to clinical practice. As mentioned in the limitations above, examining the use of multimodal therapy given repeatedly as in a clinical treatment schedule in a larger animal project would be important to assess.

Although we did see that MSCs interact with primary tumor, using larger animal numbers, assessing the exact size of tumor nodules in which MSCs become problematic to use would be of great importance. While this work was focused on microscopic disease, knowing the critical size in which MSCs become dangerous would be an important next project.

Our project focused on the acute use of MSCs – that is, they were given within 24 hours of removal of the primary tumor such as would be the case if the cells were used for the initial limb reconstruction. However, a project looking at the use of MSCs at further time-points would also be useful information. Two cases in particular should be addressed – the first would be the use of the cells injected into the site following the end of chemotherapy and radiation treatment to help heal the bone after these destructive treatments were complete. The second case would be to mimic the use of cells during revision surgery, as would be done to aid in patient healing. This revision surgery also could benefit from MSCs but it is unknown from the work above whether the cells would be safe in these patients.

Finally, as the goal of this work was to determine if MSCs could eventually be utilized for limb reconstruction in patients with a history of osteosarcoma, using established methods to create a

model of limb salvage would be of great interest. One such way to do this would be to use a xenograft of tumor into a surgically reconstructive site. Following primary tumor removal, limb salvage using an allograft should be completed. This model would allow for better testing of MSC safe use in a product and could also be used to test bone healing and MSC behavior when cells are subjected to tumor signals as well as inflammation and healing signals.

The work presented in this dissertation was critical to begin the process of addressing the safety of using mesenchymal stromal cells in a tumor microenvironment. Future projects building on these results will strengthen the findings and further answer the question for physicians as to whether mesenchymal stromal cells should be used in patients with a history of osteosarcoma.

APPENDICIES

Appendix A: Laboratory Operating Procedures

Appendix A - I: Osteosarcoma Cell Protocols

DLM8 Growth Media – Type I

Purpose: To culture DLM8 osteosarcoma cells for growth and propagation

Usage: Chapter 3 (partial)

Safety Precautions: Wear PPE for a BSL2 Lab

Preparation:

Materials:

- a. Sterile Pipettes
- b. 70% Ethanol
- c. Rapid-Flow Bottle Top Filter, 0.2 μm (150 mL or 500 mL; Thermo Fisher Scientific, Inc.)
- d. 500 mL Sterile Bottle

Equipment:

- a. Culture Hood

Reagents:

- a. 500 mL MEM
- b. 50 mL Fetal Bovine Serum (FBS)
- c. 10 mL MEM Vitamin Solution
- d. 5 mL Antibiotic-Antimycotic (100X)
- e. Non-essential Amino Acids (10 mM)
- f. Sodium Pyruvate Solution (100 mM)
- g. If selecting for luc positive cells, also add 3.5 mL G418

Procedure:

1. Thaw and warm reagents in 37° water bath
2. Sterilize the biological hood using 70% ethanol
3. Combine all reagents into MEM media bottle
4. Run reagent compound through filter into 500 mL bottle
5. Label media and store in 4° refrigerator until needed

DLM8 Growth Media – Type II

Purpose: To culture DLM8 osteosarcoma cells for growth and propagation

Usage: Chapter 3 (partial), Chapters 4-7

Safety Precautions: Wear PPE for a BSL2 Lab

Preparation:

Materials:

- a. Sterile Pipettes
- b. 70% Ethanol
- c. Rapid-Flow Bottle Top Filter, 0.2 μm (150 mL or 500 mL; Thermo Fisher Scientific, Inc.)
- d. 500 mL Sterile Bottle

Equipment:

- a. Culture Hood

Reagents:

- a. 500 mL DMEM, 4.5 g/L glucose
- b. 50 mL Fetal Bovine Serum (FBS)
- c. 5 mL Antibiotic-Antimycotic (100X)
- d. If selecting for luc positive cells, also add 3.5 mL G418

Procedure:

1. Thaw and warm reagents in 37° water bath
2. Sterilize the biological hood using 70% ethanol
3. Combine all reagents into DMEM media bottle
4. Run reagent compound through filter into 500 mL bottle
5. Label media and store in 4° refrigerator until needed

DLM8 Freeze Media – Type I

Purpose: To freeze DLM8 osteosarcoma cells for cryopreservation

Usage: Chapter 3 (partial)

Safety Precautions: Wear PPE for a BSL2 Lab

Preparation:

Materials:

- a. Sterile Pipettes
- b. 70% Ethanol
- c. Rapid-Flow Bottle Top Filter, 0.2 μm (150 mL; Thermo Fisher Scientific, Inc.)
- d. 250 mL Sterile Bottle

Equipment:

- a. Culture Hood

Reagents:

- a. 45 mL MEM
- b. 45 mL Fetal Bovine Serum (FBS)
- c. 11 mL DMSO, sterile

Procedure:

1. Thaw and warm reagents in 37° water bath
2. Sterilize the biological hood using 70% ethanol
3. Add FBS and MEM to filter
4. Run reagent compound through filter into 250 mL bottle
5. Add DMSO to sterile compound
6. Label media and store in 4° refrigerator until needed

DLM8 Freeze Media – Type II

Purpose: To freeze DLM8 osteosarcoma cells for cryopreservation

Usage: Chapter 3 (partial), Chapter 4, Chapter 5

Safety Precautions: Wear PPE for a BSL2 Lab

Preparation:

Materials:

- a. Sterile Pipettes
- b. 70% Ethanol
- c. Rapid-Flow Bottle Top Filter, 0.2 μm (150 mL or 500 mL; Thermo Fisher Scientific, Inc.)
- d. 500 mL Sterile Bottle

Equipment:

- a. Culture Hood

Reagents:

- a. 45 mL DMEM, 4.5 g/L glucose
- b. 45 mL Fetal Bovine Serum (FBS)
- c. 11 mL DMSO, sterile

Procedure:

1. Thaw and warm reagents in 37° water bath
2. Sterilize the biological hood using 70% ethanol
3. Add FBS and DMEM to filter
4. Run reagent compound through filter into 250 mL bottle
5. Add DMSO to sterile compound
6. Label media and store in 4° refrigerator until needed

DLM8 Freeze Media – Type III

Purpose: To freeze DLM8 osteosarcoma cells for cryopreservation

Usage: Chapter 6, Chapter 7

Safety Precautions: Wear PPE for a BSL2 Lab

Preparation:

Materials:

- a. Sterile Pipettes
- b. 70% Ethanol
- c. 15 mL Conical Tube

Equipment:

- a. Culture Hood

Reagents:

- a. 4 mL Type II Growth Media for OSA Cells
- b. 4 mL Fetal Bovine Serum (FBS)
- c. 2 mL DMSO

Procedure:

1. Thaw and warm reagents in 37° water bath
2. Sterilize the biological hood using 70% ethanol
3. Combine all reagents into conical tube
4. Label media and store in 4° refrigerator until needed *

*Fresh media made immediately before usage is best.

DLM8 Freezing Cells – Procedure I

Purpose: Cryopreservation of DLM8 osteosarcoma cells

Usage: Chapter 3 (partial)

Safety Precautions: Wear PPE for a BSL2 Lab

Preparation:

Materials:

- a. Sterile Pipettes
- b. 70% Ethanol
- c. 1mL Cryovial tubes

Equipment:

- a. Culture Hood
- b. Vortex

Reagents:

- a. Freeze Media Type I
- b. Type I Growth Media for OSA Cells as needed (see procedure)

Procedure:

1. Thaw and warm Growth media in 37° water bath
2. Sterilize the biological hood using 70% ethanol
3. Count cells (*See cell counting procedure) – put in 1 mL of Type I Freeze Media for OSA Cells for every 1.5×10^6 cells
4. Transfer 1 mL of cells and media to cryovial. Repeat as needed.
5. Label vials and place in -80° freezer

DLM8 Freezing Cells – Procedure II

Purpose: Cryopreservation of DLM8 osteosarcoma cells

Usage: Chapter 3 (partial), Chapter 4, Chapter 5

Safety Precautions: Wear PPE for a BSL2 Lab

Preparation:

Materials:

- a. Sterile Pipettes
- b. 70% Ethanol
- c. 15 mL Conical Tube
- d. 1mL Cryovial tubes

Equipment:

- a. Culture Hood
- b. Vortex

Reagents:

- a. Freeze Media Type II
- b. Type II Growth Media for OSA Cells as needed (see procedure)

Procedure:

1. Thaw and warm Growth media in 37° water bath
2. Sterilize the biological hood using 70% ethanol
3. Count cells (*See cell counting procedure) – put in 1 mL of Type I Freeze Media for OSA Cells for every 1.5×10^6 cells
4. Transfer 1 mL of cells and media to cryovial. Repeat as needed.
5. Label vials and place in -80° freezer

DLM8 Freezing Cells – Procedure III

Purpose: Cryopreservation of DLM8 osteosarcoma cells

Usage: Chapter 6, Chapter 7

Safety Precautions: Wear PPE for a BSL2 Lab

Preparation:

Materials:

- a. Sterile Pipettes
- b. 70% Ethanol
- c. 15 mL Conical Tube
- d. 1mL Cryovial tubes

Equipment:

- a. Culture Hood
- b. Vortex

Reagents:

- a. Freeze Media Type III
- b. Type II Growth Media for OSA Cells as needed (see procedure)

Procedure:

1. Thaw and warm Growth media in 37° water bath
2. Sterilize the biological hood using 70% ethanol
3. Count cells (*See cell counting procedure) – put in 1 mL of Type II Growth Media for OSA Cells for every 3×10^6 cells
4. Place cells with media on vortex and slowly agitate while adding equal volume of Freeze media dropwise
5. Transfer 1 mL of cells and media to cryovial. Repeat as needed.
6. Label vials and place in -80° freezer

DLM8 Splitting Cells (Subculture and Injection) – Procedure I

Purpose: Culture of DLM8 osteosarcoma cells and Prepare for Injection

Usage: Chapter 3 (partial), Chapter 5

Safety Precautions: Wear PPE for a BSL2 Lab

Preparation:

Materials:

- a. Sterile Pipettes
- b. 70% Ethanol
- c. 1mL Cryovial tubes (*for injection)

Equipment:

- a. Culture Hood
- b. Centrifuge

Reagents:

- a. Culture Media Type I
- b. 0.25% Trypsin with 2.21 mM EDTA
- c. HBSS

Procedure:

1. Thaw and warm Growth media in 37° water bath
2. Sterilize the biological hood using 70% ethanol
3. Aspirate used Media and discard
4. Pipette HBSS into flasks and gently rock flask to coat bottom
5. Aspirate and discard HBSS
6. Pipette trypsin into flasks, allow for five – seven minutes exposure time (*incubator may be better if cells are not lifting up)
7. Pipette out trypsin and cells into tube or flask
8. Mix solution with fresh Culture Media and place into flasks, or if in flask, just add required media to flask containing trypsinized cells
9. *If using for injection, rinse two – three times in centrifuge at 1200 rpm with Culture Media without FBS and resuspend in desired volume after counting

DLM8 Splitting Cells (Subculture and Injection) – Procedure II

Purpose: Culture of DLM8 osteosarcoma cells and Prepare for Injection

Usage: Chapter 3 (partial), Chapter 4, Chapter 6, Chapter 7

Safety Precautions: Wear PPE for a BSL2 Lab

Preparation:

Materials:

- a. Sterile Pipettes
- b. 70% Ethanol
- c. 1mL Cryovial tubes (*for injection)
- d. Cell Scraper

Equipment:

- a. Culture Hood
- b. Centrifuge

Reagents:

- c. Culture Media Type II
- d. HBSS

Procedure:

1. Thaw and warm Growth media in 37° water bath
2. Sterilize the biological hood using 70% ethanol
3. Aspirate used Media and discard
4. Pipette HBSS into flasks and gently rock flask
5. Aspirate and discard HBSS
6. Pipette 1-5 mL Culture media into flasks
7. Gently scrape bottom of flask to remove cells
8. Mix solution with fresh Culture Media and place into flasks
9. *If using for injection, rinse two – three times in centrifuge at 1200 rpm with Culture Media without FBS and resuspend in desired volume after counting

DLM8 Harvesting– Procedure

Purpose: To select luciferase positive tumor cells from murine lungs

Usage: Entire Study

Safety Precautions: Wear PPE for a BSL2 Lab

Preparation:

Materials:

- a. Mouse with confirmed bioluminescent pulmonary metastasis (*See IVIS Imaging Protocol)
- b. # 10 blades (x2)
- c. Scalpel handles (optional)
- d. Sterile Stir Bar
- e. 50 mL Erlenmeyer Flask
- f. 50 mL conical tube
- g. Sterile Forceps (x2)
- h. Sterile small Scissors (x2)
- i. Sterile 60 mm plates (x3)
- j. 70% ethanol (spray bottle)
- k. T-25 culture flask
- l. 70 μ m mesh cell filter

Equipment:

- a. Culture Hood
- b. Centrifuge
- c. Stir Plate
- d. Incubator

Reagents:

- a. Sterile prepared 2x Collagenase and Elastase (Worthington Biochemicals. Cat. No, CLS-4 and ESL – prepare as: 2X: Collagenase IV at 2 mg/ml and Elastase at 2 units/mL in HBSS; Filter.)
- b. HBSS
- c. DLM8 Culture Media

Procedure:

1. Euthanize mice with cervical dislocation once anesthetized
2. Spray with ethanol and bring into culture hood
3. Add enough HBSS to just cover bottom of 2 plates
4. Remove skin in “X” pattern with first set of sterile surgical instrument
5. Spray mouse with ethanol
6. Open mouse with second set of sterile instruments and remove lungs en bloc
7. Transfer lungs from mouse into first plate.

8. Transfer lungs from first plate to second plate
9. Transfer lungs from second plate to third plate
10. Mince tissue with #10 blades until very fine
11. Remove all tissue to Erlenmeyer flask containing stir bar
 - a. Should be able to transfer with 10 mL pipette – if not, then mince more
 - b. Add 833 μ L HBSS and rinse plate x3
 - c. Add 2.5 – 5.0 mL 2x Collagenase and Elastase to Erlenmeyer flask
12. Place in incubator on stir plate for 2 hours at medium-low speed (~250 rpm)
13. Pass resultant mixture through mesh filter into 50 mL conical tube
14. Centrifuge at 1400 rpm for 5 minutes
15. Aspirate out supernatant and wash pellet with HBSS
16. Spin at 1400 rpm for 5 minutes
17. Aspirate out supernatant and wash pellet with HBSS
18. Spin at 1400 rpm for 5 minutes
19. Aspirate supernatant, leaving behind cell pellet
20. Add 5 mL of DLM8 Culture Media to tube, reconstitute pellet, and move to 25 mL flask or plate
 - a. Change media 48 hours following harvest
 - b. Change media every 3-4 days until colonies form
 - c. Select colonies with bioluminescent expression using IVIS protocol

Stable Transfection of Adherent Cells

Purpose: For the transfection of DLM8 osteosarcoma tumor cell lines with the pGL3 Luciferase Reporter Vector (Promega catalog #E1741) and pCI-neo Mammalian Expression Vector (Promega catalog #E1841) using the SuperFect Transfection Reagent from Qiagen (Catalog #301305).

Procedure:

1. Plate 100,000 cells/mL of the appropriate growth medium in a 60mm dish
2. Incubate the cells under their normal growth conditions
3. Dilute 4.5 μ L pGL3 Luciferase Reporter Vector and 0.5 μ L pCI-neo Mammalian Expression Vector with cell growth medium containing no serum, proteins, or antibiotics (MEM only) to a total volume of 150 μ L. Mix and spin down the solution for a few seconds to remove drops from the top of the tube
4. Add 20 μ L Superfect Transfection Reagent to the DNA solution. Mix by pipetting up and down 5 times or vortexing for 10s
5. Incubate the samples for 10 minutes at room temperature to allow transfection-complex formation
6. While complex formation takes place, gently aspirate the growth medium from the dish and wash cells once with 4mL HBSS
7. Add 1 mL cell growth medium containing serum and antibiotics to the reaction tube containing the transfection complexes. Mix by pipetting up and down twice and immediately transfer the total volume to the cells in the 60mm dishes
8. Incubate the cells with the transfection complexes for 3 hours under their normal growth conditions
9. Remove medium containing the remaining complexes from the cells by gentle aspiration and wash cells 3-4 times with 4mL HBSS
10. Add fresh cell growth medium (containing serum and antibiotics) and incubate for 48 hours
11. Passage cells at 1:10 into the appropriate selective medium (G418). Maintain cells in selective medium under their normal growth conditions until colonies appear

*Normal growth conditions include complete cell media, 37°C and 5% CO₂ (incubator) conditions.

*See DLM8 Media Protocol for contents of growth medium

Appendix A - II: Mesenchymal Stromal Cell Protocols

MSC Growth Media

Purpose: To culture mesenchymal stromal cells for growth and propagation

Usage: Entire Study

Safety Precautions: Wear PPE for a BSL2 Lab

Preparation:

Materials:

- a. Sterile Pipettes
- b. 70% Ethanol
- c. Rapid-Flow Bottle Top Filter, 0.2 μm (150 mL or 500 mL; Thermo Fisher Scientific, Inc.)
- d. 500 mL Sterile Bottle

Equipment:

- a. Culture Hood

Reagents:

- a. 1 L Dulbecco's Modification of Eagle's Medium (w/ 1 g/L glucose, L-glutamine, sodium pyruvate) – Cellgro, Mediatech, Inc, Manassas, VA
- b. 150 mL Fetal Bovine Serum (FBS) – Atlas Biologicals, Fort Collins, CO
- c. 20 mL MEM Vitamin Solution – Cellgro, Mediatech, Inc, Manassas, VA
- d. 10 mL Antibiotic-Antimycotic (10,000 I.U/mL Penicillin, 10,000 $\mu\text{g}/\text{mL}$ Streptomycin, 25 $\mu\text{g}/\text{mL}$ Amphotericin B) – Cellgro, Mediatech, Inc, Manassas, VA
- e. 10 mL MEM Non-essential Amino Acids – Cellgro, Mediatech, Inc, Manassas, VA

Procedure:

1. Thaw and warm reagents in 37° water bath
2. Sterilize the biological hood using 70% ethanol
3. Combine all reagents into DMEM media bottle
4. Run reagent compound through filter into 500 mL bottle
5. Label media and store in 4° refrigerator until needed

MSC Freeze Media

Purpose: To cryopreserve MSCs for future use

Usage: Entire Study

Safety Precautions: Wear PPE for a BSL2 Lab

Preparation:

Materials:

- a. Sterile Pipettes
- b. 70% Ethanol
- c. Rapid-Flow Bottle Top Filter, 0.2 μm (150 mL or 500 mL; Thermo Fisher Scientific, Inc.)
- d. 50 mL Sterile Bottle

Equipment:

- a. Culture Hood

Reagents:

- a. 45 mL Dulbecco's Modification of Eagle's Medium (w/ 1 g/L glucose, L-glutamine, sodium pyruvate) – Cellgro, Mediatech, Inc, Manassas, VA
- b. 45 mL Fetal Bovine Serum (FBS) – Atlas Biologicals, Fort Collins, CO
- c. 11 mL DMSO

Procedure:

1. Thaw and warm reagents in 37° water bath
2. Sterilize the biological hood using 70% ethanol
3. Run FBS and DMEM through filter into 50 mL bottle
4. Carefully add sterile DMSO to bottle
5. Label media and store in 4° refrigerator until needed

MSC Splitting Cells (Subculture and Injection) – Procedure

Purpose: To culture mesenchymal stromal cells for propagation and injection

Usage: Entire Study

Safety Precautions: Wear PPE for a BSL2 Lab

Preparation:

Materials:

- a. Sterile Pipettes
- b. 70% Ethanol
- c. Sterile flasks or plates

Equipment:

- a. Culture Hood

Reagents:

- a. Hank's Balanced Salt Solution (HBSS) – Cellgro, Mediatech, Inc, Manassas, VA, USA
- b. 0.25% Trypsin, 2.21 mM EDTA, 1X [-] sodium bicarbonate – Cellgro, Mediatech, Inc, Manassas, VA, USA
- c. MSC Media

Procedure:

1. Remove old media from flasks or plates using glass pipette
2. Rinse with HBSS
3. Add enough trypsin to just cover bottom of flask or plate
4. Allow trypsin to remain on cells for 5-8 minutes
5. Transfer cells to new sterile flask or plate
6. Feed new flasks and plates as well as old flasks and plates with complete MSC media
7. If injecting, rinse cells two-three times, count, and resuspend in amount required for injection
 - a. Resuspension: PBS + 100 units/mL Heparin (**make sure it is 100 units/ml!**) for IV injection and sterile PBS alone otherwise

MSC Freezing Cells – Procedure

Purpose: To cryopreserve mesenchymal stromal cells for future studies

Usage: Entire Study

Safety Precautions: Wear PPE for a BSL2 Lab

Preparation:

Materials:

- a. Sterile Pipettes
- b. 70% Ethanol
- c. Rapid-Flow Bottle Top Filter, 0.2 μm (150 mL or 500 mL; Thermo Fisher Scientific, Inc.)
- d. 500 mL Sterile Bottle
- e. Sterile Flasks or plates

Equipment:

- a. Culture Hood

Reagents:

- a. Hank's Balanced Salt Solution (HBSS) – Cellgro, Mediatech, Inc, Manassas, VA, USA
- b. 0.25% Trypsin, 2.21 mM EDTA, 1X [-] sodium bicarbonate – Cellgro, Mediatech, Inc, Manassas, VA, USA
- c. MSC Freeze Media

Procedure:

1. Remove old media from flasks or plates using glass pipette
2. Rinse with HBSS
3. Add enough trypsin to just cover bottom of flask or plate
4. Allow trypsin to remain on cells for 5-8 minutes
5. Count cells (*See cell counting procedure) – put in 1 mL of MSC Freeze Media for every 1.5×10^6 cells
6. Transfer 1 mL of cells and media to cryovial. Repeat as needed.
7. Label vials and place in -80° freezer

MSC Harvesting– Procedure

Purpose: To collect mesenchymal stromal cells from adipose

Usage: Entire Study

Safety Precautions: Wear PPE for a BSL2 Lab

Preparation:

Materials:

- a. # 10 blades (x2)
- b. Scalpel handles (optional)
- c. Sterile Stir Bar
- d. 25 - 50 mL Erlenmeyer Flask
- e. 50 mL conical tube
- f. Sterile Forceps (x2)
- g. Sterile small Scissors (x2)
- h. 60 mm plates (x4)
- i. 70% ethanol (spray bottle)
- j. T-25 culture flask

Equipment:

- a. Culture Hood
- b. Centrifuge
- c. Stir Plate
- d. Incubator

Reagents:

- a. Type IA (cat # C9891, Sigma Aldrich) Collagenase (5 mL per mouse; 1 mg/mL)
- b. DMEM (low glucose) + 10% antibiotics/antimycotics
- c. MSC Culture Media

Procedure:

1. Euthanize mice with cervical dislocation once anesthetized
2. Spray with ethanol and bring into culture hood
3. Add enough DLM8+abx to just cover bottom of 3 plates
4. Remove skin in "X" pattern with first set of sterile surgical instrument
5. Spray mouse with ethanol
6. Open peritoneal membrane with second set of surgical instruments and remove abdominal adipose
7. Transfer adipose from mouse into first plate.
8. Transfer adipose from first plate to second plate
9. Transfer adipose from second plate to third plate
10. Transfer adipose to empty plate
11. Mince fat with #10 blades until very fine

12. Add collagenase and transfer fat to Erlenmeyer flask containing stir bar
 - a. Should be able to transfer with 10 mL pipette – if not, then mince more
13. Place in incubator on stir plate for 30 minutes at medium-low speed
14. Transfer resultant mixture to 50 mL conical tube and add of DMEM + antibiotic-antimycotic to get a total volume of 50 mL
15. Centrifuge at 2000 rpm for 5 minutes
16. Shake gently to resuspend pellet
17. Spin at 2000 rpm for 5 minutes
18. Aspirate supernatant, leaving behind cell pellet
19. Add 5 mL of Culture Media to tube, reconstitute pellet, and move to 25 mL flask or plate
 - a. Change media on fourth day following harvest

Quantum Dot Cell Labeling – Procedure

Purpose: To label adherent cells for tracking purpose

Usage: Chapter 3

Safety Precautions: Wear PPE for a BSL2 Lab

Preparation:

Materials:

- a. Cells to label
- b. Sterile Micro-Pipet tips
- c. 2 mL cryovial tube
- d. Sterile Flasks or plates

Equipment:

- a. Culture Hood
- b. Centrifuge
- c. Incubator

Reagents:

- a. MSC Culture Media
- b. Quantum Dot Labeling Kit (Qtracker Cell Labeling Kit cat. #Q25021MP, Invitrogen, Life Technologies, Carlsbad, CA)

Procedure (for 1×10^6 cells):

1. Add 1 μ L of Component A and 1 μ L of Component B (from Qtracker kit) to a 1.5 mL tube and let sit at room temperature for 5 minutes
2. Add 0.2 mL of media and vortex for 30 seconds
3. Add 1×10^6 cells to tube and place in incubator for 1 hour
4. Spin at 4000 rpm for 5 minutes
5. Aspirate supernatant and reconstitute pellet in 0.5 mL media
6. Spin at 4000 rpm for 5 minutes
7. Aspirate supernatant and reconstitute pellet in 0.5 mL media
8. Spin at 4000 rpm for 5 minutes
9. Visualize cells using IVIS imaging or fluorescent microscope
10. Use cells immediately or put into flask with culture media

Appendix A - III: Injection Protocols

DLM8 Cell Injection

Preparation:

a. Surgical Tools:

- i. Cotton gauze pads (small)
- ii. Surgical Gloves
- iii. Injection needles (22 gage; short and 22 gage; long – 1 per mouse)
- iv. 1 mL syringes (Luer-lock better)

b. Cell Preparation:

- i. Sterile 3 mL centrifuge tubes or sterile 2 mL cryovial tubes
- ii. 1 mL pipette with sterile tips
- iii. 15 mL and 50 mL conical tubes
- iv. DLM8 Splitting Cells (Subculture and Injection) – Procedure
- v. DLM8 cells – at least 2×10^6 per mouse (to inject 1×10^6)
 1. Add 75 μ L of Luciferase (sterile) to sample flasks and image before injection to verify expression

c. Other Equipment:

- i. Clean recovery cage with heating pad
- ii. Buprenorphine SR – inject using insulin needles (29 ½ G)
 1. amount depends on mouse weight, 0.6 mg/kg per mouse
- iii. Surgical prep wipes (4% chlorhexidine & 70% ethanol)
- iv. Isoflurane
- v. Oxygen
- vi. Ear tags and punch
- vii. Saline – 1 mL syringe, 25g needle (0.5 – 1.0 mL per mouse – if needed)

Procedure

d. Pre-operative:

- i. Weigh mice
- ii. Tag mice
- iii. Give Buprenorphine SR (0.6 mg/kg)
- iv. Shave and prepare mice with prep wipes (Tumor side, up to femoral head, mid-line)
- v. Bring to table, tumor free side down

e. Injection:

- i. Fill isoflurane container
- ii. Check oxygen level
- iii. Non-sterile table cover over heating pad
- iv. Turn on heating pad
- v. Pipette cells until well mixed (before every injection!)

- vi. Draw up cells using long 22g needle into 1 mL syringe (0.5 mL good amount), push to top of syringe, removing bubbles
- vii. Change to short 22g needle, push cells until no more bubbles and all the way to tip of needle
- viii. Place mouse in nose cone, tape down – VERIFY CORRECT SIDE
- ix. Locate patella, insert needle just proximal and gently rotate left and right to “drill” into tibial plateau
 1. STOP when in bone, before the needle slides into the diaphysis
- x. Inject 30 μ L into the site slowly over 30 seconds
 1. May need to reduce isoflurane to “1.5” (low) during injection
- xi. Slowly remove needle
 1. Gauze may be needed for blood
- xii. **NOTE: if mouse looks weak, turn off isoflurane and allow to recover under oxygen**

f. *Post-injection*

- i. Remove mouse to recovery cage set to “low” with towel in bottom of cage
- ii. Check mouse until moving regularly on their own
- iii. Move mouse to cage, label card with number, “injected DLM8 cells date”
- iv. Return mice to animal room at end of day
- v. **NOTE: if mouse recovery is slow or excessive bleeding seen, give saline before taking down at end of day**

MSC Cell Injection

Preparation:

a. Surgical Tools:

- i. Cotton gauze pads (small)
- ii. Insulin (29 ½ G) needles

b. Cell Preparation:

- i. Sterile 2 mL cryovial tubes
- ii. 1 mL pipette with sterile tips
- iii. 15 mL and 50 mL conical tubes
- iv. MSC Splitting Cells (Subculture and Injection) – Procedure
- v. MSC cells – at least 1×10^6 per mouse (to inject 5×10^5) – in PBS (+ 100 units/mL Heparin if injecting intravenously)

c. Other Equipment:

- i. Clean recovery cage
- ii. Isoflurane
- iii. Oxygen
- iv. Saline – 1 mL syringe, 25g needle (0.5 – 1.0 mL per mouse – if needed)

Procedure

d. Pre-operative:

- i. Weigh mice
- ii. Place in cage with towel and warming light above for at least 5 minutes (IV injections)

e. Injection:

- i. Fill isoflurane container
- ii. Check oxygen level
- iii. Non-sterile table cover over heating pad
- iv. Turn on heating pad
- v. Pipette cells until well mixed
- vi. Draw up cells using insulin needle, push to top of syringe, removing bubbles
- vii. Place mouse in nose cone, tape down – VERIFY CORRECT SIDE (for local injection)
 1. Gauze may be needed for blood
- viii. Place mouse in restraining device with tail accessible (for IV injection)
 1. Do not anesthetize mice first
 2. Make sure syringe has no air bubbles

f. Post-injection

- i. Remove mouse to recovery cage
- ii. Check mouse until moving regularly on their own
- iii. Move mouse to cage, label card with number, “injected MSC cells date”
- iv. Return mice to animal room at end of day
- v. **NOTE: if mouse recovery is slow or excessive bleeding seen, give saline before taking down at end of day**

Appendix A - IV: Imaging Protocols

Equipment:

- a. Luciferin (30 mg/mL)
- b. Luciferase transfected cells and/or mouse with luciferase transfected cells present
- c. Syringe with 27 G needle or insulin syringe (29 ½ G)
- d. Micropipette with 100 µL tip
- e. Isoflurane
- f. Oxygen
- g. Anesthesia chamber for live imaging
- h. IVIS 100 In Vivo Imaging System (Perkin Elmer, Waltham, USA)

Cell Procedures:

1. Inject luciferin (50-100 µL) into flask using micropipette, allow 5 minutes for exposure
2. Place flask in IVIS camera at Stage B
3. Capture image using Living Image Software set to medium binning for 30s – 1 minute
4. Remove flask from chamber after image is complete

Animal Procedures:

1. Inject luciferin IP or SQ (100 µL) into mouse using syringe, allow ambulation for 5 minutes
2. Place mouse in anesthesia chamber with moderate flow rate of isoflurane and Oxygen until immobile
3. Move mouse to IVIS imaging chamber and position with area of interest upward
4. Capture image using Living Image Software with stage set to A, medium binning, 1-3 minutes
5. Remove mouse from chamber after image has been obtained and return to cage – monitor until awake and moving normally

Appendix A - V: Surgical Protocols

Preparation:

a. Surgical Tools:

- i. Cauterizer + 2 tips
- ii. Suture scissors
- iii. Small surgical scissors
- iv. Drapes (long – mouse hole)
- v. Cotton gauze pads (small)
- vi. Cotton tipped applicator swabs
- vii. Stapler + extra staples
- viii. Needle Driver
- ix. Forceps
- x. #15 blades
- xi. #3 Blade Handle
- xii. 5-0 Biosyn suture
- xiii. Surgical Gloves
- xiv. Mask
- xv. Surgical Cap
- xvi. Towel Pack
- xvii. Stapler Remove (optional)
- xviii. Hemostat (optional)

b. Other Equipment:

- i. Clean recovery cage with heating pad
- ii. New clean cage with food on cage floor
- iii. Tissue Cassettes
- iv. Formaldehyde in large containers
- v. Lidocaine – long 22g needle, 1 mL syringe
 1. amount varies, ~20uL per mouse (2 drops)
- vi. Buprenorphine SR – insulin needles (29 ½ G)
 1. amount depends on mice, 0.6 mg/kg per mouse
- vii. Luciferin – 27 gage needle (100 µL per mouse)
- viii. Saline – 1 mL syringe, 25g needle (1 mL per mouse) – WARMED first
- ix. Surgical prep wipes (4% chlorhexidine & 70% ethanol)
- x. Isoflurane
- xi. Oxygen
- xii. Ear tags and punch (optional)

Procedure

c. Pre-operative:

- i. Give Luciferin (100 µL)
- ii. Weigh mice
- iii. Tag mice (if needed)

- iv. Image Mice (30s-3 minutes, med, A, lateral view AND 2-3 minutes, med, A, chest upward for metastasis)
- v. Give Buprenorphine SR (0.6 mg/kg)
- vi. Shave and wipe mice – VERIFY CORRECT SIDE
- vii. Bring to table

d. Operative:

- i. Set cauterize to “4”
- ii. Turn on water heating pad
- iii. Fill isoflurane container
- iv. Check oxygen level
- v. Move nose cone to ~7 in from end of table
- vi. Non-sterile table cover over heating pad
- vii. Prepare surgical instrument table – KEEP STERILE
- viii. Place mouse in nose cone, tape down – VERIFY CORRECT SIDE
- ix. Prepare cassette for leg, place leg in formaldehyde containers when removed
- x. After removal of leg, place 2-4 drops of Lidocaine into side before closure.
- xi. Suture and staple mouse closed
- xii. **NOTE: if mouse looks shaky, turn off isoflurane and allow to recover under oxygen**

e. Post-operative

- i. Remove mouse to recovery cage set to “low” with towel in bottom of cage
- ii. Give saline (1mL – half per side)
- iii. Check mouse until moving regularly on their own
- iv. Move mouse to new clean cage
- v. Re-weigh and re-image mice at or > 3 hours post-amp
 - 1. Re-image mice (100uL luciferin) for **3 minutes**, med, A
- vi. Return mice to animal room at end of day
- vii. **NOTE: if mouse recovery is slow or excessive bleeding seen, give more saline before taking down at end of day**

Appendix A - VI: Bioquant Protocols

Purpose: To assess area of lung tissue and tumor tissue, follow the steps below in the Bioquant Osteo program.

Procedure:

1. File > Open Dataset
2. New quick data set > Rename with "Mouse #, 1st/2nd cut"
3. Click "Measure" > Calibration > BQOSTEO > scope calibration file (9-9-13_Nikon Scope.cal used for this project) – Close box after selection
4. Click File > Open Image > Click the square symbol on "Large Image Nav" to fit window
5. Select "Arrays" (double click) > D3 & A2, confirm magnification matches slide file
6. Type > Irregular (spacebar to end if not continuous trace)
7. Outline tissue with define; click "Preview"
8. Apply color select to get R, G, and B values to remove white spaces
 - a. R (240, 91) G (155, 22) B (198, 47) used for analysis
9. Conversion factor should be 1.69899 (for 2X)

Tips:

1. Ctrl+Alt+I inserts new line or will add to current line if multiple areas selected
2. A1 array is for all tissue on slide and D3 is for area
3. Right click to escape drawing box

When finished, click "Edit > copy data > all selected arrays", then open excel and paste information.

Appendix B: Scoring Assessments

Appendix B – I: Post-Amputation Scoring Assessment

RODENTS – Pain assessment score chart for amputation surgery & Post-surgical monitoring

1. **BODY WEIGHT – based on “time 0” values**
 - 0 = < - 5 % decrease
 - 1 = 6 - 10 % decrease
 - 2 = 11 - 20 % decrease
 - 3 = 21 - 25 % decrease
 - 4 = > - 25% decrease

2. **LAMENESS**
 - 0 = none
 - 1 = mild, single limb lameness
 - 2 = moderate, multiple limb lameness
 - 3 = severe, non-weight bearing on any limb

3. **APPEARANCE**
 - 0 = normal
 - 1 = huddled, mild piloerection, moves when stimulated
 - 2 = huddled, moderate piloerection, reluctant to move
 - 3 = huddled, ungroomed, severe piloerection, no movement or moribund

4. **ARTHRITIS SCORE**
 - 0 = normal
 - 1 = mild erythema, no swelling or limb deformity
 - 2 = moderate erythema, mild swelling, no limb deformity
 - 3 = moderate erythema, moderate swelling, mild limb deformity
 - 4 = severe erythema, severe swelling, moderate to severe limb deformity

Score

0-3 total score or <1 score in a category: No intervention

4-9 total score or >1 score in a category: Administer Buprenorphine SR (1 dose of 0.6 mg/kg, subcutaneously)

10 – 11: Administer Buprenorphine SR (1 dose of 0.6 mg/kg, subcutaneously) and re-evaluate pain score in 1 hour. If still not controlled the animal will be examined by a veterinarian and euthanized based upon results of exam.

Appendix B – II: Scoring Assessment for Survival Study

Appearance

| | |
|--|---|
| Normal (coat smooth, eyes/nose clear) | 0 |
| Reduced Grooming | 1 |
| Dull/rough coat, ocular/nasal discharge | 2 |
| Absence of grooming, piloerection, hunched | 4 |

Body Weight

| | |
|---|---|
| Normal (no weight loss) | 0 |
| Up to 10% weight loss since time 0 | 1 |
| 10 to 25% weight loss since time 0 or 15% over 2 days | 2 |
| > 25% weight loss since time 0 or 20% over 2 days | 4 |

Clinical Signs

| | |
|-------------------------|---|
| Normal | 0 |
| Ataxia | 1 |
| Loss of righting reflex | 2 |
| Cold to touch | 4 |

Natural Behavior

| | |
|--|---|
| Normal | 0 |
| Minor changes, less peer interaction | 1 |
| Little peer interaction, less mobile and alert, isolated | 2 |
| No peer interaction, self-mutilation, restless or still | 4 |

Provoked Behavior

| | |
|---|---|
| Normal | 0 |
| Subdued, but normal when stimulated | 1 |
| Subdued even when stimulated | 2 |
| Unresponsive when stimulated, weak, precomatose | 4 |

Score Total

Interpretation:

Normal: 0 – 4; Continue to monitor daily

Near Moribund: 5 – 14; Veterinary exam, increase monitoring for higher scoring

Moribund (consider euthanasia): 15 – 20; Euthanize with secondary veterinarian opinion

The above scoring assessment was utilized for Specific Aim 3, survival of mice after removal of primary tumor and treatment with MSC and chemotherapy for micrometastatic disease. However, we found there were several issues with the scoring criteria, such as not taking metastatic disease burden or dyspnea into account. Thus, based on our observations throughout the study, we are introducing a scoring assessment we think would work better with this model in future studies. If the budget is available, the use of a MouseOx (pulse oximeter) would help to measure breath rate, heart rate, and other clinical signs. Another consideration not accounted for in this assessment would be measuring IVIS expression of the metastatic regions and accounting for those in the overall score in addition to measureable metastatic nodules.

Modified Scoring Assessment for Survival Study

Appearance

| | |
|--|---|
| Normal (coat smooth, eyes/nose clear) | 0 |
| Reduced Grooming | 1 |
| Dull/rough coat, ocular/nasal discharge | 2 |
| Absence of grooming, piloerection, hunched | 4 |

Body Weight

| | |
|--|---|
| Normal (no weight loss) | 0 |
| Up to 10% weight loss since time 0 | 1 |
| 10 to 25% weight loss/gain since time 0 or 15% over 2 days | 2 |
| > 25% weight loss/gain since time 0 or 20% over 2 days | 4 |

Clinical Signs

| | |
|-------------------------|---|
| Normal | 0 |
| Ataxia | 1 |
| Loss of righting reflex | 2 |
| Cold to touch | 4 |

Natural Behavior

| | |
|--|---|
| Normal | 0 |
| Minor changes, less peer interaction | 1 |
| Little peer interaction, less mobile and alert, isolated | 2 |
| No peer interaction, self-mutilation, restless or still | 4 |

Provoked Behavior

| | |
|---|---|
| Normal | 0 |
| Subdued, but normal when stimulated | 1 |
| Subdued even when stimulated | 2 |
| Unresponsive when stimulated, weak, precomatose | 4 |

| | | |
|--------------------------|---|-------|
| Dyspnea | | |
| | Normal, no breathing issues | 0 |
| | Mild, some breathing issues | 1 |
| | Moderate, obvious “air hunger” | 2 |
| | Severe breathing issues, extreme “air hunger” | 4 |
| Lameness | | |
| | Normal | 0 |
| | Present | 1 |
| Metastatic Burden | | |
| | Normal, no palpable metastatic disease | 0 |
| | Palpable metastatic disease less than 10.0 cm | 1 |
| | Palpable metastatic disease > 10.0 cm | 3 |
| Score Total | | _____ |

Interpretation:

Normal: 0 – 6; Continue to monitor daily

Near Moribund: 7 – 20; Veterinary exam, increase monitoring for higher scoring

Moribund (consider euthanasia): 21 – 29; Euthanize with secondary veterinarian opinion

LIST OF ABBREVIATIONS

MSC = Mesenchymal Stromal (or Stem) Cell

BM-MSC = Bone Marrow Mesenchymal Stromal Cell

AD-MSC = Adipose Derived Mesenchymal Stromal Cell

CSC = Cancer Stem Cell

OS = Osteosarcoma

EWS = Ewing's Sarcoma

MFH = Malignant Fibrous Histiocytoma

GFP = Green Fluorescent Protein

BMP = Bone Morphogenetic Protein

IV = Intravenous

IA = Intra-arterial

BM = Bone Marrow

FUS-CHOP = Fused in Sarcoma, Translocated in LipoSarcoma-C/EBP Homologous Protein

SDF = Stromal derived factor

STAT = signal transducer and activator of transcription

TRAIL = tumor necrosis factor-related apoptosis-inducing ligand

IL = Interleukin

MEM = minimum essential medium eagle

DMEM = Dulbecco's modified eagle medium

FBS = fetal bovine serum

HBSS = Hanks' Balanced Salt Solution

G-418 = Geneticin 418